

THESIS  
3  
2001

This is to certify that the

dissertation entitled

CHARACTERIZATION OF INTERFACIAL STRUCTURE AND  
PROPERTIES OF COLLOIDAL LIQUID APHRONS  
FOR BIOCATALYSIS

presented by

Prashant Srivastava

has been accepted towards fulfillment  
of the requirements for

Ph.D. degree in Chemical Engineering

R. Mark Worden

Major professor

Date 10/25/00

**LIBRARY  
Michigan State  
University**

**PLACE IN RETURN BOX to remove this checkout from your record.  
TO AVOID FINES return on or before date due.  
MAY BE RECALLED with earlier due date if requested.**

DATE DUE	DATE DUE	DATE DUE

**Characterization of interfacial structure and properties of Colloidal Liquid  
Aphrons for biocatalysis**

By

Prashant Srivastava

A DISSERTATION

Submitted to  
Michigan State University  
in partial fulfillment of the requirements  
for the degree of

DOCTOR OF PHILOSOPHY

Department of Chemical Engineering  
2000

Dr. R. Mark Worden

## **ABSTRACT**

**Characterization of interfacial structure and properties of Colloidal Liquid Aphrons  
for biocatalysis**

**By**

**Prashant Srivastava**

**Colloidal liquid aphrons (CLA) are surfactant-stabilized droplets (1-50 microns in diameter) of a nonpolar liquid dispersed in a continuous aqueous phase. The small dimensions of CLA provide very large interfacial areas and short diffusion path lengths; consequently interphase solute transfer can often be completed within seconds. The interfacial structure and mass transfer properties of CLA emulsions were investigated in this research. Applications of CLA emulsions in multiphase enzymatic and whole-cell biocatalysis were also developed.**

**A variety of experimental tools were used to characterize the interfacial structure of CLA emulsions, including freeze fracture transmission electron microscopy, differential scanning calorimetry, small angle x-ray scattering, and Isothermal titration calorimetry. Results indicate the presence of liquid crystalline bilayers surrounding the organic phase in CLA emulsions. These layers are formed by the interaction between the two surfactants used in CLA formulation. The energetics and stoichiometry of the surfactant interaction were measured. A conceptual model of the mechanism stabilizing CLA emulsions was developed.**

**The mass-transfer properties of CLA emulsions were measured experimentally using two approaches. The first approach involved the direct**

measurement of heptanoic acid diffusion from the CLA emulsions into the water phase. The second approach involved indirect measurement via coupling the mass-transfer of the solute (p-tolyl acetate) to a chemical reaction (alkaline hydrolysis). The local mass transfer coefficient of the surfactant shell ( $K_{L,shell}$ ) was estimated to be about  $\sim 30 \times 10^{-3}$  cm/s, which is comparable to  $K_L$  values for surfactant-free, liquid-liquid systems at an equivalent void fraction ( $\phi$ ). The volumetric mass transfer coefficient ( $K_L a$ ) for CLA were 5 to 20 times higher than those for conventional emulsions.

Application of CLA emulsions to enzymatic and whole cell biocatalysis was demonstrated. The dynamic resolution of L,D phenylalanine was carried out in a multiphase system using porcine pancreatic lipase. The CLA emulsions were found to reduce the time required to attain equilibrium by about four-fold over conventional contacting methods. A statistical design of experiment approach was used to identify the major variables affecting equilibrium conversion and enantiomeric excess. The use of CLA emulsions in the biotransformations of cinnamaldehyde by Baker's yeast at high cell densities (250g/L) using a non-toxic solvent (2,2,4 trimethyl pentane) was also studied. The selectivity of this transformation was influenced by the presence of CLA emulsions.

Reversible emulsions formed using novel block-graft copolymeric emulsifiers (Polymethacrylic acid (PMAA)-g-Ethylene Glycol (EG)) were investigated. Such emulsions show considerable promise in multiphase contacting, since the emulsions produced can be maintained stable as long as desired and then coalesced on demand by a small pH change.

**Dedicated to my granddad, Mr. B.N.Srivastava, and my parents who have been a  
constant source of motivation and strength**

## ACKNOWLEDGMENTS

I would like to thank Dr. R. M Worden for his invaluable guidance and support during this research project. I would also like to thank Dr. Alec Scranton, Dr Charles Petty, Dr. Bruce Dale and Dr. Pat Oriel, for their service on my guidance committee. This work would not have been possible without my principal collaborators, John W. Heckman, at the Center for Electron Optics, and Olaf Hahr, at the Technical University of Berlin. Invaluable intellectual discussions with Robert C Saunders, a fellow student at MSU, have contributed immensely to my insight into the interfacial structure. His knowledge of interfacial science and measurement has been a constant inspiration for this work. I would like to thank Dr. Charles Petty, for access to the particle characterization facility, and inspiring discussions over coffee. Special thanks goes to Dr. Wilson, Professor in the Department of Biochemistry, for letting us use the Omega titration microcalorimeter. I would also like to thank Dr. M.M. Sharma, Hon.Professor, Jawaharlal Nehru Center for Advanced Scientific Research (Bangalore) and Dr. G.J. Karabatsos, Professor Emeritus, Department of Chemistry, Michigan State University for their guidance for the p-tolyl acetate studies. Dr. Dennis Gilliland, at the Department of Statistics, MSU, contributed immensely to the statistical design and analysis presented in Chapter 4. I would also like to thank Frank Jere and Mike Shaffer, fellow students in Dr Miller's group, for being such a great listener for all my crazy ideas. It was a pleasure working with some tremendous undergraduates; Jason Shellnut, Derek Hodges, Andrew Brinks, Anna Johnson, and Christopher Loose, in the course of this work. Special thanks to the

Chemical Engineering office staff : Faith Peterson, Julie Caywood, Candace  
Mcmaster, Nancy Albright, Mary Lehnert and Paula Holzheur for all their support  
during my stint in graduate school.

## TABLE OF CONTENTS

<b>List of Figures.....</b>	<b>xiv</b>
<b>List of Tables.....</b>	<b>xix</b>
<b>Introduction.....</b>	<b>1</b>
<b><i>1. Interfacial Structure of Colloidal Liquid Aphrons .....</i></b>	<b><i>15</i></b>
<b>1.1 Introduction .....</b>	<b>15</b>
<b>1.2 Preparation of CLA emulsions .....</b>	<b>20</b>
<b>1.3 Differential Scanning Calorimetry.....</b>	<b>20</b>
<b>1.4.1 Description .....</b>	<b>20</b>
<b>1.4.2 Materials and Methods .....</b>	<b>22</b>
<b>1.4.3 Results.....</b>	<b>22</b>
<b>1.4 Freeze-Fracture/Freeze Etch Transmission Electron Microscopy .....</b>	<b>24</b>
<b>1.4.1 Description .....</b>	<b>24</b>
<b>1.4.2 Materials and methods .....</b>	<b>27</b>
<b>1.4.3 Results.....</b>	<b>28</b>
<b>1.5 Small Angle X ray Scattering.....</b>	<b>38</b>
<b>1.5.1 Description .....</b>	<b>38</b>
<b>1.5.2 Materials and Methods .....</b>	<b>42</b>
<b>1.5.3 Results.....</b>	<b>42</b>
<b>1.6 Isothermal Titration Calorimetry .....</b>	<b>45</b>
<b>1.6.1 Description .....</b>	<b>45</b>

<b>1.6.2 Materials and Methods</b> .....	<b>47</b>
<b>1.6.3 Results</b> .....	<b>48</b>
<b>1.7 Development of a conceptual model for lamellar micelles stabilizing CLA interfaces</b> .....	<b>51</b>
<b>1.8 Interpretation of CLA properties</b> .....	<b>54</b>
<b>1.8.1 Ease of formation and small droplet sizes</b> .....	<b>54</b>
<b>1.8.2 High dispersed phase volume ratios</b> .....	<b>55</b>
<b>1.8.3 Influence of nature of the dispersed phase on maximum phase volume ratios</b> .....	<b>57</b>
<b>1.8.4 High stability</b> .....	<b>58</b>
<b>1.9 Conclusions</b> .....	<b>59</b>
<b>1.10 References</b> .....	<b>59</b>
<b>2. Enhancement of Mass Transfer Using Colloidal Liquid Aphrons :</b>	
<b>Measurement of Mass Transfer Coefficients in Liquid-Liquid Extraction</b> ....	<b>64</b>
<b>2.1 Introduction</b> .....	<b>64</b>
<b>2.2 Materials and Methods</b> .....	<b>69</b>
<b>2.2.1 Mass-Transfer System</b> .....	<b>69</b>
2.2.1.1 Surfactants .....	69
2.2.1.2 Continuous and Dispersed Phases.....	69
2.2.1.3 Transferred Solute .....	70
<b>2.2.2 Measurement of Heptanoic Acid Concentration</b> .....	<b>71</b>
<b>2.2.3 CLA Preparation</b> .....	<b>73</b>

<b>2.2.4 CLA Size Measurement.....</b>	<b>74</b>
<b>2.2.5 Mass Transfer Measurement .....</b>	<b>74</b>
2.2.5.1 <i>Stirred-Cell Experiments. ....</i>	74
2.2.5.2 <i>Stirred-tank experiments.....</i>	74
<b>2.3 Data Analysis .....</b>	<b>77</b>
<b>2.4 Results and Discussion.....</b>	<b>81</b>
2.4.1 <b>Measurements in Stirred Cell .....</b>	<b>81</b>
2.4.2 <b>.Measurements in Baffled Tank.....</b>	<b>81</b>
2.4.3 <b>Influence of Surfactant Concentration. ....</b>	<b>88</b>
<b>2.5 Conclusions .....</b>	<b>92</b>
<b>2.6 Nomenclature .....</b>	<b>92</b>
<b>2.7 References.....</b>	<b>94</b>
<b>3. Enhancement of Mass Transfer using Colloidal Liquid Aphrons:</b>	
<b>Measurement of Mass-Transfer Coefficients Using Chemical Reaction.....</b>	<b>99</b>
<b>3.1 Introduction.....</b>	<b>99</b>
<b>3.2 Theory.....</b>	<b>100</b>
3.2.1 <b>Mass-transfer resistances in series.....</b>	<b>100</b>
3.2.2 <b>Coupling of mass transfer and reaction.....</b>	<b>101</b>
3.2.3 <b>Relative rates of mass transfer and reaction .....</b>	<b>101</b>
<b>3.3 Materials .....</b>	<b>105</b>

<b>3.4 Methods</b> .....	<b>106</b>
<b>3.4.1 CLA preparation</b> .....	<b>106</b>
<b>3.4.2 CLA size measurement</b> .....	<b>107</b>
<b>3.4.3 Mass-transfer rate measurement</b> .....	<b>107</b>
<b>3.4.4 Physical-property determination</b> .....	<b>108</b>
<b>3.5 Results and Discussion</b> .....	<b>109</b>
<b>3.5.1 Physicochemical properties</b> .....	<b>109</b>
<b>3.5.2 Effect of Ionic Strength</b> .....	<b>111</b>
<b>3.5.3 Mass-transfer coefficients</b> .....	<b>111</b>
<b>3.5.4 Effect of surfactant concentration on <math>\overline{d_{32}}</math> and <math>K_L</math></b> .....	<b>114</b>
<b>3.6 Conclusions</b> .....	<b>117</b>
<b>3.7 Nomenclature</b> .....	<b>118</b>
<b>3.8 References</b> .....	<b>119</b>
<b>4. LIPASE CATALYZED DYNAMIC RESOLUTION OF AMINO ACIDS</b> .....	<b>121</b>
<b>4.1 Introduction</b> .....	<b>121</b>
<b>4.2 Model System</b> .....	<b>124</b>
<b>4.3 Materials and methods</b> .....	<b>126</b>
<b>4.3.1 Experimental Methods</b> .....	<b>127</b>
<b>4.3.1.1. Immobilization efficiency</b> .....	<b>127</b>

4.3.1.2. Chiral resolution experiments.....	128
4.3.1.3. HPLC assay.....	129
<b>4.3.2 Conversion and enantiomeric excess measurements .....</b>	<b>133</b>
4.3.2.1. Central Composite Design.....	133
<b>4.4 Results and discussion .....</b>	<b>136</b>
<b>4.4.1 Enzyme interactions with CLA .....</b>	<b>136</b>
<b>4.4.2 Reaction rate measurements .....</b>	<b>137</b>
<b>4.4.3 Chiral Resolution.....</b>	<b>137</b>
4.4.3.1. Conversion ( $Y_c$ ).....	140
4.4.3.2. Enantiomeric excess ( $Y_{ee}$ ).....	152
<b>4.5 Conclusion .....</b>	<b>156</b>
<b>4.6 References.....</b>	<b>157</b>
<b>5. Whole Cell Biotransformations using Colloidal Liquid Aphrons.....</b>	<b>160</b>
<b>5.1 Introduction.....</b>	<b>160</b>
<b>5.1.1 Whole Cell Biocatalysis .....</b>	<b>161</b>
<b>5.1.2 Organic solvents in whole cell biocatalysis.....</b>	<b>163</b>
<b>5.1.3 Colloidal Liquid Aphrons .....</b>	<b>164</b>
<b>5.1.4 Model system.....</b>	<b>164</b>
<b>5.2 Experimental Methods.....</b>	<b>169</b>
<b>5.2.1 Determination of solvent biocompatibility .....</b>	<b>169</b>
<b>5.2.2 Preparation of Colloidal Liquid Aphrons.....</b>	<b>169</b>

<b>5.2.3 Biotransformation Methods</b> .....	170
<b>5.2.4 Analytical procedures</b> .....	171
<b>5.3 Results and discussion</b> .....	174
<b>5.3.1 Biocompatibility</b> .....	174
<b>5.3.2 Biotransformations in presence of CLA</b> .....	176
<b>5.3.3 Mechanisms for changing selectivity of whole cell biotransformations</b> .....	178
5.3.3.1. <i>Effect of concentration on product composition</i> .....	178
5.3.3.2. <i>Effect of time on product composition</i> .....	178
<b>5.3.4 Selectivity control using hydrophobic resins</b> .....	181
<b>5.4 Conclusion</b> .....	181
<b>5.5 References</b> .....	184
<b>6. Reversible emulsions</b> .....	187
<b>6.1 Introduction</b> .....	187
<b>6.2 Materials and Methods</b> .....	189
<b>6.3 Results</b> .....	191
<b>6.4 Conclusions</b> .....	193
<b>6.5 References</b> .....	196
<b>7. Summary</b> .....	197

## List of Figures

Figure 1 Ideal substrate (Modified from Csuk et al., 1991).....	2
Figure 2. Limitations of common biocatalytic substrates and strategies to overcome those limitations (redrawn from Van Sonsbeek et al. 1993).....	4
Figure 3. Possible biocatalytic systems involving an organic liquid.....	5
Figure 1.1. Model for CLA droplets (Redrawn from Sebba, 1987) .....	18
Figure 1.2. Schematic diagram of Differential Scanning Calorimeter (DSC) .....	21
Figure 1.3. DSC endotherm for CLA dispersion containing 0.1% Tergitol 15-S-3 in Limonene and 0.4% Tween 80 in Water (PVR 0.25).....	23
Figure 1.4 Freeze Fracture and Freeze etching of "membraned" cells or emulsions.....	25
Figure 1.5 Schematic diagram of sample preparation in Freeze Fracture TEM. .	26
Figure 1.6. Phase contrast micrographs of A. CLA emulsion and B. Conventional emulsions.....	32
Figure 1.7 Fracture surfaces of separate phases. A. Water and Tween 80 frozen in liquid propane at $-190^{\circ}\text{C}$ . B. Limonene and Tergitol frozen in a nitrogen slurry at $\approx -210^{\circ}\text{C}$ . .....	33
Figure 1.8 Replicas of conventional emulsions. A. Freeze fracture and B. Freeze etch. Inset shows the detail of the droplet matrix interface for each at 5X increased magnification. ....	34

Figure 1.9 A. Freeze fracture of CLA suspension showing the multilamellar phase boundary. B. Enlargement of the boundary showing varying surface steps approximately 20 to 40 nm high. ....	35
Figure 1.10 A. Freeze etch of a CLA emulsion showing enhanced detail of the phase boundary. B. Enlargement showing the 20 to 40 nm steps and additional ridges running parallel to the step faces. ....	36
Figure 1.11 A. Freeze fracture surface of a mixture of Tergitol and Tween at the concentrations used to form the CLA. B. The same solution, etched for 8 min prior to shadowing.....	37
Figure 1.12 X-ray diffraction from lattice planes (Braggs law).....	41
Figure 1.13. SAXS data for 0.1% Tergitol, 0.4% Tween 80 solution in water ....	44
Figure 1.14. Typical ITC experimental data and analysis (MicroCal Inc, MA).....	46
Figure 1.15 Heat flow/sec vs. time data for ITC Runs 1. Deionized water titrated deionized water, 2. Deionized water titrated 0.1% Tergitol, 3. 2% Tween 80 titrated deionized water, 4. 2% Tween 80 titrated 0.1% Tergitol.....	49
Figure 1.16 Analysis of ITC data based on two site model. ....	50
Figure 1.17. Conceptual model for mixed lamellar micelles formed by Tergitol 15-S-3 and Tween 80 in water. ....	53
Figure 1.19. CLA emulsion comprising Limonene (0.1% Tergitol 15-S-3) and water (0.4% Tween 80) at a PVR of 14 (magnification 400x).....	56
Figure 2.1. Proposed structure for a single colloidal liquid aphron (CLA) when dispersed in a continuous aqueous phase (Redrawn from Sebba (1984)). ....	68
Figure 2.2 Calibration curve for heptanoic acid.....	72

Figure 2.3a: Agreement of experimental data with the linear trend predicted by Eqn. 3. (stirred cell at 60 rpm).....	78
Figure 2.3b: Agreement of experimental data with the linear trend predicted by Eqn. 3. Run 10 in baffled tank at 427 rpm.....	79
Figure 2.3c. Agreement of experimental data with the linear trend predicted by Eqn. 3. Run 8 in baffled tank at 550 rpm, 0.4% (v/v) Tween 80 in aqueous phase and 0.1% (v/v) Tergitol 15-S-3 in CLA phase.....	80
Figure 2.4. Variation in experimental volumetric mass transfer coefficient ( $K_{L,a}$ ) with $N_{RE}$ measured in a baffled tank.....	83
Figure 2.5. Effect of $N_{RE}$ on experimental $K_L$ values ( $\blacklozenge$ ) measured in a baffled, stirred tank and predicted $K_{L,continuous}$ values ( $\square$ ) calculated using Eqn. 4 (Skelland <i>et al.</i> , 1981).....	86
Figure 2.6 Variation of CLA droplet diameter with Tween 80 concentration in the aqueous phase at Tergitol 15-S-3 concentrations of 0.1% v/v ( $\square$ ) and 0.01% v/v ( $\blacklozenge$ ).....	89
Figure 3.1: Semi log plot of specific reaction rate (R) vs. ionic strength (I) at 550 ( $\square$ ) and 300 ( $\blacklozenge$ ) rpm. ....	112
Figure 3.2. Effect of $N_{RE}$ on $K_L$ values measured in baffled stirred tank at initial alkali concentrations of 0.75M ( $\square$ ) and 0.5M ( $\blacklozenge$ ). The solid line represents the prediction of Equation 9 (Skelland <i>et al.</i> , 1981).....	113
Figure 3.3. Variation of CLA Sauter mean diameter ( $\blacklozenge$ ) and volumetric mass transfer coefficient ( $K_{L,a}$ , $\square$ ) with Tween 80 concentration (% v/v) in the aqueous phase. ....	115

Figure 4.1 Lipase catalysed resolution of D,L-Phenylalanine using hydrolysis of D,L Phenylalanine methyl ester (PAM). .....	126
Figure 4.2. Reaction products of L,D PA with TAGIT .....	131
Figure 4.3. Sample HPLC Chromatogram of the enantiomeric separation of L and D Phenylalanine .....	132
Figure 4.4 Conversion vs. time for chiral resolution experiments with (■) and without ( ) CLA dispersions. Reaction conditions: pH 5, Void fraction 30%, 80 mg crude enzyme, 0.2M Phe-me in decanol.....	138
Figure 4.5 Residuals vs. fitted values for full set of experimental data. (Note: The fitted value for one of the data points (experiment 25) is negative, and the residual is extreme).....	142
Figure 4.6a. Plot of residuals vs. order of data for regression model represented by equation 1. ....	144
Figure 4.6b. Normal Probability plot for residuals based on Equation 1.....	145
Figure 4.6c. Plot of residuals vs. Fitted values for regression model given by Equation 1.....	146
Figure 4.7. Contour plot for $Y_c$ for P and V ranging from -1 to 1, using Equation 1. ....	150
Figure 4.8. Plot of conversion vs. void fraction at varying initial concentrations of Phe-Me in the decanol phase .....	151
Figure 4.9 Plot of residuals vs. order of data for $Y_{ee}$ . ....	154
Figure 4.10 Contour plots for $Y_{ee}$ , for P and V ranging from -1 to 1, based on equation 2. ....	155

Figure 5.1. Biotransformation of Cinnemaldehyde by Baker's yeast. ....	165
Figure 5.2. Structure of L- amiacetose .....	167
Figure 5.3. Compounds synthesised from (4) .....	168
Figure 5.4. Typical NMR spectrum of biotransformation products .....	173
Figure 5.6. Effect of CLA volume on % diol in product.....	177
Figure 5.7. Change in product composition with initial concentration of cimmemaldehyde.....	179
Figure 5.8. Effect of time on product composition. Plotted are data at different initial substrate (1) concentrations .....	180
Figure 5.9. Effect of hydrophobic resins on product composition.....	183
Figure 6.1 Complex formation in MAA-MPEGMA copolymers (redrawn from Mathur (1998)). .....	188
Figure 6.2. Titration curves for block copolymeric emulsifiers.....	194
Figure 6.3 Percentage recovery of organic phase vs. pH for reversible emulsions, formed using different polymeric emulsifiers, and CLA emulsions. ....	195

## List of Tables

Table 1. Literature review of CLA in chronological order, upto 2000.....	1
Table 2.1. Summary of conditions for mass-transfer experiments. ....	76
Table 2.2. Effect of $N_{RE}$ on $K_L$ , $K_{L,continuous}$ , and $K_{L,shell}$ . ....	87
Table 2.3. Effect of surfactant concentrations on $K_L$ and $K_L a$ .....	90
Table 3.1. Physicochemical data for p-tolyl acetate-water system.....	110
Table 3.2. Variation of interfacial area ( $a$ ), overall mass-transfer coefficient ( $K_L$ ), and volumetric mass-transfer coefficient ( $K_L a$ ) with Tween 80 concentration in aqueous phase. ....	116
Table 4.1. Buffer recipes for chiral resolution experiments .....	126
Table 4.2. Central Composite Design (coded variables are defined as shown in Table 4.3).....	135
Table 4.3 Coding of variables for Central Composite Design.....	136
Table 4.4 % Enzyme immobilized using different nonionic and .....	136
emulsifiers to form CLA emulsions at pH 5. ....	136
Table 4.5 Effect of pH on % enzyme immobilized on CLA emulsions formed using Tween 80.....	137
Table 4.6. Experimental data for chiral resolution experiments.....	139
Table 4.7 Regression analysis for data presented in Table 4.6 .....	141
Table 4.8. Regression analysis results for model represented by Equation 1...	143
Table 4.9 Regression analysis for the model represented by Equation 2 .....	153

<b>Table 6.1. Size distribution and mass transfer coefficients obtained for reversible emulsions and CLA.....</b>	<b>192</b>
---	------------

# INTRODUCTION

## Challenges in Biocatalysis

Biocatalysis has enormous commercial potential. Enzymes or whole cells can convert chemical precursors into a wide variety of product classes, including pharmaceuticals (steroids, isoflavonoids, taxol), fragrance and flavor compounds (lactones, pyrazines, essential oils), fuels (ethanol, butanol, biodiesel), as well as a broad range of miscellaneous oils, fatty acids, and terpenoids. Most biocatalysts are amazingly specific, and it is this ability to carry out a reaction on a single substrate or, conversely, to utilize multiple substrates to produce a single product or product family, that gives them wide applicability. An important limitation to the use of conventional biological processes arises from the observation that many of the feedstocks and/or resulting products have only limited or negligible water solubility. Biocatalysts, such as microorganisms (which may be considered as complex, multifunctional, enzyme systems) or isolated enzymes, are designed by nature to be effective in an aqueous medium, which would suggest that they are poorly suited for use in an application that requires them to function in a non aqueous environment. The ability to use biocatalysts in non-natural environments, such as non-aqueous media, would facilitate the application of bioprocesses in a wide range of operations. Development of efficient biocatalytic processes involving nonpolar reactants or products having low aqueous solubility is challenging (Mattiasson, *et al.* 1991). In such cases, a multiphase approach can be effective, in which the continuous aqueous phase contains the biocatalyst, and the dispersed phase serves as a reservoir for the

reactant or product. The dispersed phase may transfer a reactant to the aqueous phase to replenish what is consumed by reaction. Alternatively, the dispersed phase may extract an inhibitory or labile product from the aqueous phase as it is formed (Larsson, et al. 1989). Most multiphase contacting processes are mass transfer limited, and high surface area approaches (emulsions) are most effective in overcoming mass transport resistances (Scott et al., 1995).

### **Mass transfer limitations in biocatalytic processes**

An ideal whole-cell biocatalytic process would involve a substrate that would conform to all the conditions listed in Figure 1.

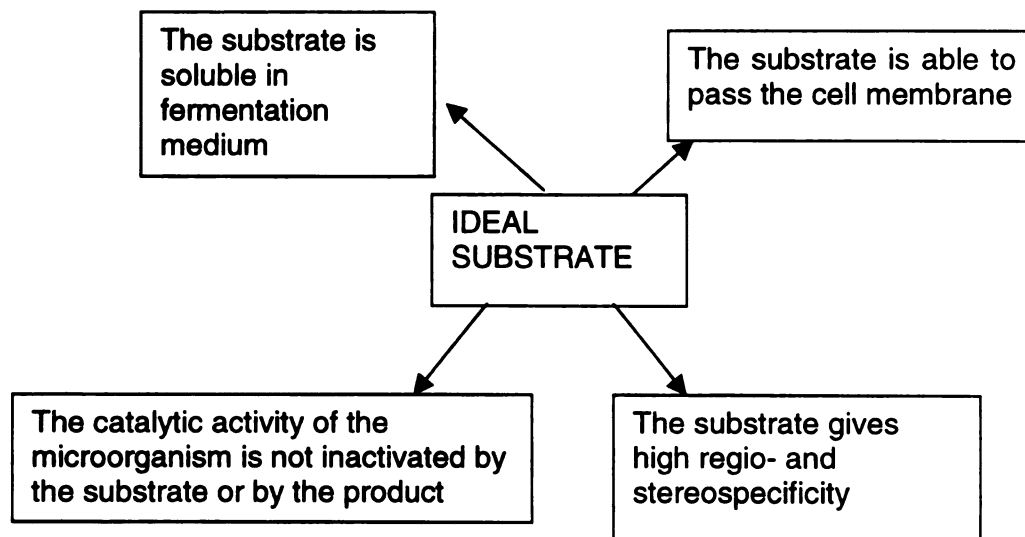


Figure 1. Ideal substrate (Modified from Csuk, R et al., 1991).

However, ideal interactions between the substrate and the microorganism are scarcely found in practice. Some of the techniques used to overcome the limitations of real substrates are shown in Figure 2. The techniques highlighted involve mass transfer from one phase to another. In most aqueous organic two-phase systems, mass transfer limitations and rapid inactivation of cells are often perceived to be the main drawbacks (Van Sonsbeek et al., 1993).

Scott et al. (1995) have identified at least four types of reaction systems containing a water immiscible organic liquid (Figure 3). Three of these utilize a dispersion of either the organic or aqueous phase in an aqueous or organic phase, respectively, with the biocatalyst being in the aqueous phase, but with interfacial contact with the organic phase. However, there has been only limited work on the investigation of the potential multiphase bioreactor systems and operating parameters. A fundamental understanding of interfacial contact and transport mechanisms, and the effects of system parameters on intrinsic biocatalytic kinetics, is needed so that an optimum configuration for such reactor systems can be developed (Lily et. al., 1985). This research is aimed at understanding the fundamental aspects of interfacial stabilization to minimize transport limitations that occur in multiphase catalytic systems and enhance the productivity and selectivity of biocatalytic processes.

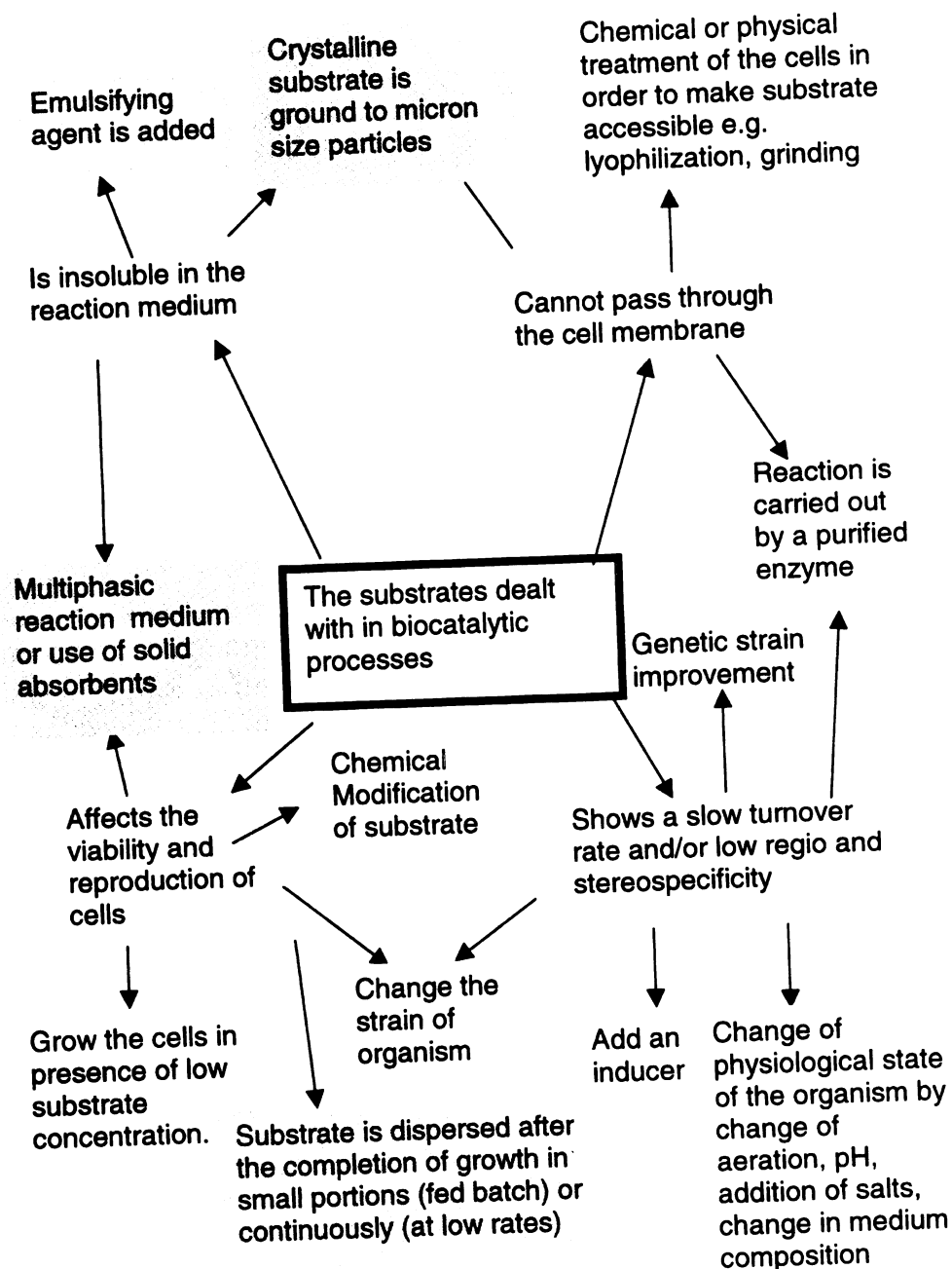
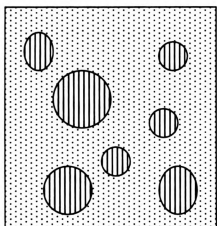
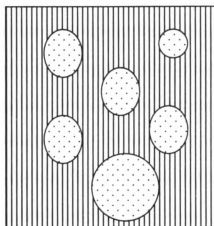


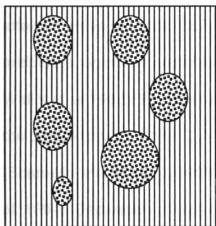
Figure 2. Limitations of common biocatalytic substrates and strategies to overcome those limitations (Redrawn from Van Sonsbeek et al. 1993)



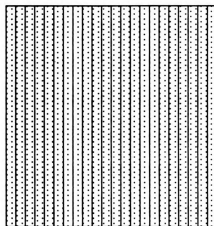
Organic dispersed in aqueous  
with aqueous soluble Biocatalyst



Aqueous with soluble biocatalyst  
dispersed in organic



Aqueous with insoluble biocatalyst  
dispersed in organic



Organic with solubilized or particulate  
biocatalyst

Figure 3. Possible biocatalytic systems involving an organic liquid (Scott et al. 1995.)

## **Colloidal Liquid Aphrons**

Colloidal Liquid Aphrons (CLA) are micron sized spherical droplets of organic solvent (1-50 microns in diameter), each encapsulated in a surfactant shell. Sebba (1972) proposed that the CLA are stabilized by a mixture of surfactants: one in the aqueous phase and another in the dispersed organic phase. Since Sebba's original reports on biliquid foams (Sebba, 1972) and subsequent description of "minute oil droplets encapsulated in a water film (Sebba, 1979), CLA have been investigated for use in pre-dispersed extraction processes. The small dimensions of CLA provide a very large mass transfer area (typically 10,000-20,000 m<sup>2</sup>/m<sup>3</sup> CLA), and allowing extraction equilibrium to be attained within seconds. CLA have been applied successfully to the separation of antibiotics, epoxides and ethanol (Lye and Stuckey, 1996; Rosjidi et al, 1994, Wallis et. al 1985). Furthermore, the addition of various ion-exchange reagents to the organic phase of the CLA has enabled polar solutes like phenylalanine (Scarpello and Stuckey, 1996), and several metal ions to be extracted (Save et al. 1994). Separation of CLA from dispersions and their reconcentration can be effected by micro-filtration or centrifugation (Lye and Stuckey, 1996; Rosjidi et. al, 1994).

A brief literature review of studies previously undertaken on CLA systems is given in Table 1. Most studies have emphasized the applications of the CLA dispersions, and limited fundamental aspects have been studied. However, understanding the relationship between the structure and the macroscopic properties of CLA is essential to their optimal use.

Table 1 Literature Review of CLA in chronological order, up to 2000

Reference	Oil Phase Surfactant	Water Phase Surfactant	Dispersed Oil Phase	Parameters and Conditions	Applications
Sebba, 1984	Tergitol 15-S-3	NaDBS	Kerosene	Type of cations ( $\text{Ca}^{2+}$ , $\text{Mg}^{2+}$ ), cation concentration, Surfactant concentration, type of surfactant, Area exposed to air	---
Wallis et al. 1985	Tergitol 15-S-3	NaDDBS	Decanol	Flotation time (3, 6, 10 min) Settling time (1-5 min) Contact time (0-30 min)	Recovery of biological products
Sebba, 1987	Tergitol 15-S-3	NaDDBS	Kerosene	---	---
Matsushita et al. 1992	CTMAB DTMAB Softanol Synperonic Atlas G1300 Tergitol	SDS SDBS	Decalin Octane Toluene P-xylene Decanol 1-octanol hexan-1-ol, 1-pentanol, acetates	HLB number (8-16) Oil- phase surfactant concentration (0-5% w/v) oil addition rate (slow, fast) mixing speed (400-600 rpm) CLA flotation, stirring time (0.5-2 min) surfactant type	Pre-Dispersed Solvent Extraction
Stuckey et al. 1993	Softanol 120 Softanol 30 DTMAB	SDS	Decanol	pH (4, 8.4) CLA concentration (0.1, 1.1 g/L)	Pre-dispersed solvent extraction of dilute fermentaion products

Lye et al. 1994	Softanol 120	SDS	Decan-1-ol	pH (4-11), erythromycin concentration (0-0.25 g/L), aqueous phase ionic strength (0.02-1.0 M), phase volume ratio (1:50-1:300)	Pre-Dispersed solvent extraction
Lye et al. 1994	Softanol 30 Softanol 120 Atlas G1300	SDS	Octanol n-butyl acetate	pH (2-12), CLA:Feed Ratio (1:25-1:300), repeated equilibrium stages, ionic strength (10-500 mM)	Removing dilute organics from model waste waters
Rosjidi et al. 1994	Softanol 120	SDS	1-Decanol 2-Decanone	CLA:feed volume ratios (1-4%) Pressure (0.17, 0.33 and 0.65 bar)	Pre-Dispersed solvent extraction
Save et al. 1994	Lauryl Alcohol Ethylene Oxide Condensa- te	Dodecyl Pyridinium Chloride	Kerosene Alamine 336 IN LIX 622	CGA flow rate, Type of LA system (film, dilution water) LA flow rate, LA dilution (0:1-4:1)	Pre-Dispersed solvent extraction
Lye et al. 1996	Softanol 120 Softanol 30	SDS	Decan-1-ol n-decane	Enzyme concentration (1-15 mg/mL) continuous phase pH (5-8), repeated dispersion steps (1-3), substrate concentration (0.2-1.6 mM) solvent type	Enzyme immobilization

Zhang et al. 1996	Tergitol 15-S-3	SDBS HTAB Brij 35 Tween 80	Kerosene	Water-based surfactants, storage time (70, 230 days) SDBS concentration (0.25, 1, 4, 8 g/L)	Pre-dispersed solvent extraction
Zhang et al. 1996	Tergitol-15-S-3	NaDDBS	Kerosene	Flow rate of CGA dispersion (19.5 +/- 2.5 mL/min) Flotation time (1, 5, 10 min) Quality of CGA dispersion (0.34 to 0.67)	Pre-dispersed solvent extraction
Lye, et al. 1998	Softanol 120 Softanol 30	SDS	Decan-1-ol Decane	Ionic strength (0-1 M) cation type (Li, Na, K, Mg, Ca) pH (3-11) temperature (10-60 C) additives (lipase and erythromycin)	Structure and Stability of CLA
Scarpello et al. 1999	Softanol 120	Synperonic A20	1-Octanol Aliquat 336	Ionic strength (0-0.4 M) Aliquat concentration (100-400 g/dm3) SA20 concentration (2.5-10 g/dm3)	Pre-Dispersed Solvent Extraction

Lamb et al. 1999	Softanol 30	SDS DTMAB CTMAB Atlas G1300 Synperonic A20	n-decane	pH (4-10), enzyme concentration (0.5-20 mg/mL) type of enzyme (lysozyme, lipase, trypsin, ribonuclease-A, $\alpha$ -amylase, $\beta$ -galactosidase)	Enzyme immobilization
Lamb et al. 2000	Softanol 30 Softanol 120	SDS Brij 78 Atlas G1300 DTMAD CTMAD AOT80, Synperonic A20 SDS	n-decane hexadecane decene ethyl decanoate decanal 2-decanone Decanol	pH (3-9) aqueous phase ionic strength (0-400 mM) SDS concentration (0.5-5 % w/v) surfactants, solvents, temperature (0-80 C)	Enzyme Immobilization
Lye et al. 2000	Softanol 120	SDS	Decanol	Extraction pH, effect of individual surfactants on erythromycin partitioning	Pre-Dispersed solvent extraction

The principal objectives of this study may be summarized as follows:

- 1) To elucidate the fundamental structure of CLA, including the hypothesized “shell” structure;
- 2) To characterize mass transfer properties for CLA dispersions in agitated vessels for bio-extractive and catalytic processes;
- 3) To demonstrate novel applications of CLA, including enhancement of yields, regioselectivity and enantioselectivity of biocatalytic processes.

## References

Csuk, R , Glanzer B. I., 1991. Bakers Yeast mediated transformations in organic chemistry, *Chem. Rev.*, 91, 49-47.

Lamb, S.B. and Stuckey, D.C., 1999. Enzyme immobilization on colloidal liquid aphrons (CLAs): the influence of protein properties. *Enzyme Microb. Technol.* 24, 541-548

Lamb, S.B. and Stuckey, D.C., 2000. Enzyme immobilization on colloidal liquid aphrons (CLAs): the influence of system parameters on activity. *Enzyme Microb. Technol.* 26, 574-581

Larsson, M., Arasaratnam, V. and Mattiasson, B. 1989. Integration of bioconversion and down-stream processing. Starch hydrolysis in an aqueous two-phase system, *Biotechnol. Bioeng.* 33:758-766.

Lily MD, and Woodley JM, 1985, Biocatalytic reactions involving water-insoluble organic compounds, in Biocatalysis in organic syntheses, ed. by A Tramper, HC Van Der Pas and Linko P, Elsevier, Amsterdam. 179-192.

Lye GJ and Stuckey DC, 1996. Predispersed solvent extraction of microlide antibiotics using colloidal liquid aphrons, in *Proceedings International Solvent Extraction Conference, University of Melbourne, Australia*, ed. by Shallcross DC, Paimin R and Prvcic LM, 1399-1405

Lye, G.J, and Stuckey, D.C., 1994. Extractions of Macrolide Antibiotics Using Colloidal Liquid Aphrons (CLAs) In: D.L. Pyle (ed.), *Separations for Biotechnology III*, SCI Publishing, 280-286

Lye, G.J. and Stuckey, D.C. 1998. Structure and stability of colloidal liquid aphrons. *Coll. Surf. A.: Physiochem. Eng. Asp.* 131, 119-136

Lye, G.J., Pavlou, O.P., Rosjidi, M. and Stuckey, D.C. 1996. Immobilization of *Candida cylindracea* Lipase on Colloidal Liquid Aphrons (CLAs) and Development of a Continuous CLA-Membrane Reactor. *Biotechnol. Bioeng.* 51, 69-78

Lye, G.J., Poutiainen, L.V., Stuckey, D.C. 1994. Removal of dilute organics from industrial waste waters: extraction of 3,4-dichloroaniline using colloidal liquid aphrons. In: *Proceeding 2<sup>nd</sup> International Symposium on Environmental Biotechnology*, IchemE Publishers, 25-27

Matsushita, K., Mollah, A.H., Stuckey, D.C., del Cerro, C., and Bailey, A.I., 1992  
Predispersed solvent extraction of dilute products using colloidal gas aphrons  
and colloidal liquid aphrons: aphron preparation, stability and size. *Coll. Surf.*  
69, 65-72

Mattiasson B. and Olle Holst 1991. Objectives for extractive Bioconversion, in  
*Extractive Bio Conversions*, ed. Bo Mattiasson and Olle Holst, Marcel Dekker,  
New York NY.

Rosjidi M, Stuckey DC and Leak DJ, 1994. Downstream Separation of chiral  
epoxides using colloidal liquid aphrons (CLAs), in *Separations for Biotechnology*,  
Ed by Pyle DL, SCI publishing. London. 280-286.

Rosjidi, M. , Stuckey, E.D. and Leak, D.J., 1994. Downstream Separation of chiral  
epoxides using colloidal liquid aphrons (CLAs), *Separations for Biotechnology* 3,  
440-446

Save SV, Pangarkar VG and Kumar SV, 1994. Liquid-Liquid extraction using  
aphrons, *Separation Technology*, 4: 104-111.

Scarpello JT and Stuckey DC 1996. Extraction of Phenylalanine using colloidal  
liquid aphrons (CLAs) : stability in dispersion and rates of mass transfer, in  
*Proceedings of International Congress on Membranes and membrane  
processes*, Yokohama, Japan. 988-989.

Scarpello, J.T. and Stuckey, D.C. ,1999,. The influence of system parameters on  
the stability of colloidal liquid aphrons. *Chem. Technol. Biotechnol.* 74, 409-416

Scott, C.D., T.C. Scott, H.W. Blanch, A.M. Klibanov, and A.J. Russell 1995.  
Bioprocessing in Nonaqueous Media: Critical Needs and Opportunities.  
ORNL/TM-12849, U.S. National Technical Information Service, Springfield, VA.

Sebba F, 1972. *J. Colloid Interface Sci.* 40, 468.

Sebba, F. 1987. Predispersed solvent extraction. *Chem. Ind.* 185-187

Sebba, F., 1984. Preparation and properties of polyaphrons (bilibiquid foams),  
*Chem. Ind.*, 367-372

Stuckey, D.C., Matsushita, K., Mollah, A.H., and Bailey, A.I. 1993. The  
Extractions of Dilute Fermentation Products Using High Internal Phase  
Emulsions (Aphrons). 3<sup>rd</sup> Int. Conf. On Effective Membrane Processes: New  
Perspectives, BHR Group Publications, 3-19

Van Sonsbeek, H.M., Beertink, H.H., Tramper, J., 1993. Two phase liquid –phase  
bioreactors. *Enzyme Microb. Technol.* 15 722-729.

Wallis DA, Michelson DL, Sebba F, Carpenter JK and Houle D, 1985.  
Applications of aphron technology to biological separations., *Biotech. Bioeng.*  
*Symp* 15 : 399-408.

Zhang, C., Valsaraj, K.T., Constant, W.D. and Roy, D. 1996. Studies in Solvent  
Extractions Using Polyaphrons. I. Size Distribution, Stability, and Flotation of  
Polyaphrons. *Sep. Sci. Technol.*, 31, 1059-1074

Zhang, C., Valsaraj, K.T., Constant, W.D. and Roy, D. 1996. Studies in Solvent  
Extractions Using Polyaphrons. II. Semibatch and Continuous Countercurrent  
Extraction/Flotation of a Hydrophobic Organic Dye from Water. *Sep. Sci.*  
*Technol.* 31, 1463-1482.

# Chapter 1

## 1. Interfacial Structure of Colloidal Liquid Aphrons

### 1.1 Introduction

Many industrially important chemical, biochemical, and environmental processes involve a phase-contacting operation intended to transfer a solute between two immiscible liquids. The rate of solute mass transfer is often a rate-limiting factor that limits the overall efficiency of the process. For example, the nitration of aromatic substances like benzene, toluene, phenol, and naphthalene is practiced on large scales for the manufacture of intermediates for dyestuffs, polymers, pharmaceuticals and explosives. Most of these nitrations involve two phases: an organic phase and an aqueous, mixed acid ( $\text{HNO}_3 + \text{H}_2\text{SO}_4$ ) phase. Albright and Hanson (1975) determined that under industrial conditions the rate of nitration is typically controlled by diffusional factors. Similarly, the rates of alkaline hydrolysis of several formate esters and the rates of reduction of substituted nitroaromatics in mechanically agitated, liquid-liquid contactors are dependent on interfacial area per unit volume ( $a$ ), indicating that interphase mass transfer is rate-limiting. Interphase mass transfer is often the rate-limiting step in multiphase biocatalysis, due to the inherent tradeoff between biocompatibility and solute capacity. Biocompatible solvents tend to have low distribution coefficients, and consequently, low mass-transfer driving forces (Roffler, 1986). Increasing the interphase mass-transfer rate would allow a more rapid approach to

equilibrium, thereby optimizing the use of the total solute bearing capacity of the chosen solvent for a given contacting time.

The volumetric, interphase mass-transfer rate ( $R_A$ ) is given by the product of overall, interphase mass-transfer coefficient ( $K_L$ ), the interfacial area per unit volume ( $a$ ) and the concentration driving force ( $C^*-C$ ), where  $C^*$  is the equilibrium solubility of the transferring solute. Although  $K_L$  varies somewhat with the environmental conditions, its range is relatively small. The concentration driving force is also typically small, due to the inherently low aqueous solubilities of nonpolar solutes. Under mass-transfer-limiting conditions, the volumetric solute-transfer rate can be increased by decreasing the size of the dispersed-phase droplets, and thereby increasing " $a$ " (Kafarov *et al.*, 1974; Bhave and Sharma, 1981). Mechanical agitation (e.g. a mixer settler) is commonly used in mass-transfer-limited systems for this purpose. However, this approach is energy-intensive and thus costly, particularly in large-scale systems (Bredwell, *et al.* 1998).

Colloidal liquid aphrons (CLA) are surfactant-stabilized droplets (1-50 microns in diameter) of a nonpolar liquid dispersed in a continuous aqueous phase. The small dimensions of CLA provide very large " $a$ " values (typically 10,000-20,000  $m^2/m^3$ ); consequently solute transfer can often be completed within seconds. A surfactant film surrounding each droplet stabilizes the CLA against coalescence. Surfactants are added to both the aqueous and hydrophobic phases to stabilize the CLA dispersion. An advantage of CLA is that they can be produced at very high phase volume ratios (PVR) which defined as

the volume ratio of dispersed phase to continuous phase; PVR values as high as 20 have been obtained with CLA without phase inversion or coalescence. The CLA emulsions are also very stable; they have been stored in a stoppered bottle for years without visible deterioration.

Due to the large interfacial area offered by CLA emulsions, there have been a number of reported applications in multiphase contacting (Table 1, Introduction). Most studies have emphasized the applied aspects of the CLA emulsions, such as their stability and rates of extraction for various applications, rather than exploring their fundamental properties. However, understanding the relationship between the structure and the macroscopic properties of CLA is essential to their optimal use.

In order to explain the small size and high stability of the CLA dispersion, Sebba<sup>1</sup> postulated that a multi-layered, surfactant-stabilized "shell" surrounds the hydrophobic core. This shell was thought to include an entrapped-water layer, as shown schematically in Figure 1.1. Sebba (1987) originally used fluorescent dyes to probe the structure of polyaphrons and CLA and presented indirect evidence for the existence of a shell, but the structure of the shell has not yet been determined. Researchers investigating CGA and CLA emulsions since 1982 have generally accepted this structure. However, as yet, no studies have provided conclusive evidence of this or indeed any other structure. Lye et al (1998) have investigated the structure of the CLA using cryo TEM, DSC and other light scattering techniques. However, these studies did not

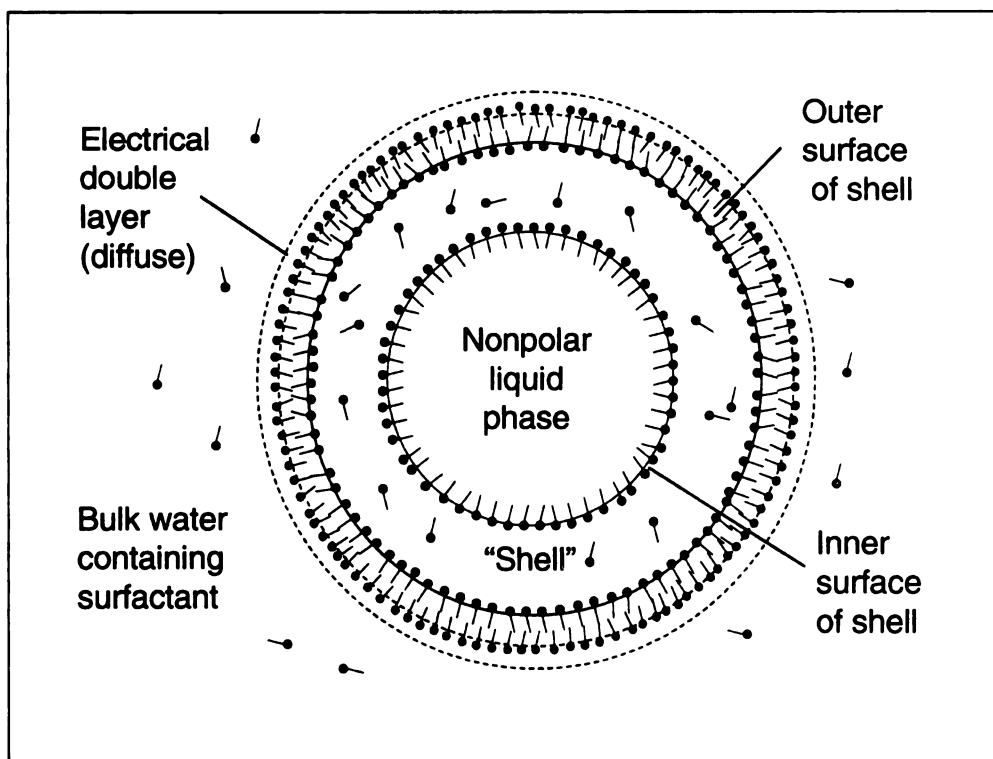


Figure 1.1. Model for CLA droplets (Redrawn from Sebba, 1987)

provide direct evidence for the structure of the surfactant-laden interfaces responsible for the stabilization of CLA.

In spite of a substantial body of literature concerning gas and liquid aphrons, the structure of these systems has often been disputed. It is suggested that CLA and high internal phase emulsions (HIPE) are in fact the same, and the term aphron be dropped to avoid confusion (Princen, 1988). This may well be the case since the macroscopic properties of the two systems are very similar, notably creaming and high stability. However, the literature suggests that there are some significant differences between CLA and HIPE, particularly relating to their formulation. HIPEs generally contain between 10-50% water soluble surfactants (Lissant et al 1974, Mannheimer 1972, Princen 1980, Schwartz and Princen, 1985), whereas CLA emulsions have been generally formulated using 0.1-2 % oil soluble surfactant in oil phase and 0.1-2 % surfactant in the aqueous phase. Lye and Stuckey (1998) emphasized a need for a definitive structural study to rationalize the understanding and nomenclature in this area and the effects of these differences.

The objective of this study was to characterize the structure of the CLA dispersion and identify the factors responsible for CLA formation and stability. A variety of techniques, including DSC, FFTEM, SAXS and ITC, were used to characterize the interfacial properties of CLA emulsions. Surfactant theory was applied to gain a better understanding of the fundamental aspects of CLA formulation and develop a model for micellar stabilization of CLA emulsions.

## **1.2 Preparation of CLA emulsions**

CLA were prepared by dropping the oil phase (0.1% v/v Tergitol (15-S-3) in limonene (Sigma Chemical Co.)) via a burette into a well stirred aqueous solution containing 0.4% v/v Tween 80 (Sigma Chemical Co.), until the desired phase volume ratio ( $PVR = V_{\text{organic}} / V_{\text{aqueous}}$ ) was attained. Comparative conventional emulsions were made using identical techniques except that the oil phase was free of the Tergitol surfactant used in the CLA.

## **1.3 Differential Scanning Calorimetry (DSC)**

### ***1.3.1 Description***

Differential scanning calorimetry (DSC) measures the temperatures and heat flows associated with transitions in materials. These measurements provide quantitative as well as qualitative information about the physical and chemical changes that the sample undergoes. Differential scanning calorimetry (DSC) is widely used to determine the thermophysical and thermochemical properties of unknown mixtures or poorly characterized phases. Examples of thermal transitions are melting, recrystallization, decomposition, out-gassing, or a change in heat capacity; DSC also measures the transition onset and ending temperatures, as well as the temperature at the transition maximum. The calorimeter measures both endothermic (heat absorbed) and exothermic (heat released) processes, or changes in heat capacity.

The DSC uses a two-pan system, where the sample is placed in one pan and the other pan is left empty as a reference (Figure 1.2). Sample size is usually

between 5-10mg of material. The two pans are exposed to the same heat source and the difference between the heat evolution or absorption amongst the two pans is measured. In either case, the objective is to measure the amount of energy absorbed or released from the sample. Samples can be tested from -150°C to 725°C. The resulting energy absorbed or released by the sample is then plotted against the temperature ramp.

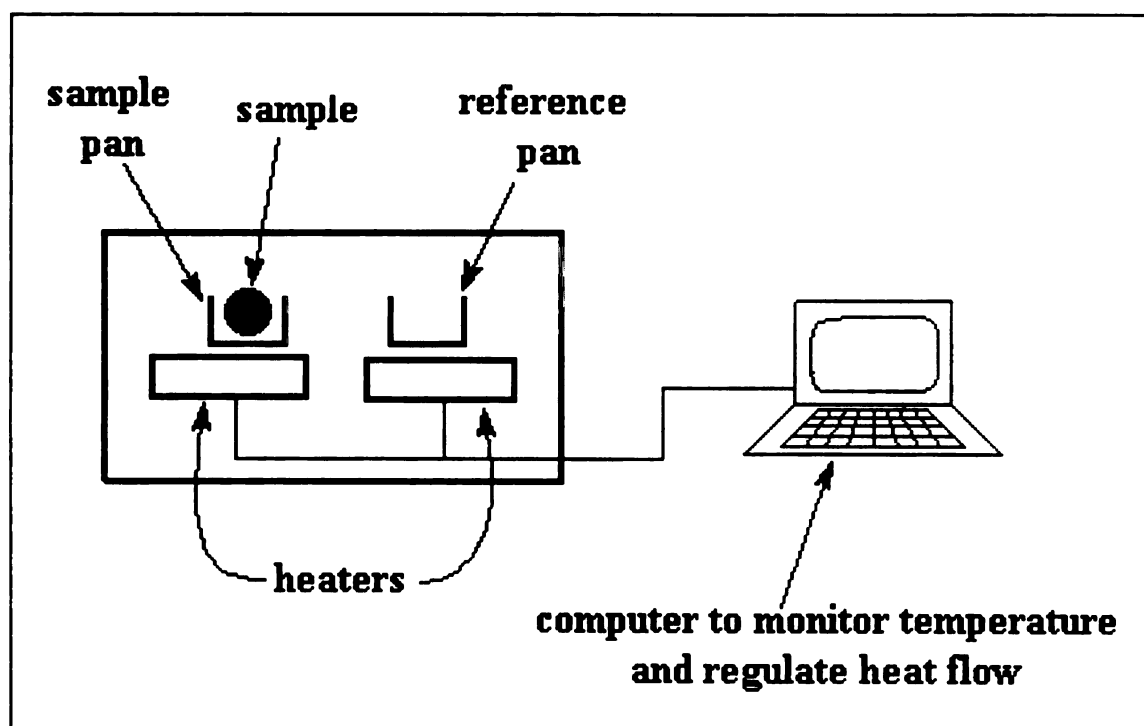


Figure 1.2. Schematic diagram of Differential Scanning Calorimeter (DSC)

### **1.3.2 Materials and Methods**

DSC measurements were carried out using a heat flux Mettler TA 4000 system. A glass disk provided the primary means of transferring heat to the sample and reference positions, while also functioning as one element of the temperature measuring thermoelectric junctions. The CLA sample was placed in an aluminum pan fitted with a lid which could be sealed using a Mettler press. A sealed empty pan was used as a reference. Both the sample and reference pans were placed on the glass disk that was gradually heated, while the temperature was monitored. The melting of the phases in the emulsions was accompanied by an endothermal peak which was automatically recorded. Measurements were carried out between  $-50^{\circ}\text{C}$  and  $30^{\circ}\text{C}$ .

### **1.3.3 Results**

Melting endotherms of CLA emulsions are shown in Figure 1.3 between  $-10^{\circ}\text{C}$  and  $15^{\circ}\text{C}$ . At least two separate phase transitions can be seen in the CLA samples around the melting point of water, indicating the presence of two distinct phases containing water. The colligative properties of the surfactants in water would be expected to lower the melting point of the "shell" phase as is indicated by the freezing point depression of the smaller of the two peaks. The sharp transitions observed during melting indicate the crystalline nature of the phase. Further studies were undertaken using Freeze fracture transmission electron microscopy to visualize the internal structure of this "shell" phase.

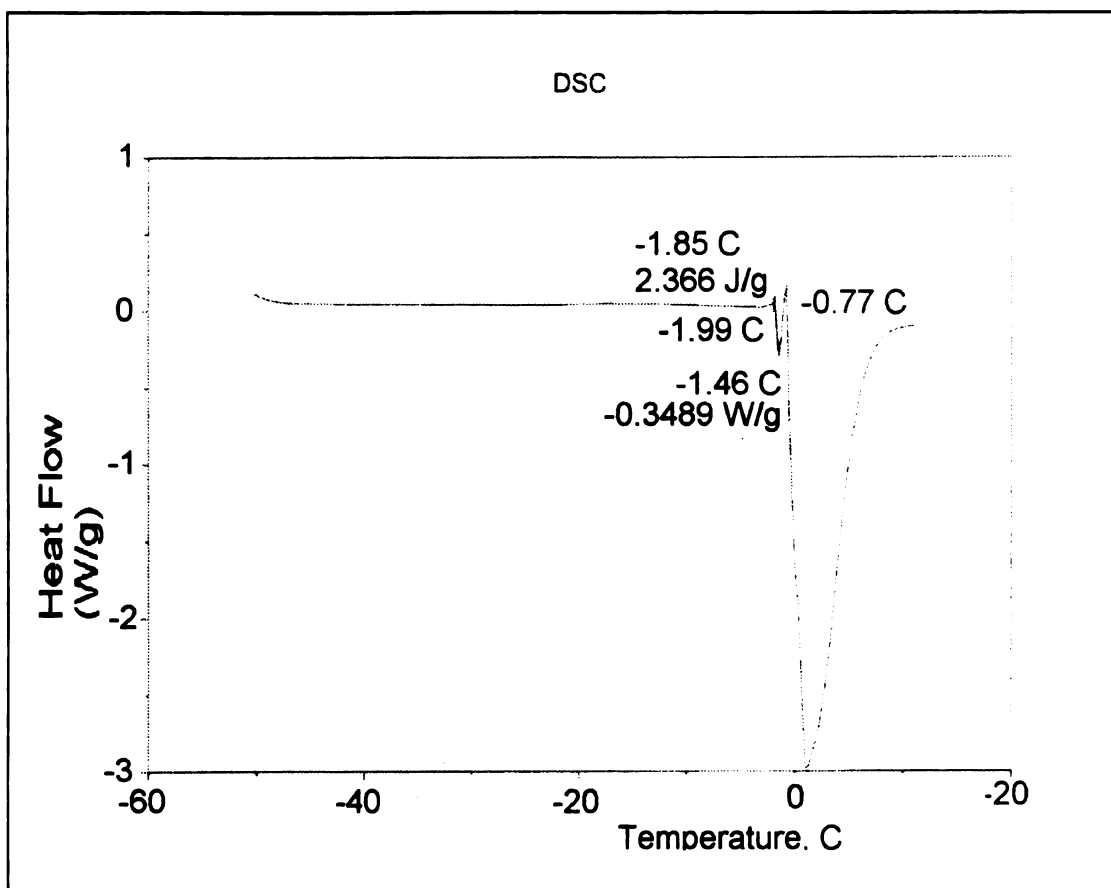


Figure 1.3. DSC endotherm for CLA dispersion containing 0.1% Tergitol 15-S-3 in Limonene and 0.4% Tween 80 in Water (PVR 0.25).

## **1.4 Freeze-Fracture/Freeze Etch Transmission Electron Microscopy**

### **1.4.1 Description**

Detailed studies of the interfacial regions of fine aqueous suspensions require resolution below the approximately 300 nm limit of visible-light optical means. However, electron microscopy must be accomplished in near perfect vacuum conditions that preclude the direct observation of such samples. Conventional TEM sample fixation, used in the life sciences, provides no regimen that would yield relatively artifact free preparations with sufficient electron contrast to study aprotic matrix interfaces (Dawes, 1971). An alternative is to create a high resolution topographical replica of the area of interest. Freeze-fracture and freeze-etch are TEM replica techniques where two-staged replicas are formed on the fractured surface of frozen samples (Rash and Hudson, 1979; Severs and Shotton (1995)). The initial fracture surface, in both cases, follows the path where the fracture strength of the frozen sample is at a minimum. In the case of frozen cells, for example, the fracture path always follows the middle of the unit membranes with integral membrane proteins either pulled from one of the leaflets or snapped by breakage of covalent bonds. In freeze-fracture, the contrasting metal (Pt) is evaporated directly on the freshly fractured surface of the sample, under vacuum. Freeze-etch incorporates a brief period of low-temperature sublimation, again under vacuum, at a temperature sufficient to drive the sublimation but below the rapid re-crystallization temperature of the phases present (Figure 1.4).

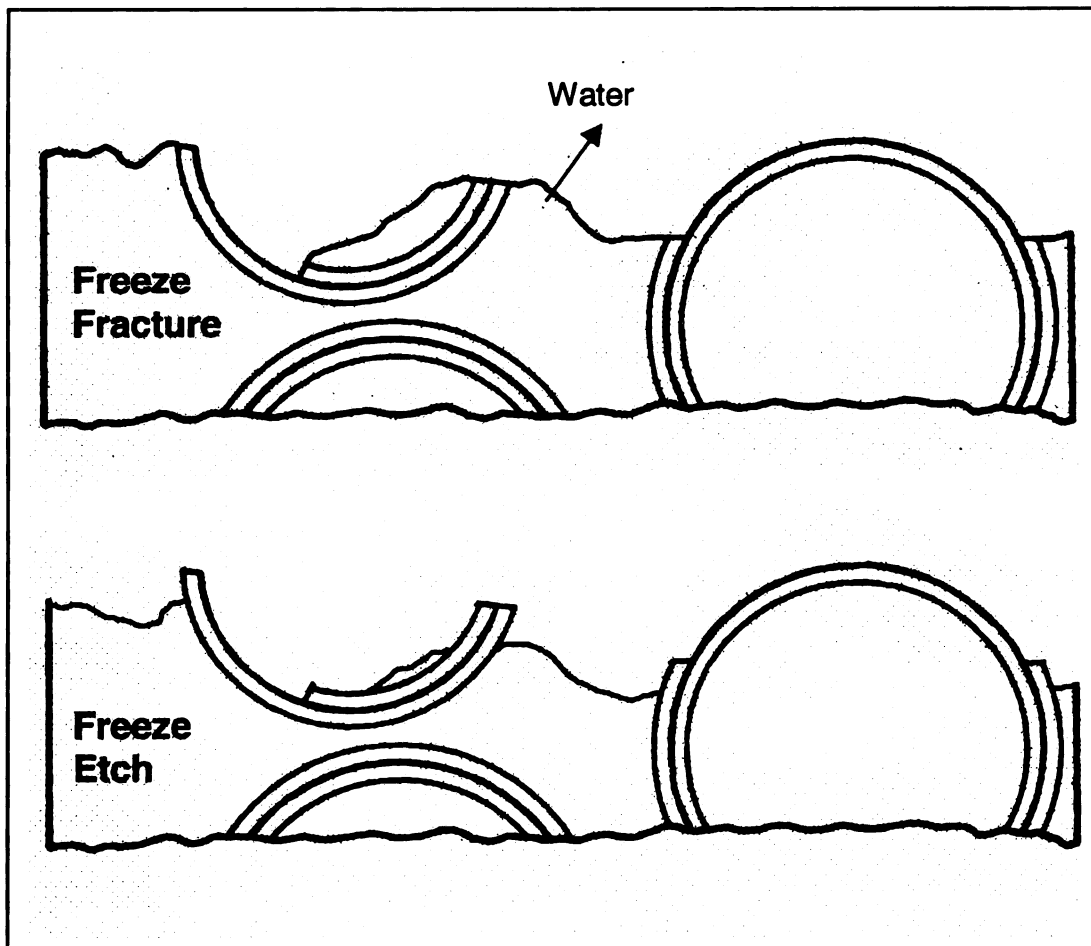


Figure 1.4 Freeze Fracture and Freeze etching of "membraned" cells or emulsions.

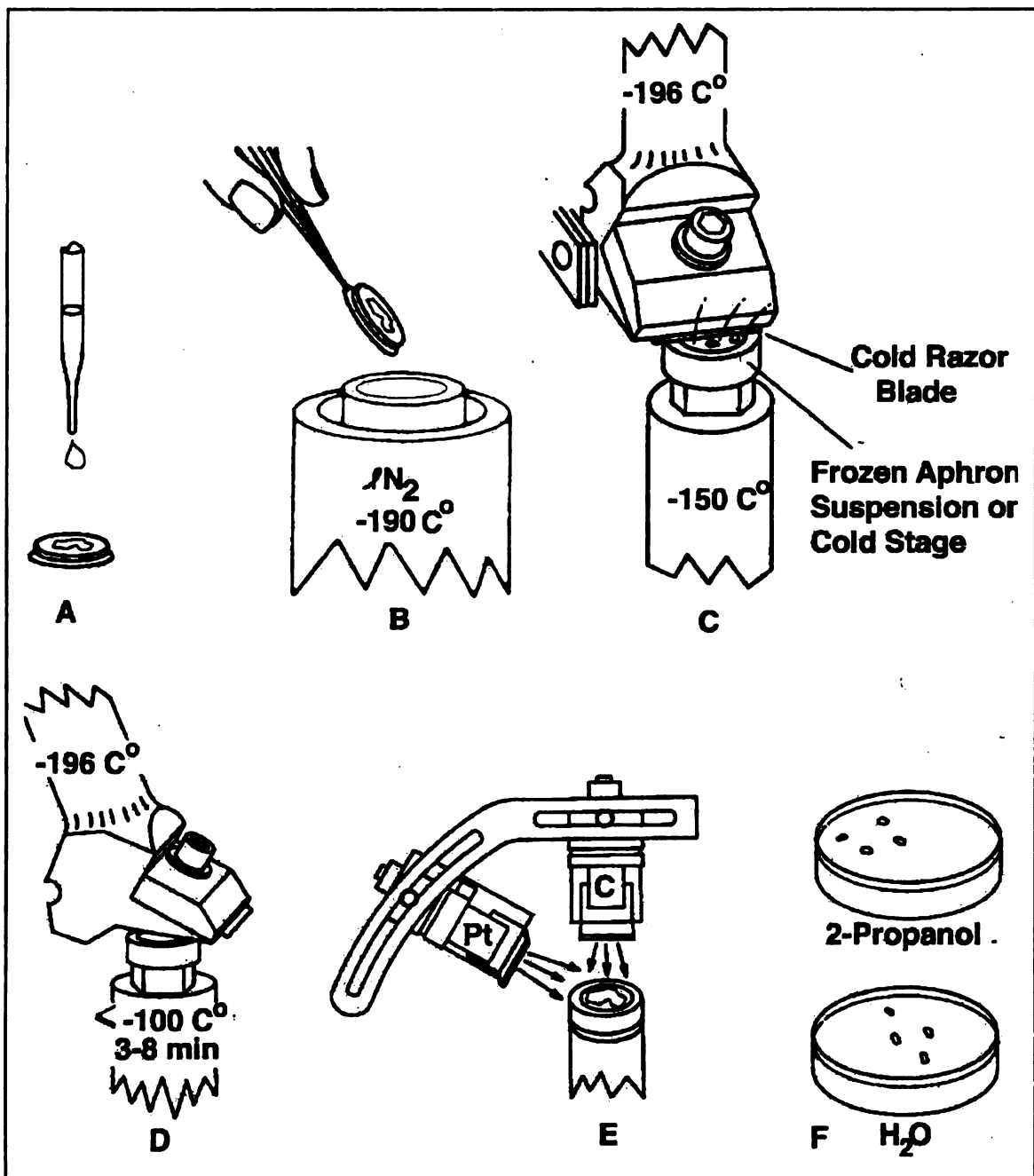


Figure 1.5 Schematic diagram of sample preparation in Freeze Fracture TEM.

In both cases the first coating applied is a discontinuous film of Pt metal with a grain size of about 1 nm. This is applied at an oblique angle to the surface and preferentially accumulates on the evaporator side of topographical features. The contrasting film is immediately stabilized by the deposition of 10 –20 nm of evaporated amorphous carbon.

After completion of the replica, the sample is dissolved away in suitable solvents and the replica cleaned and mounted on an ordinary copper TEM support grid (Figure 1.5). The resulting preparation is viewed in brightfield mode. Generally the image is presented as a negative, giving the impression that the surface is illuminated by the contrasting metal.

#### **1.4.2 Materials and methods**

For this investigation, CLA emulsions with a PVR of 0.25 were used. Aliquots (~30  $\mu\text{L}$ ) of the emulsions were spread on 0.15 mm thick, 10 mm diameter copper supports. These samples were ultra-rapidly frozen by plunging the supports in liquid propane ( $-190^{\circ}\text{C}$ ). For the pure limonene reference sample, the freezing was accomplished by plunging the support into nitrogen slush.

The frozen samples were inserted onto the pre-cooled rotary stage of a freeze-etch unit (modified Balzers BA-510) and fractured by a knife at  $150^{\circ}\text{C}$  with a residual pressure of approx.  $6.5 \times 10^{-5}$  Pa. The replicas were shadowed, with ~2nm of Pt at a  $30^{\circ}$  angle to the plane of the sample followed by 10-15 nm of carbon (at  $\approx 90^{\circ}$  angle) by arc evaporation. Etching was accomplished by raising the stage temperature to  $-100^{\circ}\text{C}$ , positioning the knife holder ( $\approx -196^{\circ}\text{C}$ ) over the

sample surface and allowing it to sublime for 3 min prior to shadowing. Deep etching of the mixed surfactant solution was allowed to progress for 8 min. The resulting replicas were washed in a 10% graded isopropanol series, rinsed in de-ionized H<sub>2</sub>O, and then mounted on 300 mesh grids. TEM was performed on a JEOL 100CX II operated at 120keV with images recorded on Kodak SO 163 film. The negatives were digitized with a Polaroid<sup>®</sup> SprintScan 45 scanner and processed with Adobe<sup>®</sup> PhotoShop. Final prints were made on a dye sublimation printer with the shadows printed dark.

### **1.4.3 Results**

Limonene emulsions and CLAs were morphologically similar at the light microscopy level. Figure 1.6 shows phase-contrast light micrographs of conventional emulsion and CLA dispersions. The overall form the CLA prepared in this study is superficially similar to a conventional emulsion. As seen in Figure 1.6, the droplet sizes averaged about 20  $\mu\text{m}$  in diameter, for both systems, with similar size distributions for each. Sebba (1984) mentions the use of differential staining and uses light microscopy to characterize the outer shell of the CLA; however no comparison with similarly formed conventional emulsions was made. Indeed, the multilamellar CLA interfacial region presented is below the resolution limit of conventional phase contrast light microscopy. In addition, accurate separation of the details of a continuous interface from diffraction artifact at the surface of spherical objects is problematic.

TEM allows resolution of macromolecular dimension; however, the sample must be rendered stable at very low pressure. Typically this is accomplished

either by keeping the specimen at a temperature below which there is no significant vapor pressure in the microscope column, or “fixing” the specimen chemically to allow the removal or conversion of the volatile phases. One of the major concerns in either direct cryogenic observation or the use of frozen samples is the possibility of freezing-rate artifacts. In general, cooling rates on the order of  $10^4$  °C/sec must be achieved to create glass like aqueous phases. However, the addition of solutes to the aqueous phase depresses the freezing point and allows accurate representation of the system at significantly slower cooling rates. The addition of cryoprotectants to freeze-fracture systems has been extensively investigated (*e.g.* Rash and Hudson, 1979).

The emulsion and CLA replicas presented here are relatively free of the typical segregation of components seen with phase separation at low cooling rates (Chiruvolu, *et al.*, 1994). If TEM resolvable ice crystals are formed during the quenching process, a eutectic is formed which gives a characteristic plate-like surface on freeze fracture (Willison and Rowe, 1985). If there are membranes present, the growth of ice crystals beneath them causes the fracture face to have a characteristic roughness (Gilkey and Staehelin, 1986). None of these features were seen in the samples prepared here. Finally, the fracture character of the aqueous phase exhibited the characteristic topography seen in glass fracture (Doremus, 1994).

In order to determine if there were any inherent ordering in either the aqueous (0.4% Tween 80) phase or in the limonene (0.1% Tergitol) phases, we compared the fracture surfaces of these two components separately. In Figure

1.7 the conchoidal fracture of the aqueous phase (Figure 1.7A) is consistent with the fracture of a glass-like material with no long-range order. The fracture characteristics of the organic phase were more planar with less evidence of the curving surface features of the aqueous phase. The limonene phase did exhibit a coarser surface texture, however.

In Figure 1.8, the replicas of the standard emulsion droplets are shown freeze-fractured (Figure 1.8A) and after 3 min of etching (Figure 1.8B). In both cases the interface between the organic phase droplet and its surroundings appear as simple fracture interfaces with no fine structure.

Freeze fracture of CLA emulsion yielded organic phase droplets with a cross fracture habit similar to the conventional emulsion. Both the freeze fractured and freeze etch preparations of the CLA's show a layered interface (Figure 1.9A), a feature clearly not present in the conventional emulsions. These lamella fractured showing varying surface steps approximately 20 to 40 nm high (Figure 1.9B). Etching the CLA fracture surface prior to replication (Figure 1.10A) further accentuated these lamellar steps. At higher magnification (Figure 1.10B), the steps can be seen to have an additional texture approximately parallel to the step faces. These were also spaced about 15-20 nm.

Figure 1.11A illustrates the ordering of the detergents in an aqueous phase, without the presence of the organic phase as can be seen in the FFT (inset) of the deeply etched combined surfactants in Figure 1.11B there is a regular periodic spacing widthwise in this material. Since the vapor pressure of the surfactants is much lower than water, especially at the temperatures used in

freeze fracture, it can be reasonably assumed that the specific dimensions revealed are due to the preferential sublimation of water. When the surface was deep etched (8 min), these areas were seen as elongated ridges spaced approximately 20 nm apart (Figure 1.11B). The average spacing between interfacial layers in the CLA (Figure 1.10B) is difficult to assess due to the problem in calculating the exact angular orientation of the cleavage plane as it varies around the spherical aphron. Planar cross fractures were not observed in the replicas viewed in this investigation. However, based on Figures 1.7 and 1.8, it appears that the lamellae are spaced further apart than is observed based on the measurements of the mixed surfactants alone. Addition of the organic phase is likely to cause a rearrangement in the packing of the surfactants, contributing to a dilation of the interlamellar regions.

The combined results from freeze fracture/TEM of the aphron interface at low PVR indicate the presence of stable multilamellar interfaces in the CLA emulsion. The lamellar liquid crystalline phase, observed in this study, is one of the most common liquid crystalline phases observed in surfactant-water systems. The formation of lamellar liquid crystalline micelles has been observed by various investigators (Dimitrova et al, 1995; He et al, 1993; Lang and Morgan, 1980). Most surfactants, at high concentrations, pack in such a manner as to form lamellar micelles. The hydrocarbon chains are in a dynamic disordered state, which is similar to that of paraffins in liquid state, and the amphiphile bilayers are separated by water layers. Small angle x-ray scattering was used to obtain the periodic spacing amongst these liquid crystals.

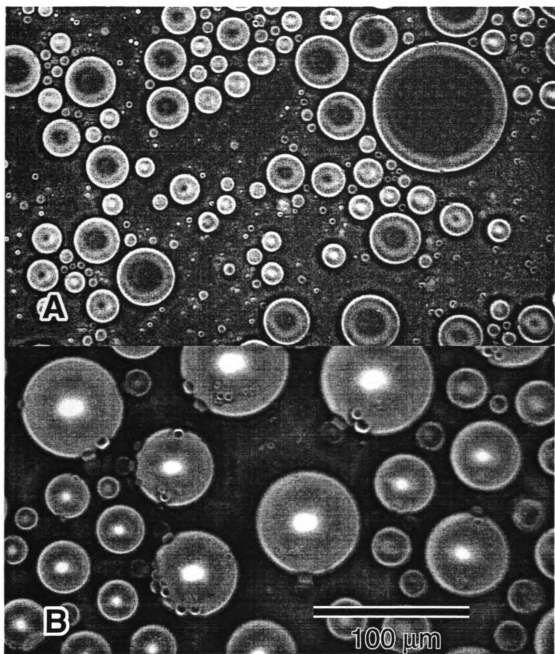


Figure 1.6. Phase contrast micrographs of A. CLA emulsion and B. Conventional emulsions. The average droplet size,  $\approx 20 \mu\text{m}$  was the same for both emulsions.

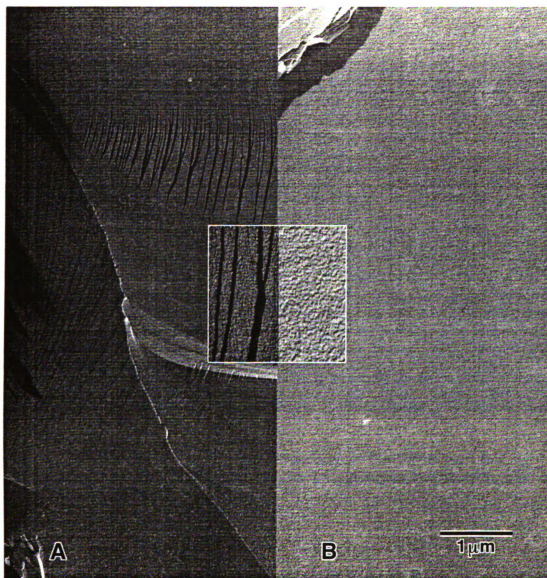


Figure 1.7 Fracture surfaces of separate phases. A. Water and Tween 80 frozen in liquid propane at  $-190^{\circ}\text{C}$ . B. Limonene and Tergitol frozen in a nitrogen slurry at  $\approx -210^{\circ}\text{C}$ .

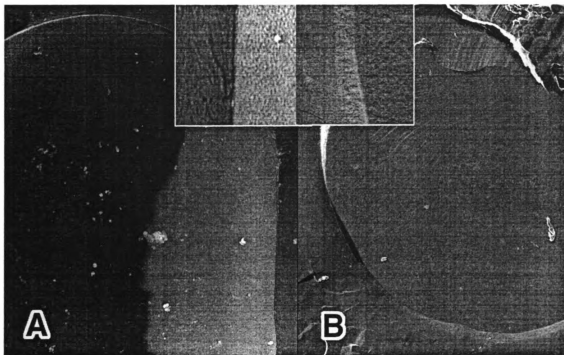
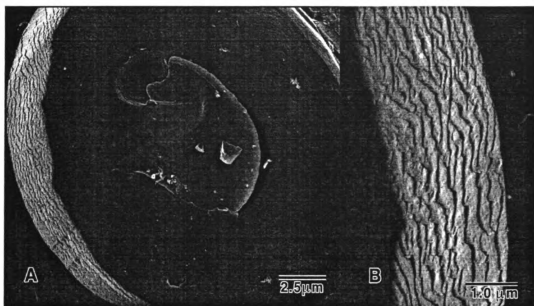


Figure 1.8 Replicas of conventional emulsions. A. Freeze fracture and B. Freeze etch. Inset shows the detail of the droplet matrix interface for each at 5X increased magnification.



**Figure 1.9** A. Freeze fracture of CLA suspension showing the multilamellar phase boundary. B. Enlargement of the boundary showing varying surface steps approximately 20 to 40 nm high.

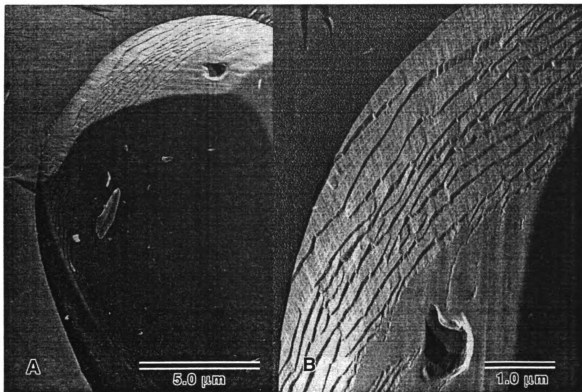


Figure 1.10 A. Freeze etch of a CLA emulsion showing enhanced detail of the phase boundary. B. Enlargement showing the 20 to 40 nm steps and additional ridges running parallel to the step faces.

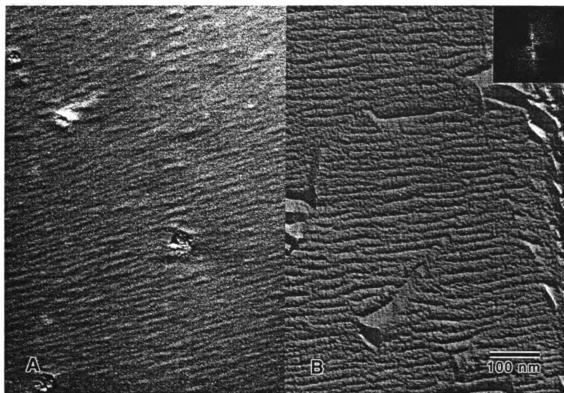


Figure 1.11 A. Freeze fracture surface of a mixture of Tergitol and Tween at the concentrations used to form the CLA. B. The same solution, etched for 8 min prior to shadowing. Inset shows a fourier transform of the etched sample.

## 1.5 Small Angle X ray Scattering

### 1.5.1 Description

Small angle x-ray scattering is a technique for studying structural features of colloidal size. The detailed theory of small angle x-ray scattering can be obtained from Glatter et al. (1982). A brief discussion is presented in this section. Any scattering process is characterized by a reciprocity law, which gives an inverse relationship between particle size and scattering angle.

The general scattering formula is

$$I(\mathbf{h}) = FF^* = \iiint \iiint dV_1 \cdot dV_2 \cdot \rho(r_1) \cdot \rho(r_2) \cdot e^{-i\mathbf{h}(r_1-r_2)} \quad (1)$$

Equation 1 is a Fourier integral, and can be simplified by integrating over all  $r = (r_1-r_2)$  that are equal, then by integrating over all the different  $r$ .

This first step is the mathematical operation of auto-correlation, and is defined by

$$\text{autocorrelation } \overline{\rho^2}(r) = \iiint dV_1 \rho(r_1) \rho(r_2) \quad (2)$$

with  $r=(r_1-r_2)=\text{constant}$ .

The resulting function, well known as the Patterson function, and widely used in crystallography, has the following properties: every electron pair with relative distance  $r$  can be represented by a point in fictitious C-space, say. The density of these points can be represented by  $\rho^2(r)$ . As every pair is counted twice with  $r$  and  $-r$ , it follows that the distribution in the C-space must show a center of symmetry.

The second step consists of integration over C-space

$$I(\mathbf{h}) = \iiint dV \cdot \bar{\rho}^2(\mathbf{r}) \cdot e^{-i\mathbf{h}\mathbf{r}} \quad (3)$$

So the intensity distribution in  $\mathbf{h}$  or reciprocal space is uniquely determined by the structure of the object, as expressed by  $\bar{\rho}^2(\mathbf{r})$ . Conversely, the latter can be drawn from  $I(\mathbf{h})$  by the inverse fourier transform

$$\bar{\rho}^2(\mathbf{r}) = (1/2\pi)^3 \iiint d\mathbf{h}_x d\mathbf{h}_y d\mathbf{h}_z \cdot I(\mathbf{h}) \cdot e^{-i\mathbf{h}\mathbf{r}} \quad (4)$$

One quite general conclusion can be drawn from (3) and (4) : there is a reciprocity between ordinary and reciprocal space. As they are connected by the phase  $\mathbf{h}\mathbf{r}$  only, the result will be the same, when  $r$  is enlarged or  $h$  is diminished by the same factor. So large particles will give a diffraction pattern concentrated at small angles.

Especially with particles of colloidal dimensions, and with a usual wavelength of about 1Å, the pattern is limited to a range of one or two degrees. This is a typical domain of small angle scattering. There are two main restrictions that enable considerable simplification of the theory of small angle scattering

1) The system is statistically isotropic. It makes no difference here whether this is a property of the structure itself or a consequence of some change in time (rotation of particles or the like).

2) There exists no long range order. This means there is no correlation between the points separated widely enough.

From restriction (1) it follows that the distribution of  $\bar{\rho}^2$  in C-space depends only on the magnitude  $r$  of the distance, though this will not hold true for  $\rho(r)$  in

ordinary space. Likewise the phase factor  $e^{-ihr}$  can be replaced by its average taken over all directions of  $r$ . This is expressed by the fundamental formula of Debye:

$$\langle e^{-ihr} \rangle = \frac{\sin hr}{hr} \quad (5)$$

by means of which (3) can be reduced to the form

$$I(h) = \int 4\pi r^2 dr \cdot \bar{\rho}^2(r) \frac{\sin hr}{hr} \quad (6)$$

Diffraction is produced by the interference of waves scattered by an object. In case of X-rays striking an object, every electron becomes a source of a scattered wave. The scattered waves are coherent. Coherence means that all amplitudes are added and the intensity is then given by the absolute square of the resulting amplitude. The amplitudes are of equal magnitude and differ only by their phase  $\phi$ , which depends on the position of the electron in space. It is convenient to represent a single secondary wave by a complex form:  $e^{i\phi}$ . The phase  $\phi$  is  $2\pi/\lambda$  times the difference between the optical path and some arbitrary reference point.

The path length difference of two rays shown in figure 1.10, is

$$AB+BC = 2 d \sin\theta \quad (10)$$

where  $\theta$  is referred to as the glancing angle. For many glancing angles the path length difference is not an integral number and the waves interfere destructively. However, when the path length difference is an integral number of wavelengths, the scattered waves are in phase and interfere constructively. It follows that a

bright reflection should be observed when the glancing angle satisfies the Bragg Law

$$n\lambda = 2d\sin\theta \quad (11)$$

Reflections with  $n=2,3,\dots$  are called second order, third order, and so on they correspond to pathlength differences of  $2,3,\dots$  wavelengths. The primary use of Bragg's law is in the determination of the spacing between layers in the lattice, for once the angle  $\theta$  corresponding to a reflection can be determined,  $d$  may be readily calculated.

The characteristic pattern of X-ray diffraction lines obtained for a liquid crystalline lamellar structure is a series of sharp lines in the relative ratio  $1:1/2:1/3:1/4$ . The first order long spacing corresponds to the net spacing between the two bilayers including the interlayer water phase. The characteristic variable reported for x-ray scattering is known as  $q$  or  $h$ , where  $q = (4\pi/\lambda) \sin\theta$ . where  $2\theta$  is the scattering

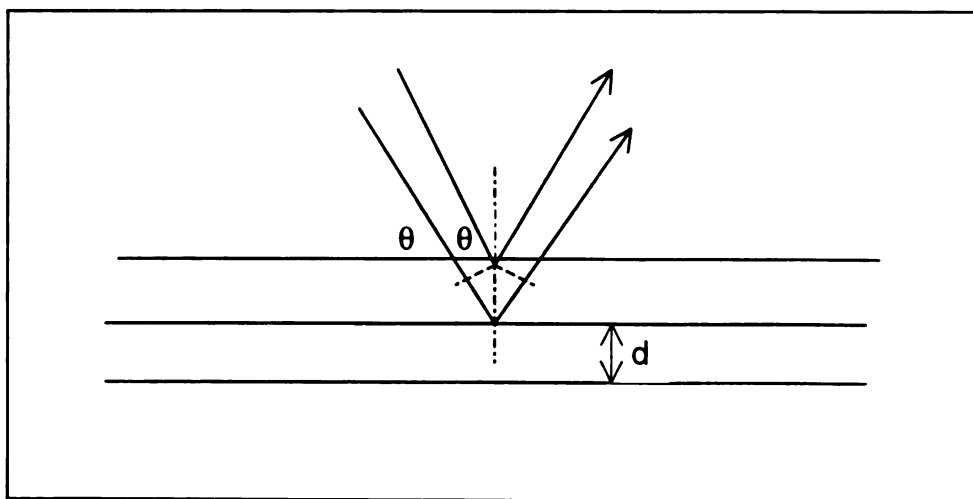


Figure 1.12 X-ray diffraction from lattice planes (Bragg's law)

angle and  $\lambda$  is the wavelength and is related to the characteristic bragg length (d-spacing) as  $d=2\pi/q$ .

### **1.5.2 Materials and Methods**

Surfactant solutions were prepared using MilliQ deionized water. Small angle X ray scattering experiments were performed using a Kratky Camera. The X-ray source was a Rigaku Rotaflex rotating anode with a copper target operating at 7.5-10W. The  $k_{\alpha}$  wavelength of 1.54 Å was selected using Nichol filters. The energy window on the 10 cm OED linear position sensitive detector was set to accept only the scattering signal with energy close to  $K_{\alpha}$ . The input collimators and rectangular holes produced a 2\*0.13mm X-ray spot on the sample, which was sealed in a special glass capillary having a diameter of 1mm. The sample to detector distance was 68.5cm. The accessible range of  $q$  was 0.01-0.4Å<sup>-1</sup>.

The scattering data accumulated over 30-240 minutes was corrected for background scattering by subtracting the scattering intensity of water and the empty capillary.

### **1.5.3 Results**

Small angle X-ray scattering by liquid crystal phases generates scattering peaks in  $I(\theta)$ , where  $I$  is the scattered intensity and  $\theta$  is the scattering angle. The SAXS studies (Figure 1.13) unambiguously identified the lamellar phase spacing in this system as 188 Å. This is in close agreement with the spacing observed in the FFTEM studies discussed earlier. Only a first order peak was observed,

which moved to a higher wavelength (corresponding to a d-spacing of 203 Å) with dilution from (1% to 0.1%v/v Tween 80 in water, keeping the molar ratio of Tween to Tergitol at 1:1) indicating swelling of the lamellar phase. These observations are in agreement with those reported for lamellar phases in dilute water-C<sub>12</sub>E<sub>5</sub> systems (Strey et al., 1990). FFTEM studies indicated that the lamellar phase formed only in the presence of both emulsifiers. Hence, it was necessary to find the stoichiometry and energetics of this interaction, in order to explain the mechanism of formation of the lamellar micelles. These studies were conducted using Isothermal titration calorimetry.

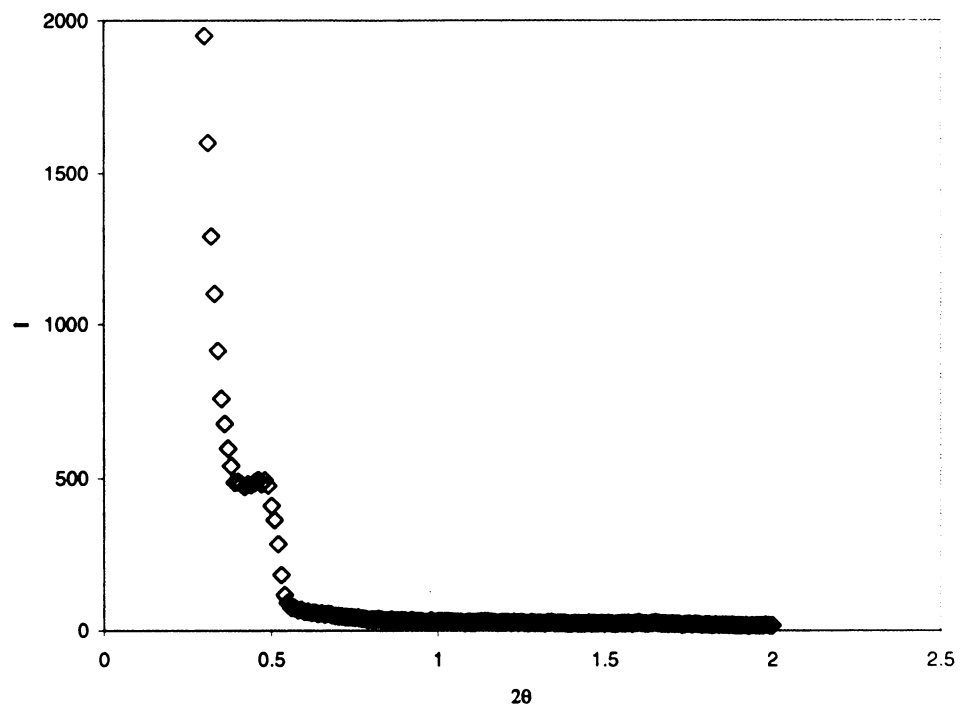


Figure 1.13. SAXS data for 0.1% Tergitol, 0.4% Tween 80 solution in water

## **1.6 Isothermal Titration Calorimetry**

### **1.6.1 Description**

Isothermal titration calorimetry (ITC) is a technique that measures the heat of interaction between two molecules. In ITC, a solution containing a ligand is titrated into a cell containing a solution of the macromolecule. As the two elements interact, heat is released or absorbed in direct proportion to the rate and energetics of binding that occurs. When the macromolecule in the cell becomes saturated with added ligand, the heat signal diminishes until only the background heat of dilution is observed. The area underneath each injection peak (Figure 1.14) is equal to the total heat released for that injection. When this area is plotted against the molar ratio of ligand added to macromolecule in the cell, a complete binding isotherm for the interaction is obtained. ITC is a true in-solution method. It does not require immobilization of binding components as in surface plasmon resonance (SPR), or chemical tagging as with fluorometry.

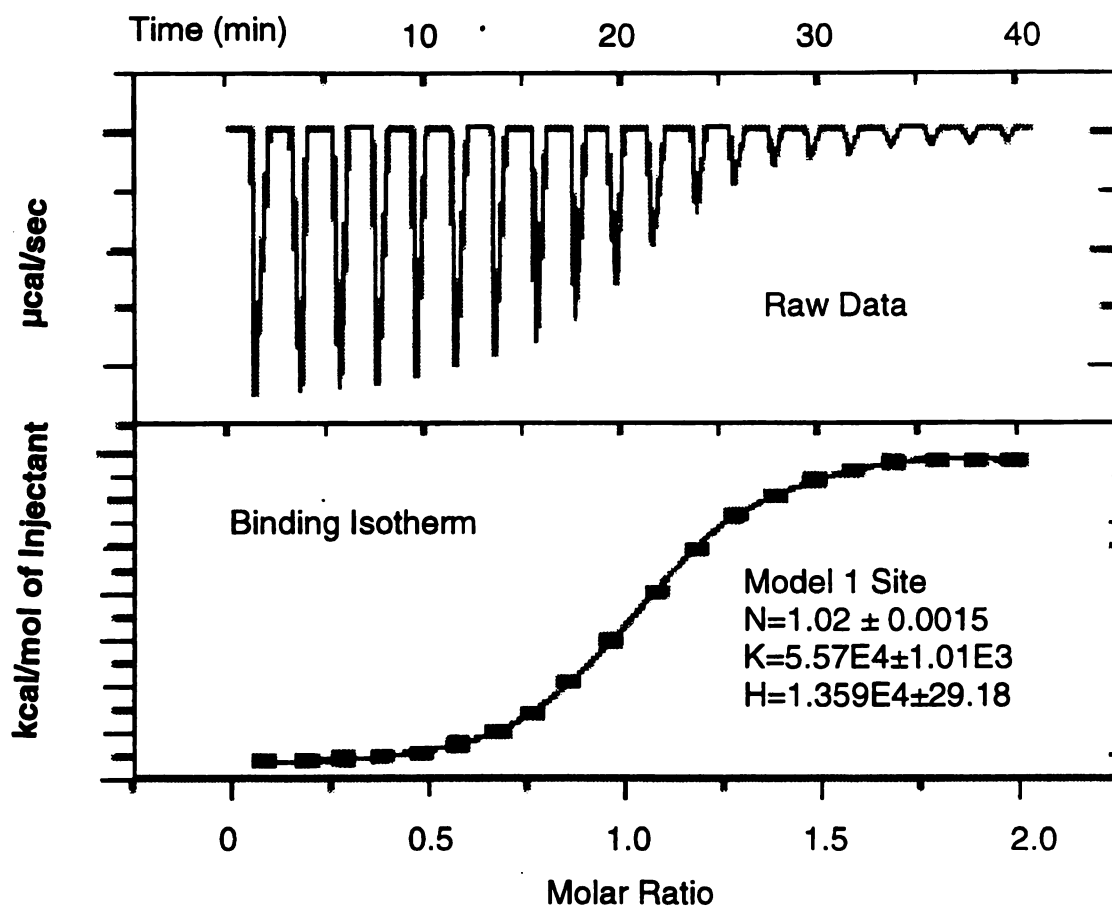


Figure 1.14. Typical ITC experimental data and analysis (MicroCal Inc, MA)

ITC has been extensively used by biochemists to study interactions in biological systems such as: protein–small molecule & enzyme-inhibitor interactions, protein–carbohydrate interactions, protein–protein interactions, protein–lipid interactions, lipid & lipid-small molecule interactions, nucleic acid-small molecule interactions, protein-nucleic acid interactions, nucleic acid-nucleic acid interactions, antibody studies, receptor interactions, and protein folding. Several reviews on the use of ITC for interaction studies have appeared in the literature (Baker et al., 1996; Blandamer et al., 1996, Ladbury, et al, 1996, Wadso, I, 1995, Cooper and Johnson, 1994).

### ***1.6.2 Materials and Methods***

Microcalorimetry experiments were performed on a Microcal, Inc VP-ITC calorimeter. The injection syringe was filled with a concentrated stock solution containing 2% (15.27mM) Tween 80 solution. Sixty injections of 3  $\mu$ L each were made into a 1.38 mL calorimeter cell, which contained 0.1% (3.14mM) Tergitol 15-S-3 solution. The cell was stirred at 400 rpm and was thermally equilibrated at 25°C for 30 min until a smooth baseline was obtained, and injections were initiated. The thermogram was allowed to return to baseline between injections (6 min between injections), and each injection had a 6s duration. In order to correct for heats of micellization/ demicellization due to dilution in the cell, three control runs were conducted. First, deionized water was titrated with deionized water using the procedure described above. Second, deionized water was titrated with 0.1% Tergitol 15-S-3 to correct for heats of demicellization caused by dilution of Tergitol in the cell. Lastly, 2% Tween 80 was titrated into deionized water to

correct for the heats of micellization/demicellization of Tween 80. Before data analysis the data for control runs was subtracted from the data points for the Tween80-Tergitol experiment to correct for the heats of mixing. Peaks were integrated using software from Microcal to yield enthalpy generated for each injection.

### **1.6.3 Results**

Figure 1.15 shows the ITC data for the sample titration along with three control runs (i.e. water titrated with water; water titrated with 0.1% Tergitol solution; and 2% Tween 80 solution titrated with water). Data in Figure 1.10 shows that the heat effects for the sample run are quite large compared to those of the control runs, and can be attributed mostly to the interaction between Tween 80 and Tergitol. The heat effects for the sample run appear to have two kinds of interactions. For the first 15 injections, heat effects are all exothermic and their magnitude decreased quite rapidly. For the next 20 injections, the injection peaks show some endothermic heat besides the exothermic heat. After 40 injections the heat effects seem to level off. Some residual heat effects were still observed and maybe attributed to the heat of mixing and a small pH mismatch between the Tween 80 (pH 6) and Tergitol (pH 6.8) solutions. The integrated data was fit to two sets of independent sites as shown in Figure 1.16. The strong sites have a binding constant of  $\sim 2.3 \times 10^5 \text{ M}^{-1}$  and the weak sites have a binding constant of  $\sim 6.3 \times 10^4 \text{ M}^{-1}$ . The binding heat for the strong site binding is

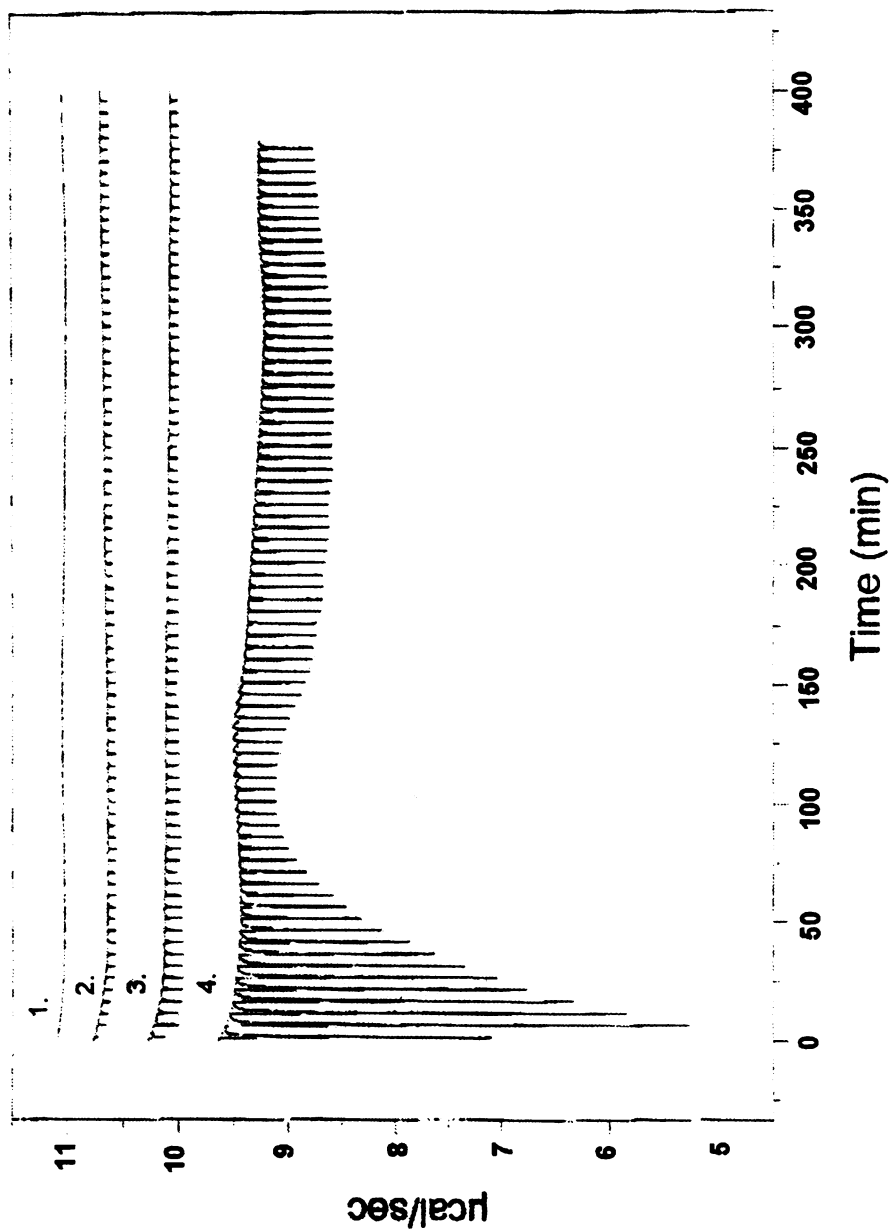


Figure 1.15 Heat flow/sec vs. time data for ITC Runs 1. Deionized water titrated deionized water, 2. Deionized water titrated 0.1% Tergitol, 3. 2% Tween 80 titrated deionized water, 4. 2% Tween 80 titrated 0.1% Tergitol

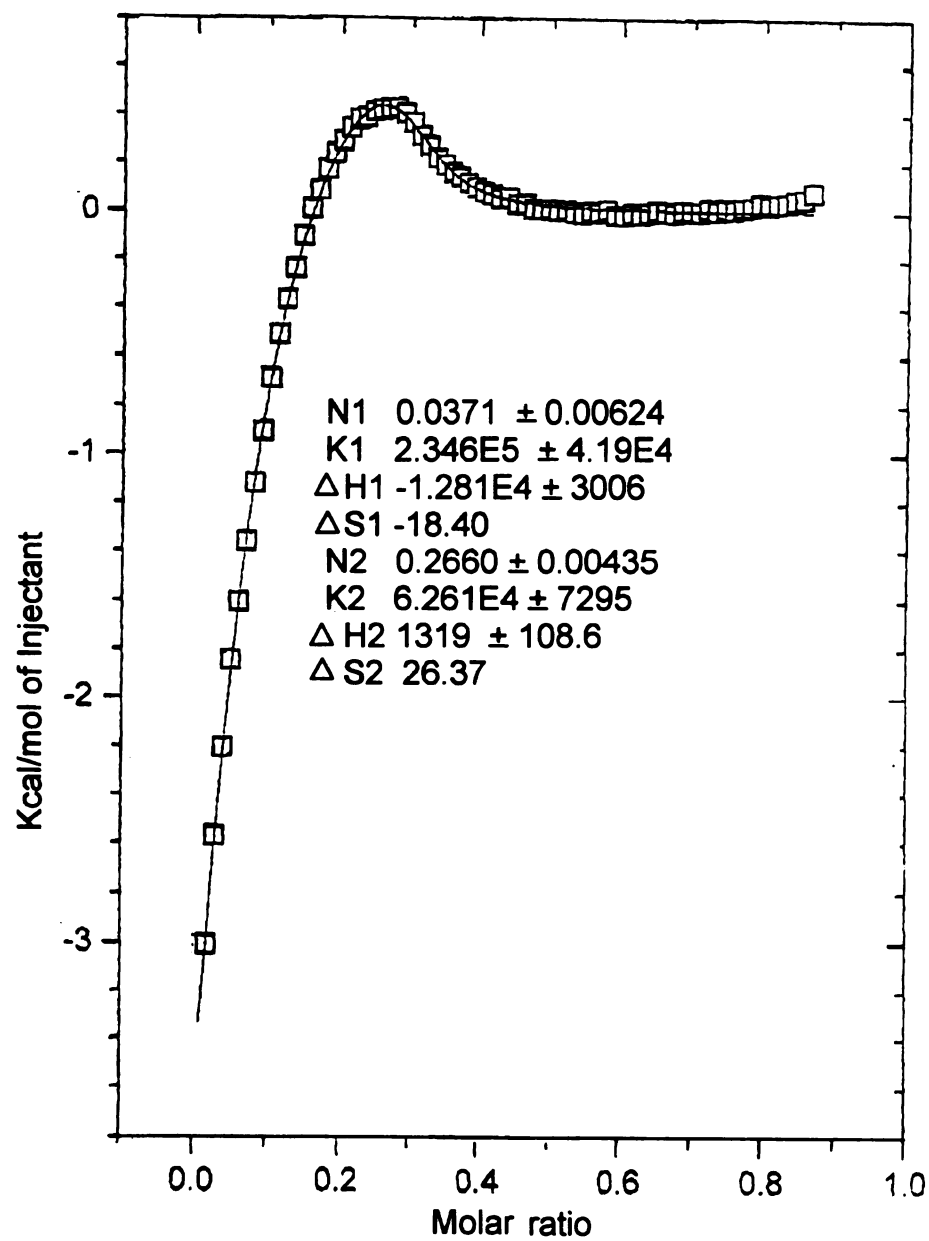


Figure 1.16 Analysis of ITC data based on two site model.

exothermic ( $\sim 12.8$  kcal/mol) while that of the weak site is endothermic (1.32 kcal/mole). The N values for the strong site (0.03) are much smaller than that for the weak site (0.27).

Since Tergitol is initially in colloidal form in water (highly turbid solution) the strong site binding may simply be the penetration of Tween 80 into the colloidal particles and their subsequent destabilization. Later the association of the two surfactants accounts for the weak site binding. The weak site binding is strongly endothermic but the entropy of the system increases considerably (26.37 kcal/ K), indicating the spontaneity and entropy driven nature of the interaction. A high positive change in entropy is expected for this system since the association of the surfactants will result in an increase in the the degree of disorder of the water molecules, surrounding the EO groups in the Tergitol molecule. Since both surfactants have some degrees of polydispersity in molecular weight, the results of this experiment are somewhat qualitative. However, an N value of 0.27 for the weak site indicates the approximate stoichiometry of interaction being approximately 4 molecules of Tergitol per Tween 80 molecule in the system.

### **1.7 Development of a conceptual model for CLA stabilization by lamellar micelles**

Based on these experimental results, a conceptual model was proposed to explain the formation of the lamellar phase observed around the CLA droplets. Lyotropic liquid crystals consist of ordered micelles and are formed by interaction

between micelles (Tiddy, 1980). A number of theories to describe micelle shapes have been published (Israelachvili et al, 1976, Tanford, 1980, Mitchell and Ninham, 1981). These theories involve the balance of repulsive forces between the alkyl chain and water, and those between adjacent head groups within micelles together. They also include surface curvature and steric effects into consideration. These geometric limitations impose restrictions on the allowed shapes of micelles and force some of the amphiphiles to assemble into those shapes, which appear to be thermodynamically unfavorable. The concept of geometry of the emulsifier, developed by Israelachvili et al (1976) was used in this study. According to their concept, the emulsifier is characterized by its volume  $v$ , the length of the hydrocarbon chain  $l$ , and the cross-sectional area of the head group  $a$ . Different values of the ratio  $v/al$  give different surfactant packing possibilities. Lamellar systems are generally found if this ratio lies between  $\frac{1}{2}$  and 1 (Mitchell et al. 1983). For lamellar liquid crystalline phases to occur this ratio has to be  $\sim 1$ . Based on our experimental evidence for these phases and the measurement of the association stoichiometry of 4 Tergitol 15-S-3 molecules per Tween 80 molecule the mixed micellar bilayer structure shown in Figure 1.17 was proposed. The highlighted molecular complex in the lamellar micelle would satisfy the geometric criteria proposed by Israelachvili et al (1976). Such a complex would be held at the interface, since one of its components (Tween 80) is appreciably soluble in water (HLB 14.0) and the other Tergitol 15 –

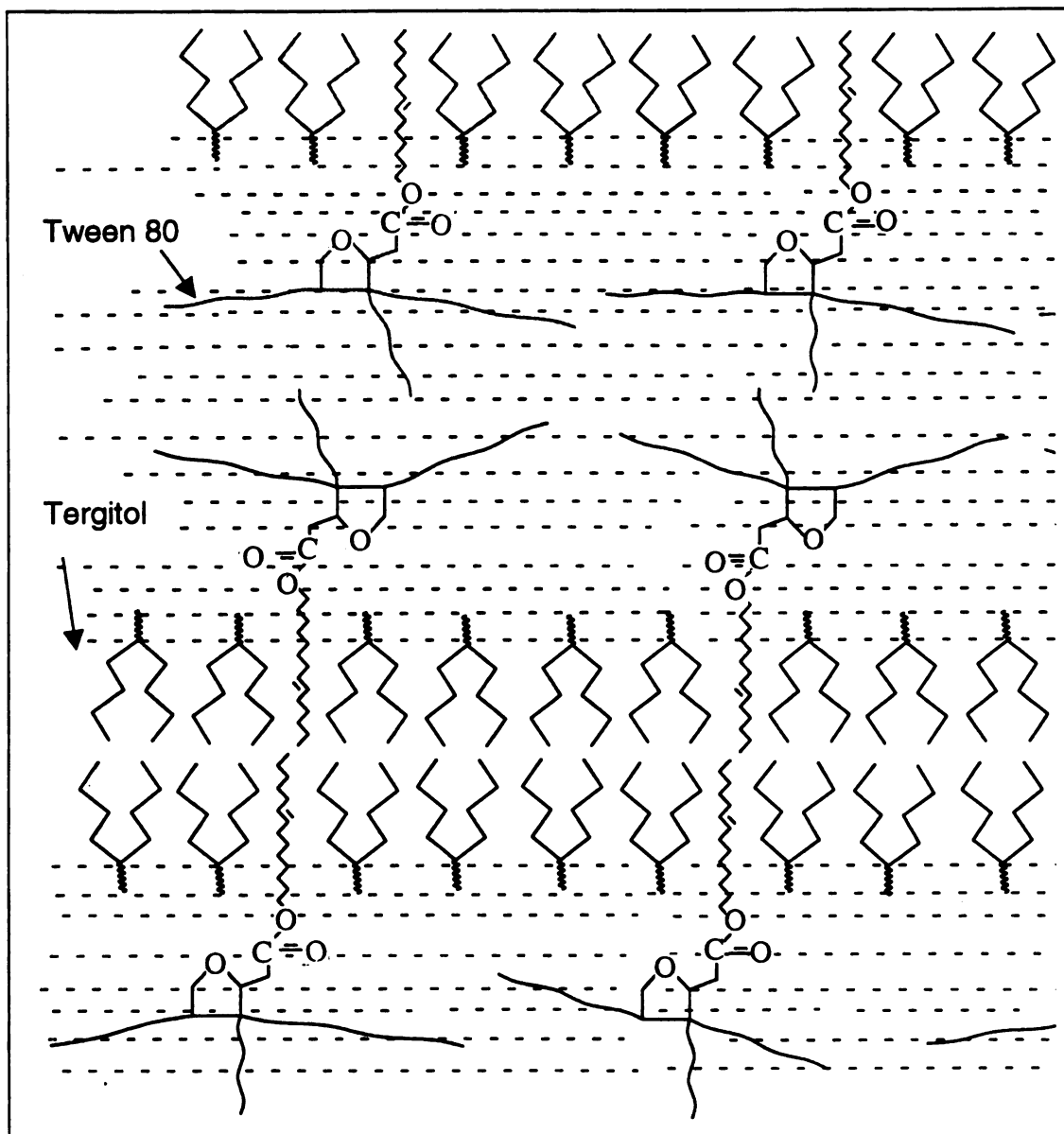


Figure 1.17. Conceptual model for mixed lamellar micelles formed by Tergitol 15-S-3 and Tween 80 in water.

S-3 is appreciably soluble in oil (HLB). Thus, the Tergitol cannot pull the Tween 80 molecules into the oil phase and the Tween 80 cannot pull the oil soluble Tergitol into the water. Each component of the complex holds the other component at the interface so that a very high concentration is obtained at the interface. The positive entropy of formation indicates that the complex is stable when formed, and hence only minute concentrations of each component are required to cover the oil/water interface and stabilize the emulsion. Similar molecular complexes at interfaces have been reported by other investigators, as early as the 1940s. Schulman and Cockbain (1940) hypothesized the presence of such complexes between cetyl sulphate and cholesterol, for stabilization of Nujol-water emulsions.

## **1.8 Explanation of CLA properties**

### ***1.8.1 Ease of formation and small droplet sizes***

Several investigators have reported the formation of CLA emulsions at relatively low shear rates (Sebba et al, 1984, Matsushita et al, 1992). The most important factor that influences the ease of formation of emulsions and their stability is the rate at which the emulsifier is adsorbed on the surface and the interfacial tension of the system. Ford et al. (1966) have reported that the adsorption of relatively hydrophilic emulsifiers usually occurs within a few milliseconds but the more hydrophobic emulsifiers may migrate slowly to the interface. Under these conditions the formation of complete interfacial film may take several minutes. In the case of CLA systems, however, the hydrophobic emulsifier is present in the organic phase, so the distance traveled to the

interface is substantially less than that for travel through the continuous aqueous phase to the interface. The interfacial tension of this system (Limonene/ Tergitol 15-S-3/ Water/ Tween 80) is very small ( $\sim 1\text{mN/m}^2$ , measured using Wilhelmy plate method), so the dispersion of the oil in water involves a small increase in surface energy. Hence the system is readily dispersible, and when the small oil drops are formed, the two emulsifiers interact at the interface forming a rigid interfacial film that prevents coalescence.

### ***1.8.2 High dispersed phase volume ratios***

The rigid interfacial film formed by the two emulsifiers is believed to be responsible for the high phase volume ratios possible using CLA. Sebba (1987) reported a PVR of 20 attainable in kerosene polyaphrons. At high internal phase ratios the CLA dispersion is transformed into a polyhedral foam (Sebba, 1987, Zhang et al., 1996a), where the individual oil polyhedral cells are prevented from coalescence by an interfacial film formed by the molecular complex (Figure 1.18). At high phase volume ratios ( $\text{PVR} > 3$ ), the interfacial properties of the CLA emulsions are similar to those of high internal phase emulsions (HIPE). Both systems consist of polyhedra surrounded by lamellar films that prevent collapse or coalescence of cells. However, since the molecular complex is stable, and because each surfactant holds the other at the interface at high interfacial concentration, the amount of emulsifiers required in CLA emulsions (0.1-1%) has been lower than that traditionally observed by HIPE researchers (5-10%).

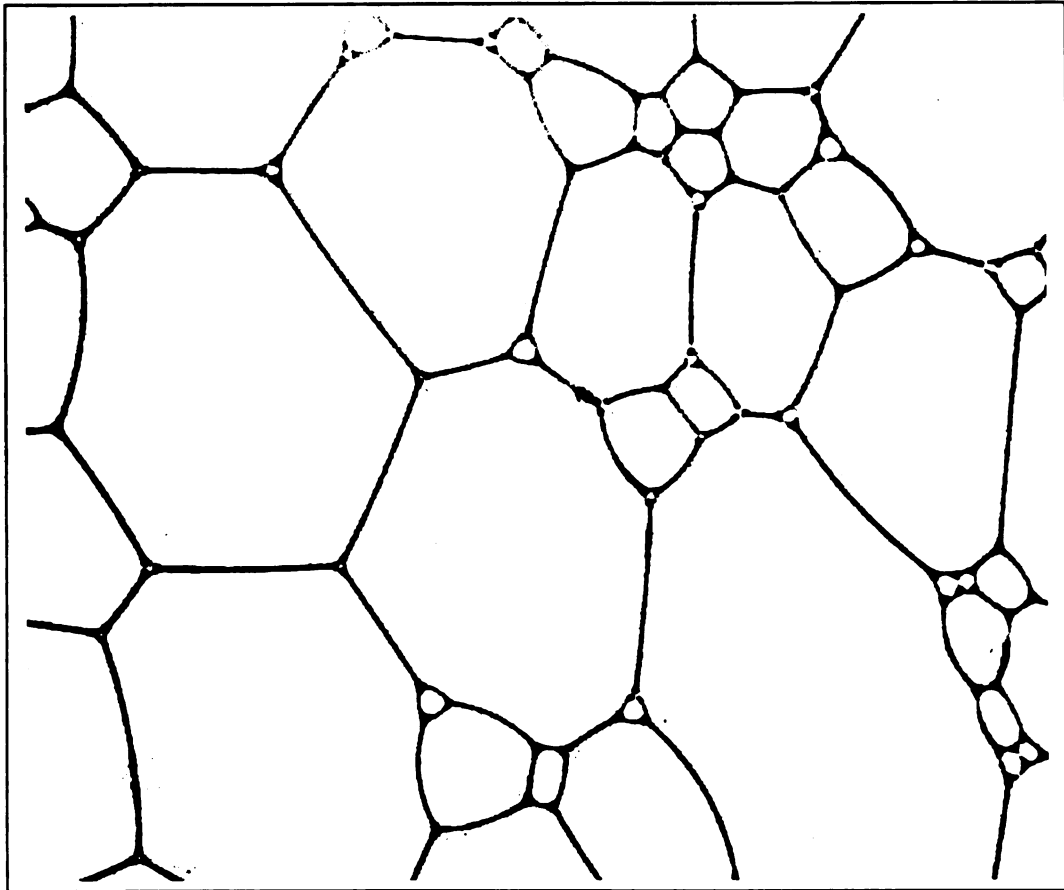


**Figure 1.18. CLA emulsion comprising Limonene (0.1% Tergitol 15-S-3) and water (0.4% Tween 80) at a PVR of 14 (photomicrograph, magnification 400x)**

### **1.8.3 Influence of nature of the dispersed phase on maximum phase volume ratios**

The polarity of the internal dispersed liquid phase also influences the packing of the emulsifiers at the interface as well as the partitioning of the emulsifiers between the bulk and the interface. These factors change the characteristics of the interfacial complex, hence changing the net surface areas that can be stabilized by the complex. Becher (1963) found that the polyoxyethylene head groups of nonionic surfactants interact with polar compounds. As a result the polar head group of the aqueous phase surfactant is no longer completely immersed in water, and a part becomes immersed in the oil phase. Such interactions do not occur with aliphatic hydrocarbons such as decane. The reduced stability of CLA emulsions formed using oils with high aqueous solubility may also be explained in terms of molecular diffusion. Small droplets formed in the emulsification process will dissolve rapidly and the larger droplets will grow at their expense. Matsushita et al (1992) could not form CLA emulsions using butan-1-ol, butan-2-ol or ethyl acetate, all of which have appreciable solubilities in water. For compounds with lower (but not negligible) water solubilities, such as butyl acetate (0.43 wt %, Dean, 1992), or amyl acetate (0.17%, Dean, 1992), maximum PVR obtained in stable systems was limited to 5. In this study, a PVR of 17 was obtained with limonene (13 mg/L; (Toxicology Update, 1995)) and up to a PVR of 32 with isooctane (0.25mg/L; McAuliffe, 1965) as the organic phase.

#### **1.8.4 High stability**

Several papers have reported that CLAs have remained stable for a period of several months or even years (Sebba, 1984; Lye and Stuckey, 1998). The high interfacial dilational viscosity of mixed emulsifier films provides viscous resistance against coalescence from the flocculated state (Kirikou and Sherman, 1979; Adamson and Gast, 1997). The rate of drainage of liquid films between two parallel plates is inversely proportional to the viscosity of the medium between the plates (Reynolds, 1886). This translates into several fold larger drainage times for CLA emulsions after creaming, thus accounting for the observed stability periods. In addition, drainage may be retarded by the Marangoni effect (Adamson and Gast, 1997). In this phenomenon, the flow of the liquid in the film and the flow of the surfactant along the interface are coupled, so that film drainage results in surfactant depletion on the draining film surface. The resulting increase in interfacial tension in the surfactant-depleted portions of the film creates an interfacial tension gradient that opposes the transport of surfactant. Because of the strong coupling between the surfactant and the film liquid, the drainage of the liquid is also retarded by this mechanism. There is evidence in the literature that hydrophilic polyoxyethylene chains (such as those present in Tween 80) may contribute to the stability of emulsions due to the strong interaction with the water in the film (Boyd et al., 1972), thus retarding film drainage.

## **1.9 Conclusions**

The interfacial structure of CLA emulsions has been characterized using DSC, FF-TEM, SAXS and ITC. Differential scanning calorimetry results indicated the presence of a separate phase, apart from the aqueous and organic phases present in the emulsion. Freeze Fracture TEM demonstrated the unique lamellar interface formed in CLA emulsions. The formation of a rigid interfacial film, due to the interaction of the two contrary emulsifiers (Tween 80 and Tergitol 15-S-3) has been shown to be responsible for the stabilization of these emulsions. Isothermal titration calorimetry was used to characterize the energetics and stoichiometry of interaction between Tween 80 and Tergitol 15-S-3. Similarities and differences between properties and formulations of HIPE and CLA emulsions were briefly addressed. A model of lamellar micelles stabilizing the CLA interfaces was proposed based on the geometric theory of surfactant packing. Properties of CLA emulsions observed in the literature were explained based on this model.

## **1.10 References**

- Adamson A.W., and Gast A.P., (1997). *Physical Chemistry of Surfaces*, Sixth ed. John Wiley & Sons, NY
- Albright, L. F., and Hanson C. (1975). *Industrial and Laboratory Nitration* (Am. Chem. Soc. Symp. Ser. No. 22), American Chemical Society, Washington D.C.
- Baker, B. M. and Murphy, P. K., 1996. *Biophysical Journal*, 71, (4), 2049-2055.
- Becher P. 1963. *J Colloid Science*, 18, 665

- Bhave R.R. and Sharma M.M. 1981. Liquid-liquid reactors: operation under refluxing conditions: measurement of effective interfacial area, *Trans ICHME*, 59 161-168.
- Blandamer, M. J., Cullis, P. M. and Engberts, J. B. F. N. 1996. *Pure and Applied Chemistry*, 68,(8),1577-1582.
- Boyd J, Parkinson C and Sherman P, 1972. *J Coll. Interface Sci.*, 41, 359.
- Bredwell M.D., Worden R.M. 1998 Mass-transfer properties of microbubbles. 1. Experimental studies, *Biotech. Prog.* 14: (1) 31-38.
- Cooper, A. and Johnson, C. M. 1994. In *Methods in Molecular Biology*, Vol. 22 (Ed's Jones, C., Mulloy, B., Thomas, A. H.), Humana Press, 109-24.
- Dawes, C.J.,1971. *Biological techniques in electron microscopy*. Barnes & Noble NY. 193.
- Dean JA, 1992. *Lange's Handbook of chemistry*, Fourteenth Edn., McGraw Hill, Inc, NY.
- Dimitrova GT, Th. F. Tadros, and Luckham PF, 1995. Investigations of the phase changes of nonionic surfactants using microscopy, differential scanning calorimetry, and rheology 1. Synperonic A7, a C<sub>13</sub>/C<sub>15</sub> Alcohol with 7 mol of ethylene oxide, *Langmuir* 11, 1101-1111.
- Ford RE and Furnidge CGL. 1966. Studies at phase interfaces: II The stabilization of water in oil emulsions using oil soluble emulsifiers, *J Coll. Interface. Science*, 22, 331-341.
- Glatter O and Kratky O, 1982. *Small angle X-ray scattering*, Academic press, NY.

He M, Hill RM, Lin Z, Scriven LE, and Davis HT, 1993. Phase behaviour and microstructure of polyoxyethylene trisiloxane surfactants in aqueous solution. *J Phys. Chem.* 97, 8820-8834.

Israelachvili JN, DJ Mitchell and BW Ninham. 1976. *J Chem. Soc. Faraday Transactions 2*, 72, 1525

Jauregi Paula and Julie Varley, 1999. Colloidal gas aphrons: Potential applications in biotechnology, *TIBTECH*, 17, 389-394.

Kafarov, V.V.; Reutskii, V. A.; Zhuravleva, T. Yu. (1974), *J. Appl. Chem USSR*, 49(12), 2724.

Kirikou M and Sherman P, The influence of Tween 40/Span 80 ratio on the viscoelastic properties of concentrated oil in water emulsions, *J Coll. Interface. Science*, 71 (1) 51-54.

Ladbury, J. E. and Chowdhry, B. Z. 1996. *Chemistry and Biology*, 3, 10, 791-801

Lang JC and Morgan RD, 1980, Nonionic surfactant mixtures I. Phase equilibria in C<sub>10</sub>E<sub>4</sub>-H<sub>2</sub>O and closed loop coexistence, *J. Chem. Phys.* 73(11) 5849-5861.

Lissant K.J., Peace BW, Wu SH, Mayhan KG, 1974. Structure of high internal phase ratio emulsions, *J. Colloid and Interface Science*, 47 (2) 416-423.

Lye G.J., and Stuckey D.C., 1998. Structure and stability of colloidal liquid aphrons, *Colloids and Surfaces A-physicochemical and engineering aspects* 131: (1-3) 119-136.

Lye G.J., Stuckey D.C. 1994. Extraction of macrolide antibiotics using Colloidal Liquid Aphrons (CLAs), In; D.L. Pyle (ed.), *Separations in Biotechnology*. 3<sup>rd</sup> edition. Royal society of Chemistry Cambridge UK. 280-286.

Lye, G.J., Poutainen, L. V., Stuckey D.C., 1994. Removal of dilute organics from industrial wastewaters: extraction of 3-4 dichloroaniline using colloidal liquid aphrons, In: Proceeding 2<sup>nd</sup> environmental symposium on Environmental Biotechnology, IChemE Publishers, Rugby, UK. 25-27

Mannheimer RJ, 1972. Anomalous rheological characteristics of a High internal phase ratio emulsion, J. Colloid and Interface Science, 40 (3), 370-382.

Matsushita K, A. H. Mollah, D.C. Stuckey, C. Del. Cerro and A.I. Bailey, 1992. Predispersed solvent extraction of dilute products using colloidal gas aphrons and colloidal liquid aphrons: aphron preparation, stability and size, *Colloids Surf.*, 69, 65.

McAuliffe C, 1965. J. Phys. Chem., 70 (4), 1267-1275.

Mitchell DJ and Ninham BW, J Chem. Soc. Faraday Trans. 2, 77, 601, (1981).

Mitchell, D.J.; Tiddy, G.J.T.; Waring L., 1983, J. Chem Soc. Faraday Trans. I , 79, 975.

Princen HM, 1980. J. Colloid and Interface science, 75, 246

Princen HM, 1988. Langmuir, 4, 486.

Rash, J.E. and C.S. Hudson (1979) Freeze fracture: methods, artifacts and interpretations. Raven Press, NY. 204

Reynolds O, 1886. Philosophical Transactions, 177, 157

Roffler, S. 1986. Extraction fermentation-lactic acid and acetone/butanol production, Ph. D. Dissertation, University of California, Berkeley.

Schulman JH and EG Cockbain, 1940. Molecular interactions at oil/water interfaces part I. Molecular complex formation and the stability of oil in water emulsions. *Trans. Faraday. Soc.* 36, 651-661

Schwartz LW, and Princen HM, 1987. *J. Colloid. Interface Science.* 118, 201

Sebba F. 1987 *Foams and biliquid Foams-aphrons.* John Wiley & sons, Inc., New York.

Sebba F., *J. Colloid and Interface Sci.*, 35 (4) (1971) 643.

Severs N.J. and D.M. Shotton (1995). *Rapid freezing, freeze fracture and deep etching.* Wiley-Liss, NY. 372

Strey R, Schomaker R, Roux D, Nallet F, and Olsson U, 1990. Dilute lamellar and L<sub>3</sub> phases in the binary water-C<sub>12</sub>E<sub>5</sub> system. *J.Chem.Soc. Faraday Trans.*, 86(12), 2253-2261.

Tanford, CJ, "The Hydrophobic effect: Formation of micelles and biological membranes", Wiley NY 1980.

Tiddy, G.J.T., *Phys. Rep.*, 57,1, (1980)

Toxicology Update *Journal of Applied Toxicology* 1995.15(6) 495-499.

## Chapter 2

# 2. Enhancement of Mass Transfer Using Colloidal Liquid Aphrons : Measurement of Mass Transfer Coefficients in Liquid-Liquid Extraction

### 2.1 Introduction

Biocatalysis has enormous commercial potential. Enzymes or whole cells can convert chemical precursors into a wide variety of product classes, including pharmaceuticals (steroids, isoflavonoids, taxol), fragrance and flavor compounds (lactones, pyrazines, essential oils), fuels (ethanol, butanol, biodiesel), as well as a broad range of miscellaneous oils, fatty acids, and terpenoids. Development of efficient biocatalytic processes involving nonpolar reactants or products having low aqueous solubility is challenging (Mattiasson, *et al.* 1991). In such cases, a multiphase approach can be effective, in which the continuous aqueous phase contains the biocatalyst, and the dispersed phase serves as a reservoir of the reactant or product. The dispersed phase may transfer a reactant to the aqueous phase to replenish what is consumed by reaction. Alternatively, the dispersed phase may extract an inhibitory or labile product from the aqueous phase as it is formed (Larsson, *et al.* 1989). Such extractive fermentations have been demonstrated for a variety of fermentation products (Roffler, *et al.* 1991; Puziiss, *et al.* 1965; Soucaille, *et al.* 1987).

To date, the commercial potential of multiphase bioprocesses has not been fully realized, because the underlying biological and engineering principles have not been sufficiently developed to allow process development, design and scale-up (Scott *et al.*, 1995). Selection of an appropriate fluid to serve as the dispersed phase is an important engineering consideration. Either nonpolar liquids or a second aqueous phase may be used when the transferred solute is nonvolatile (Roffler, *et al.* 1991; Puziss, *et al.* 1965), and gases may be used for volatile or gaseous solutes (Bredwell, *et al.* 1999). Ideally, the fluid should be biocompatible (i.e., not inhibit the biocatalyst), and it should have a high capacity for the solute.

The tendency of a solute to partition into the dispersed phase is given by its distribution coefficient ( $K_c$ ), which is the ratio of the equilibrium solubility of the solute in the dispersed phase to that in the continuous phase. The larger the  $K_c$  value, the lower the volume of dispersed phase required. Unfortunately, solvents with the highest distribution coefficients are typically not biocompatible (e.g., Roffler, 1986). Biocompatible solvents, on the other hand, tend to have low distribution coefficients, and consequently, low mass-transfer driving forces (Roffler, 1986). The relative position of a solvent in the biocompatibility/solute capacity continuum has been correlated to its distribution coefficient between octanol and water ( $K_{ow}$ ) (Bruce *et al.* 1991).

The inherent tradeoff between biocompatibility and solute capacity results in interphase mass transfer often being the rate-limiting step in multiphase biocatalysis. Kollerup and Daugulis (1985) have developed a mathematical

model to estimate the effect of key process variables on the productivity of an extractive fermentation process to produce ethanol. A key parameter in the model is the effective distribution coefficient ( $K_c'$ ) which is the product of the distribution coefficient and the fractional degree of equilibrium mass transfer ( $\eta$ ) between the two phases. The value of  $\eta$  was reported to be on the order of 0.2 for a typical set of operating conditions (Kollerup, *et al.* 1985), indicating only a 20% approach to equilibrium. Increasing the interphase mass-transfer rate would allow a closer approach to equilibrium. In this case a five-fold increase in extraction efficiency is theoretically possible.

The volumetric, interphase mass-transfer rate ( $R_A$ ) is given by the product of overall, interphase mass-transfer coefficient ( $K_L$ ), the interfacial area per unit volume ( $a$ ) and the concentration driving force ( $C-C^*$ ) where  $C^*$  is the equilibrium solubility of the solute being transferred. Although  $K_L$  varies somewhat with the environmental conditions, its range is relatively small. The concentration driving force is also typically small, due to the inherently low aqueous solubilities of nonpolar solutes. However, the value of  $a$  can be increased by orders of magnitude by decreasing the size of the dispersed droplets or bubbles.

Mechanical agitation (e.g. a mixer settler) is commonly used in mass-transfer-limited systems for this purpose. However, this approach is energy-intensive and thus costly, particularly in large-scale systems (Bredwell, *et al.* 1998). Another approach is to use surfactants to predisperse the nonpolar phase prior to its addition to the aqueous phase. This approach can give droplet sizes on the order of microns or smaller (Bredwell, *et al.* 1998; Lye and Stuckey, 1996).

The utility of CLA in multiphase extraction processes has been demonstrated at the bench scale (Lye and Stuckey, 1996, Rosjidi *et al.* 1994, Wallis, *et al.* 1985, Scarpello and Stuckey, 1996). Sebba proposed that CLA are coated with a surfactant-stabilized “shell” that contains entrapped water, as shown schematically in Figure 2.1. Formation of this shell has been reported to require two contrary surfactants (i.e., one surfactant that partitions primarily into the aqueous phase, and another that partitions primarily into the nonpolar phase). Freeze-fracture transmission electron microscopy and other techniques to provide evidence for a multilamellar shell structure (See Chapter 1). The results suggested that the two contrary emulsifiers form liquid-crystal-like bilayers that stabilize the droplets. This ordering has been shown to be a unique property of the surfactant system used to form the aphrons.

This shell is important from an engineering standpoint, because it may impart significant resistance to mass transfer that could significantly reduce  $K_L$ . However, no fundamental studies of CLA mass transfer have been published to date. Such information would be needed to optimize and scale up multiphase biocatalytic processes involving CLA (Scarpello *et al.*, 1999). This chapter presents  $K_L$  and a data for transfer of heptanoic acid from water into limonene CLA. These data are combined with a literature correlation (Skelland and Lee, 1981) for the mass transfer coefficient of the continuous phase ( $K_{L,continuous}$ ) to estimate a mass transfer coefficient for the shell ( $K_{L,shell}$ ). The effect of the

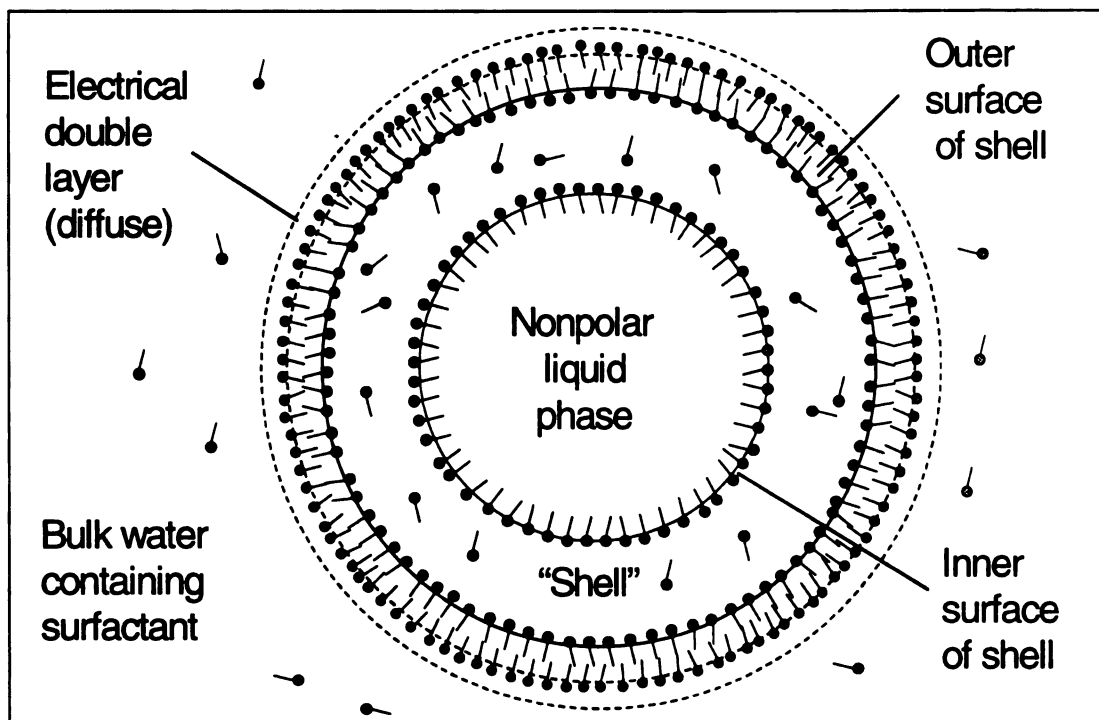


Figure 2.1. Proposed structure for a single colloidal liquid aphron (CLA) when dispersed in a continuous aqueous phase (Redrawn from Sebba (1984)).

concentration of the two surfactants on the mass-transfer properties is also presented.

## **2.2 Materials and Methods**

### **2.2.1 Mass-Transfer System**

#### *2.2.1.1 Surfactants.*

Sebba (1984) reported that two surfactants are required to form CLA--one that partitions primarily into the aqueous phase and another that partitions primarily into the nonpolar phase. Cationic and anionic surfactants form relatively strong ionic bonds with proteins that can cause denaturation. Nonionic surfactants, on the other hand, bind through much weaker hydrophobic interactions and are thus less likely to inactivate enzymes or denature proteins (Schwuber *et al.*, 1980). Bredwell *et al.* (1997) showed that nonionic Tween surfactants were non-inhibitory in batch fermentations, whereas many ionic surfactants were toxic to the cells. Consequently, two nonionic surfactants were chosen for the present study. The aqueous-phase surfactant used in this study was polyoxyethylene sorbitan monooleate (Tween 80, HLB 15.0, Aldrich Chemical Company, Milwaukee, WI ). The nonpolar-phase surfactant was a linear alcohol ethoxylate (Tergitol 15-S-3, HLB 8.3, Sigma Chemical Company, St. Louis, MO). The interfacial structure of the shell, which results from this combination of surfactants, has been described in the previous chapter.

#### *2.2.1.2 Continuous and Dispersed Phases.*

Deionized water (resistivity > 18M $\Omega$ -cm) drawn from a Milli-Q Plus<sup>®</sup> water purification system (Millipore Corporation, Bedford, MA) was used as the

continuous phase. Limonene (CAS 138-86-3, Sigma Chemical Company, 97%) was used as the dispersed phase. Limonene is a naturally occurring terpenoid found in etherial oils derived from lemons, oranges, grapefruit, and caraway. It is an important by-product of the citrus-processing industry and is currently used as a solvent in waterless hand cleaners and degreasing agents. It has extremely low solubility in water (13 mg/L at 25°C) and a log  $K_{ow}$  of 4.232 (Toxicology Update, 1995).

### ***2.2.1.3 Transferred Solute***

To ensure that the controlling mass-transfer resistance is in the continuous phase, it is necessary that the solute's  $K_c$  value be large in favor of the dispersed phase. Heptanoic acid is highly soluble in nonpolar solvents, but its aqueous solubility is only 2.5 g/L at 25°C (Dean, 1992). As a result, it has a high  $K_c$  value for the limonene/water system. Also, because heptanoic acid ionizes in water, its aqueous-phase concentration can be readily measured on-line using a conductivity probe. Heptanoic acid has been used to study interphase mass-transfer in other multiphase systems (Skelland *et al.* 1981).

### ***2.2.2 Measurement of Heptanoic Acid Concentration***

The concentration of heptanoic acid in the aqueous phase was measured by electrical conductivity, as recommended by Rushton *et al.* (1964). A YSI 3417 ( $K=1.0/cm$ ) conductivity probe (YSI Inc, Yellow Springs, OH),  $\frac{1}{2}$  in OD,  $5\frac{3}{4}$  in overall length used with a YSI Model 32 conductance meter at a range switch setting of 200  $ms^{-1}$ . The probe support ring was grounded to the (-) recorder jack to minimize electrical noise in the signal. The output of the conductance meter

was recorded by a CAMILE 2000<sup>®</sup> data acquisition system (Dow Chemical Company, Midland MI) at 1s intervals. The time constant of this probe (<1 msec) was much smaller than that of the interphase mass transfer process, so the mass-transfer dynamics could be measured accurately during the batch runs.

The apparatus was calibrated by measuring the conductivity of standard heptanoic acid solutions in the absence of a dispersed phase. Three sets of calibration solutions were independently prepared and measured. The resulting calibration curve (Figure 2.2) was linear ( $R^2 = 0.9965$ ) with respect to concentration. The conductivity of pure water was measured both in the presence and absence of limonene. At the low limonene volume fractions used, limonene had no effect on the conductivity of the aqueous phase (<1% change in conductivity).

The diffusivity value for heptanoic acid in water ( $6.8 \times 10^{-6}$  cm/s) was calculated using the Wilke-Chang correlation (Wilke *et al.*, 1955). The molal volume of heptanoic acid at its normal boiling point was obtained using Le Bas group contributions method (Reid *et al.*, 1958).

### **2.2.3 CLA Preparation**

The CLA-preparation conditions have been shown to influence the size distribution and stability of the CLA phase (Matsushita *et al.*, 1992). Consequently, the CLA were prepared under consistent conditions in all runs. The CLA emulsions were formed in a 50 mL glass beaker having an internal diameter of 40 mm. Five mL of aqueous Tween 80 solution was added to the

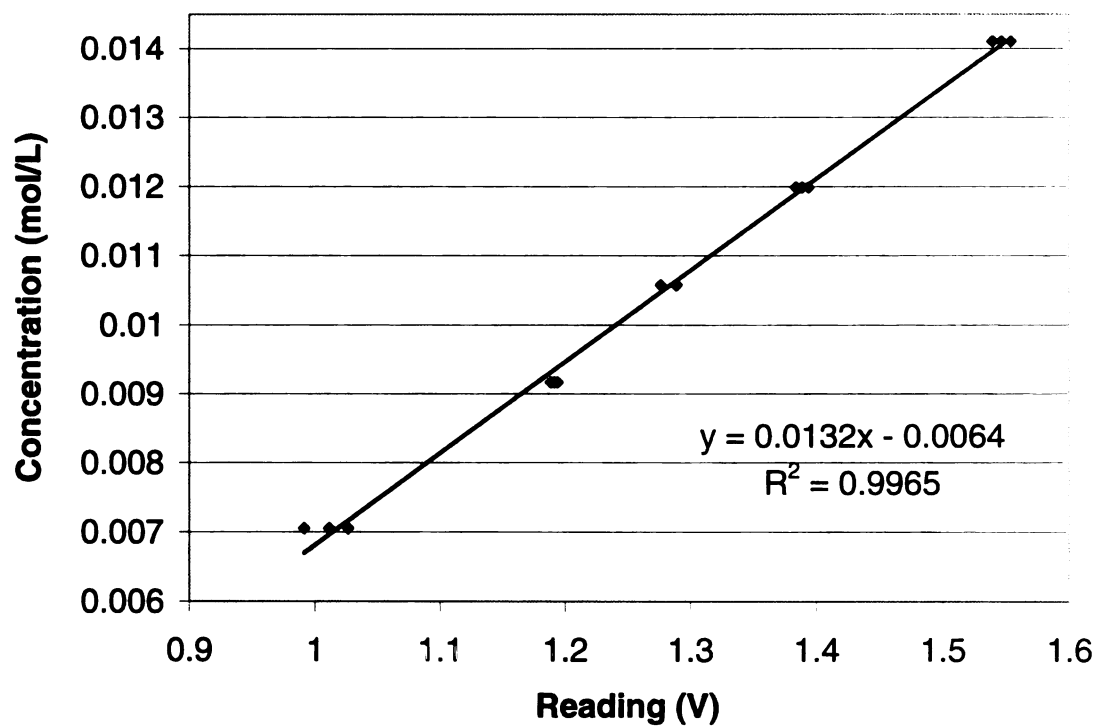


Figure 2.2 Calibration curve for heptanoic acid

beaker. The concentration of the Tween 80 solution was adjusted to achieve the desired final concentration (0.001% v/v to 0.4% v/v Tween 80). Five mL of limonene/Tergitol 15-S-3 solution (0.01% v/v to 0.1% v/v Tergitol 15-S-3) was then dispensed into the aqueous solution at a rate of 0.5 mL/min while mixing at 1,600 rpm using a 25 mm magnetic stirrer bar. The resulting CLA emulsions were creamy white, with a phase volume ratio (PVR) of 1.0. The PVR is defined as the ratio of the volume of the nonpolar phase to that of the aqueous phase. The CLA emulsions were very stable, with no phase separation evident over a period of 6 months.

#### **2.2.4 CLA Size Measurement**

Particle-size distributions of CLA emulsions were measured using a Malvern Mastersizer X particle analyzer (Malvern Instruments, Worcestershire, UK). The instrument was fitted with a 15-mL sample chamber containing deionized water. The contents of this cell were mixed using a 10 mm by 8 mm Nalgene Star Head magnetic stir bar (Fisher Scientific, Pittsburgh, PA) to ensure that the CLA remained dispersed. The size measurement was made within 10 s of the CLA being added to the cell. The average particle size was reported in terms of the Sauter mean diameter ( $\overline{d}_{32}$ ) which is defined in Eqn. 1. The precision of the particle-size measurements is  $\pm 5\%$ .

$$\overline{d}_{32} = \frac{\sum n_i d_i^3}{\sum n_i d_i^2} \quad (1)$$

## **2.2.5 Mass Transfer Measurement**

### **2.2.5.1 Stirred-Cell Experiments.**

In stirred-cell experiments, the two phases are not dispersed, but rather overlaid on one another. This approach has been widely used to measure  $K_L$  values because the interfacial area is accurately known (Nanda *et al.*, 1966; Nanda *et al.*, 1967, Fernandes *et al.*, 1967; Bhave *et al.*, 1981). The stirred cells were glass beakers having internal diameters of either 8.3 cm or 10.5 cm. Five hundred mL of 0.0141 M aqueous heptanoic acid solution was overlaid with 50 mL of pure limonene. A Rushton impeller located just below the limonene-water interface was used to gently mix the water phase without disrupting the water/limonene interface. The stainless-steel impeller had a diameter of 5 cm, a blade height of 1 cm, and blade width of 1.2 cm. The impeller was driven using a Lightnin<sup>®</sup> Labmaster II unit (Mixing Equipment Company, Rochester, NY). A wooden shaft was used to minimize the electrical noise in conductivity measurements. The impeller rate (60 rpm) allowed the interface to be continuously renewed without creating a significant vortex. The conductivity of the aqueous phase was recorded as a function of time until no further decrease was detected. The equilibrium concentration was then measured after 24 h.

### **2.2.5.2 Stirred-tank experiments**

The mass-transfer properties of the CLA were measured in a baffled, stirred tank having standard dimensions (McCabe *et al.*, 1993). The Plexiglass vessel had an ID of 15 cm and a height of 20 cm. It was fitted with four, equally spaced, vertical, wall baffles. The liquid height in the vessel was maintained at 15

cm. The Rushton impeller described above was axially centered in the tank 5 cm from the bottom. The conductivity probe was mounted close to the impeller blades. The continuous phase (2.8 L of 0.0141 M aqueous heptanoic acid) was placed in the tank, and mixing was initiated at the target rpm. Then the second phase was poured rapidly (within 1 s) near the center of the vessel to promote rapid dispersion. For CLA experiments, 10 mL of CLA dispersion having a PVR of 1.0 was added. In one control experiment conducted without any surfactants (Run 10), pure limonene was used as the dispersed phase. After the two phases were combined, the conductivity of the aqueous phase was recorded as a function of time until no further decrease was observed. A final reading was taken 30 min later to serve as the equilibrium value. All experiments were conducted at 25°C.

Table 2.1 summarizes the experimental conditions used for all runs.

Table 2.1. Summary of conditions for mass-transfer experiments.

Run No.	Vessel	Stirring rate (rpm)	Aqueous-phase surfactant conc. (% v/v)	Nonpolar-phase surfactant conc. (% v/v)
1	Stirred Cell*	60	-	-
2	Stirred Cell <sup>+</sup>	60	-	-
3	Baffled tank	200	0.4	0.1
4	Baffled tank	300	0.4	0.1
5	Baffled tank	375	0.4	0.1
6	Baffled tank	427	0.4	0.1
7	Baffled tank	500	0.4	0.1
8	Baffled tank	550	0.4	0.1
9	Baffled tank	600	0.4	0.1
10	Baffled tank	427	-	-
11	Baffled tank	427	0.02	0.01
12	Baffled tank	427	0.04	0.01
13	Baffled tank	427	0.4	0.01
14	Baffled tank	427	0.04	0.1

\*Stirred cell interfacial area = 56.72 cm<sup>2</sup> +Stirred cell interfacial area = 83.32 cm<sup>2</sup>

### 2.3 Data Analysis

The unsteady-state mass balance on heptanoic acid in the continuous phase is given below.

$$V_c \frac{dC}{dt} = K_L a V (C^* - C) \quad (2)$$

Equation 2 was integrated from the initial time ( $t_0$ ) and concentration ( $C_0$ ) to obtain Eqn. 3.

$$\ln \left[ \frac{(C^* - C)}{(C^* - C_0)} \right] = - \left[ K_L a \frac{V}{V_c} \right] (t - t_0) \quad (3)$$

The experimental data were analyzed by plotting the left-hand side of Eqn. 3 as a function of time. The value of  $K_L a$  was then obtained from the slope of the plot using the relation

$$K_L a = - \text{slope} \left[ \frac{V_c}{V} \right]$$

Example plots showing the degree to which the data followed the expected linear trend are given in Figures 2.3 (a), (b), and (c) for each of the three types of mass-transfer experiments performed.

The value of  $a$  was computed from the  $\overline{d_{32}}$  data as shown below:

$$a = 6 \frac{\phi}{d_{32}}$$

where  $\phi$  is the void fraction of the dispersed phase. The void fraction  $\phi$  was

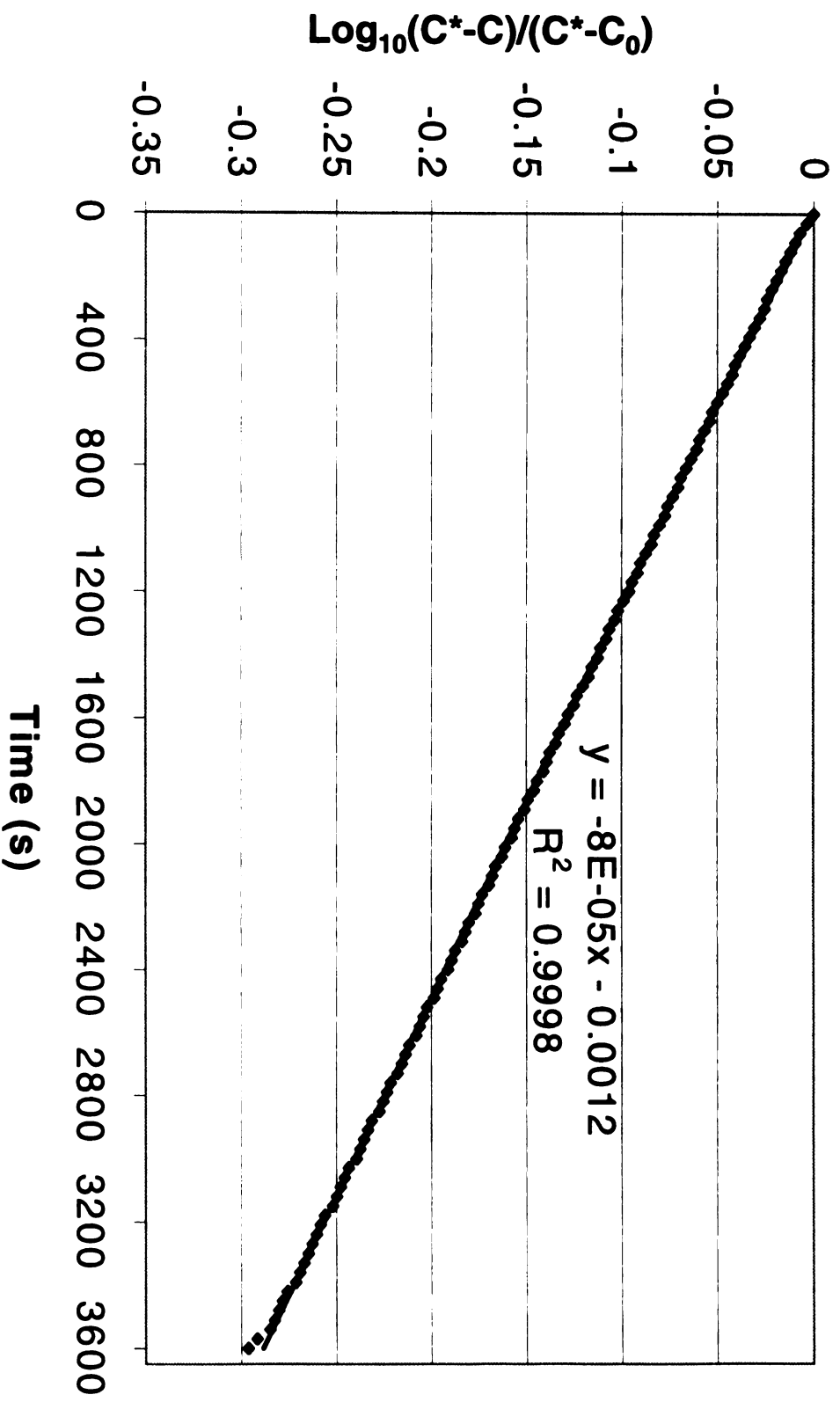


Figure 2.3a: Agreement of experimental data with the linear trend predicted by Eqn. 3. (stirred cell at 60 rpm)

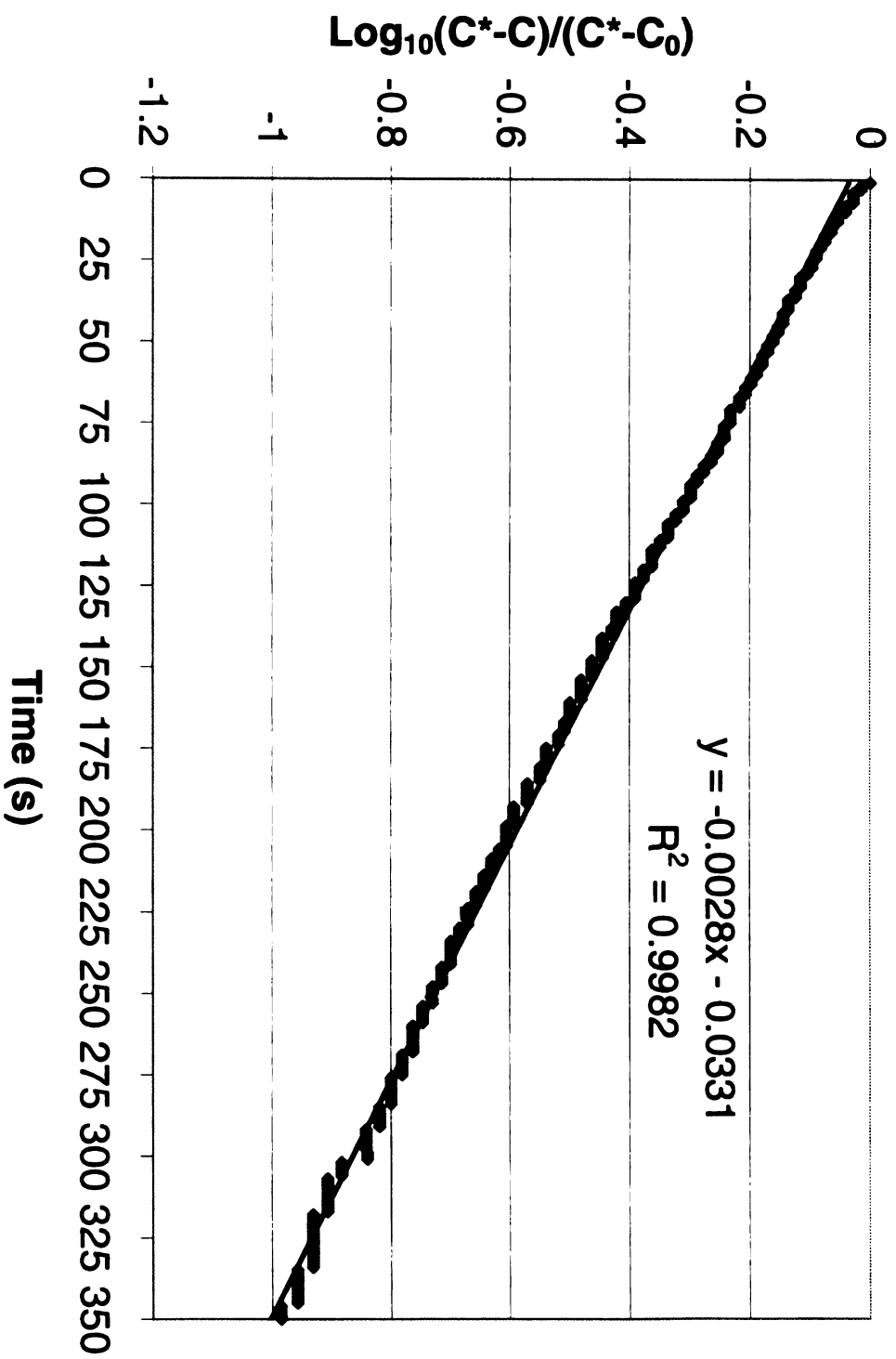


Figure 2.3b: Agreement of experimental data with the linear trend predicted by Eqn. 3.  
Run 10 in baffled tank at 427 rpm

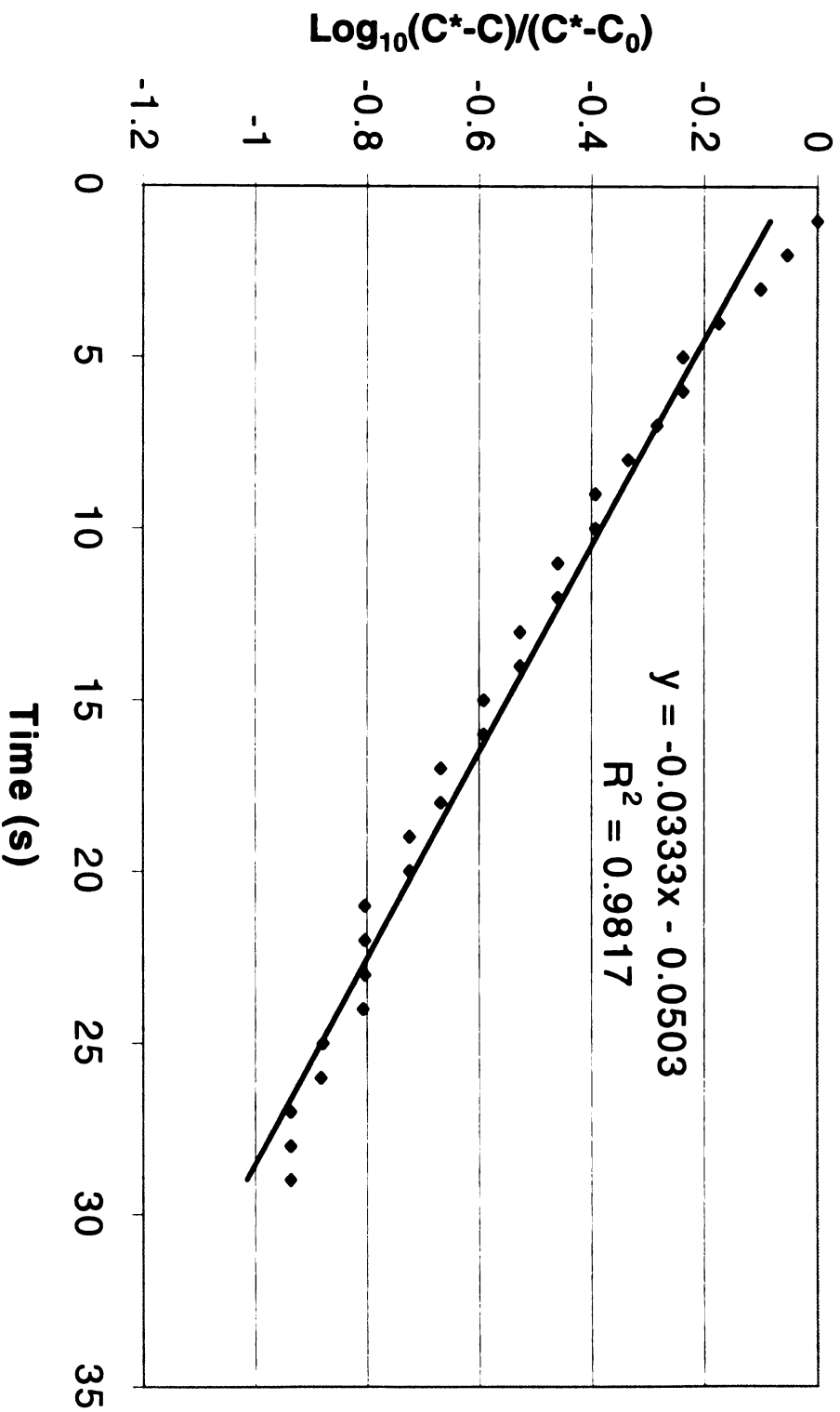


Figure 2.3c. Agreement of experimental data with the linear trend predicted by Eqn. 3. Run 8 in baffled tank at 550 rpm, 0.4% (v/v) Tween 80 in aqueous phase and 0.1% (v/v) Tergitol 15-S-3 in CLA phase.

equal to 0.0018. At such a small void fraction, collisions between droplets, and subsequent coalescence, can be ignored during the short duration of the experiments (Fernandes *et al.*, 1967). Hence, the interfacial area was assumed to be constant throughout the experiments. In the stirred-cell experiments,  $a$  was calculated as the interfacial area between the aqueous and limonene layers divided by the volume of the aqueous phase.

## **2.4 Results and Discussion**

### **2.4.1 Measurements in Stirred Cell**

Runs 1 and 2 were conducted in stirred cells of known interfacial area (56.7 cm<sup>2</sup> and 83.3 cm<sup>2</sup>, respectively). The resulting  $K_L$  values (0.0012 and 0.0011 cm/s, respectively) were well within the range of values reported for similar systems (Sharma *et al.*, 1968), indicating the suitability of the limonene/water/heptanoic-acid system for measuring interphase mass transfer. Even though the interfacial area increased by almost 50% from Run 1 to Run 2, the  $K_L$  values for the two runs were almost identical, as expected

### **2.4.2 Measurements in Baffled Tank**

Runs 3 through 9 were conducted using CLA containing 0.1% Tergitol 15-S-3 in the nonpolar phase and 0.4% Tween 80 in the aqueous phase. The interfacial area was identical in all runs. As shown in Figure 2.4,  $K_L a$  increased with  $N_{RE}$  up to about 15,000 and then became essentially independent of  $N_{RE}$ . The effect of  $N_{RE}$  on  $K_L a$  is through the  $K_L$  term, rather than  $a$ . Since the droplets in the CLA emulsions were much smaller than the maximum stable drop size

under the hydrodynamic conditions used, breakage should have been negligible in these experiments.

The  $K_L$  values obtained from experimental data are shown as a function of  $N_{RE}$  in Figure 2.5. These values reflect the overall resistance to mass transfer of heptanoic acid from the dispersed phase to the bulk continuous phase. Due to the high solubility of heptanoic acid in the nonpolar phase, the resistance to mass transfer in the non-polar phase should be negligible, and hence, there are two primary resistances to mass transfer: 1) the resistance of the continuous phase and 2) the resistance of the surfactant shell surrounding the aphrons. The resistance of the continuous phase would be expected to decrease with the degree of mixing, while the shell resistance should be relatively unaffected by mixing.

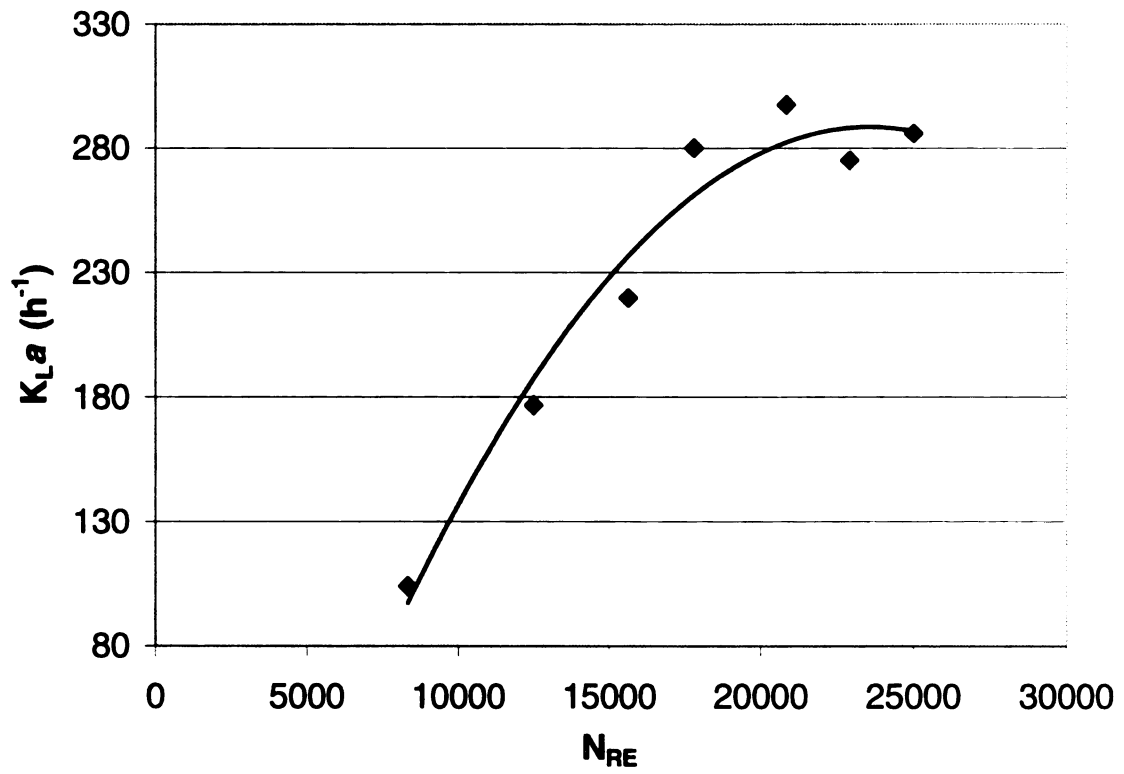


Figure 2.4. Variation in experimental volumetric mass transfer coefficient ( $K_{La}$ ) with  $N_{RE}$  measured in a baffled tank.

Skelland *et al.* (1981) developed the following correlation for  $K_{L,continuous}$  values in stirred tanks having standard dimensions:

$$\frac{K_{L,continuous}}{(ND)^{1/2}} = 1.864 \times 10^{-7} \phi^{-0.287} \left(\frac{d_I}{T}\right)^{0.548} (N_{RE})^{1.371} (N_{WE})^{-0.095} \quad (4)$$

Although this correlation was developed for mass-transfer systems without surfactants, it should reasonably predict  $K_{L,continuous}$  values for systems containing surfactants, provided the effect of the surfactant on the surface tension is taken into account through the  $N_{We}$  term. Additional mass-transfer resistance due to surfactant accumulation at the interface can be accounted for through a separate mass-transfer coefficient for the shell ( $K_{L,shell}$ ).

Figure 2.5 shows the  $K_{L,continuous}$  values predicted by this correlation along with the experimentally measured (overall)  $K_L$  values. At low  $N_{RE}$  values, the  $K_{L,continuous}$  values agree well with the  $K_L$  values, both in magnitude and the effect of impeller rate. However, above a  $N_{RE}$  of 15,000 (375 rpm), the  $K_L$  values approach an asymptote, while the  $K_{L,continuous}$  values continue to increase steadily with  $N_{RE}$ . These trends are consistent with the hypothesis that the continuous phase resistance is rate-limiting at low  $N_{RE}$ , but the shell resistance becomes rate-limiting at high  $N_{RE}$ . Based on this hypothesis, the resistances-in-series model shown in Eqn. 5 was used to estimate  $K_{L,shell}$  from the  $K_L$  and  $K_{L,continuous}$  values.

$$\frac{1}{K_{L,shell}} = \frac{1}{K_L} + \frac{1}{K_{L,continuous}} \quad (5)$$

The results are summarized in Table 2.2.

A control experiment (Run 10) was conducted to determine how well the Skelland *et al.*, (1981) correlation (Eqn. 4) applied to the limonene/water/heptanoic acid system in the absence of surfactants. This run was conducted at a  $N_{RE}$  of 17,800. Because the limonene was not predispersed as CLA, the droplet size distribution represented a dynamic equilibrium between droplet coalescence and disintegration. Under these conditions, the following correlation for  $\overline{d_{32}}$  published by Skelland *et al.* (1981) applies:

$$\frac{\overline{d_{32}}}{d_I} = 6.713 \times 10^{-4} \phi^{-1.034} (N_{RE})^{-0.558} (N_{OH})^{-1.025} \quad (6)$$

Equations 4 and 6 were used to calculate a predicted  $K_L a$  value for Run 10 of  $29 \pm 5 \text{ h}^{-1}$  and a  $\overline{d_{32}}$  value of  $241 \pm 48 \text{ }\mu\text{m}$ . This  $K_L a$  value agreed well with the experimentally measured value of  $23 \text{ h}^{-1}$ . However, the predicted  $\overline{d_{32}}$  value could not be experimentally verified; in the absence of surfactants, the droplets coalesce too fast for the Malvern Mastersizer to be used.

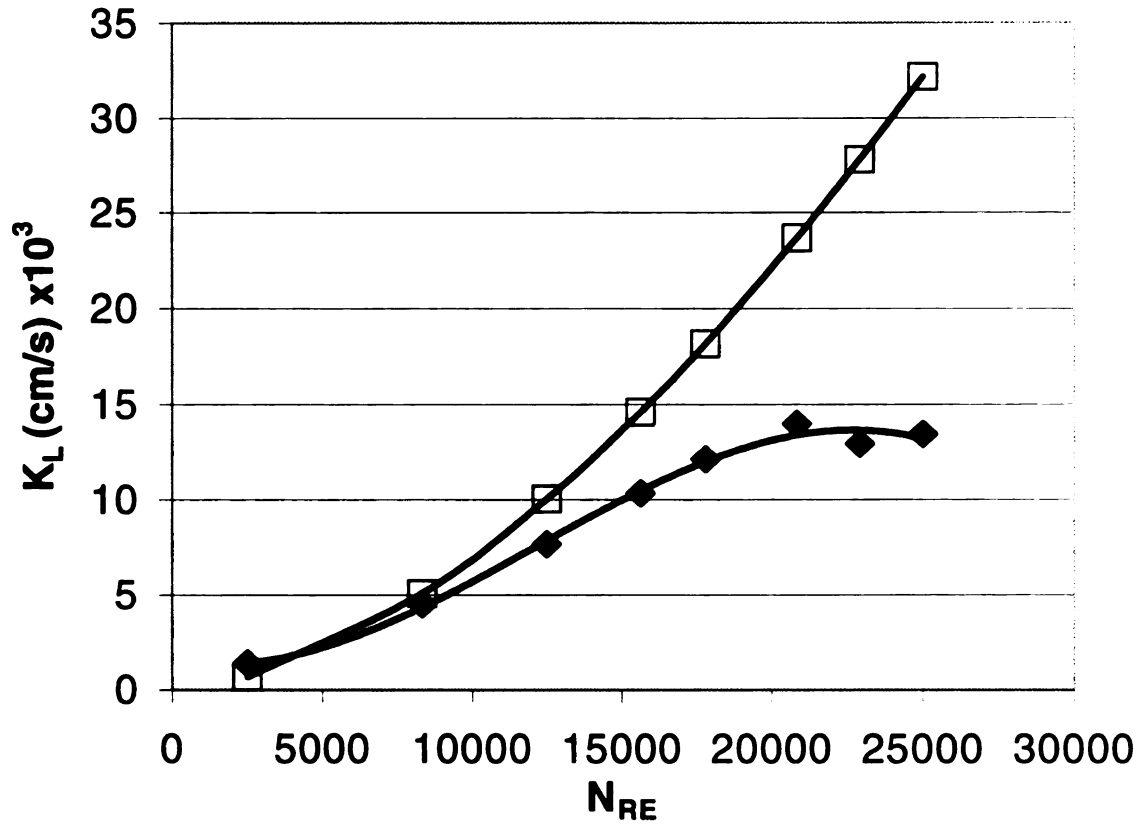


Figure 2.5. Effect of  $N_{RE}$  on experimental  $K_L$  values (◆) measured in a baffled, stirred tank and predicted  $K_{L,continuous}$  values (□) calculated using Eqn. 4 (Skelland *et al.*, 1981).

Table 2.2. Effect of  $N_{RE}$  on  $K_L$ ,  $K_{L,continuous}$ , and  $K_{L,shell}$ .

Run No.	$N_{RE}$	$K_L$ (cm/s) $\times 10^3$	$K_{L,continuous}$ (cm/s) $\times 10^3$	$K_{L,Shell}$ (cm/s) $\times 10^3$
3	8333	4.5	5.1	40.3
4	12500	7.7	10.0	32.2
5	15625	10.3	14.6	35.3
6	17792	12.1	18.2	36.5
7	20833	14.0	23.7	34.1
8	22917	12.9	27.8	24.2
9	25000	13.4	32.2	23.1

### **2.4.3 Influence of Surfactant Concentration.**

The influence of the concentrations of the two surfactants on the Sauter mean diameter of CLA droplets ( $d_{32}$ ) is shown in Figure 2.6. While the  $\overline{d_{32}}$  values were essentially unaffected by the Tergitol concentration, they decreased as much as 70% as the Tween 80 concentration increased from 0.02 to 0.4 g/L. This value is slightly higher than Critical Micelle Concentration (CMC) of 0.013 g/L for Tween 80. The CMC value is defined as the concentration at which the surfactant concentration forms a saturated monomolecular layer at the interface (Porter, 1994). Stable CLA emulsions could not be formed below a Tween 80 concentration of 0.015 g/L.

Table 2.3 shows the effect of surfactant concentration on the experimentally measured values of  $\overline{d_{32}}$ ,  $a$ ,  $K_L$ , and  $K_L a$  for the limonene CLA (Runs 6, 11, 12, 13, and 14). The  $\overline{d_{32}}$ ,  $a$ , and  $K_L$  values predicted by Eqns 4 and 6 and the measured  $K_L a$  value for the control run without surfactants (Run 10) are also listed for comparison. The  $K_L a$  values for CLA increased by a factor of about three as the Tween 80 concentration was increased from 0.02 to 0.4% v/v at a constant Tergitol-S concentration of 0.01% v/v. This effect was due almost exclusively to an increase in  $a$ , which increased by a similar factor. The value of  $K_L$  remained essentially constant for all the CLA runs. The average  $K_L$  value of the CLA runs was  $14.3 \times 10^{-3}$  cm/s, and the standard deviation was  $2.2 \times 10^{-3}$

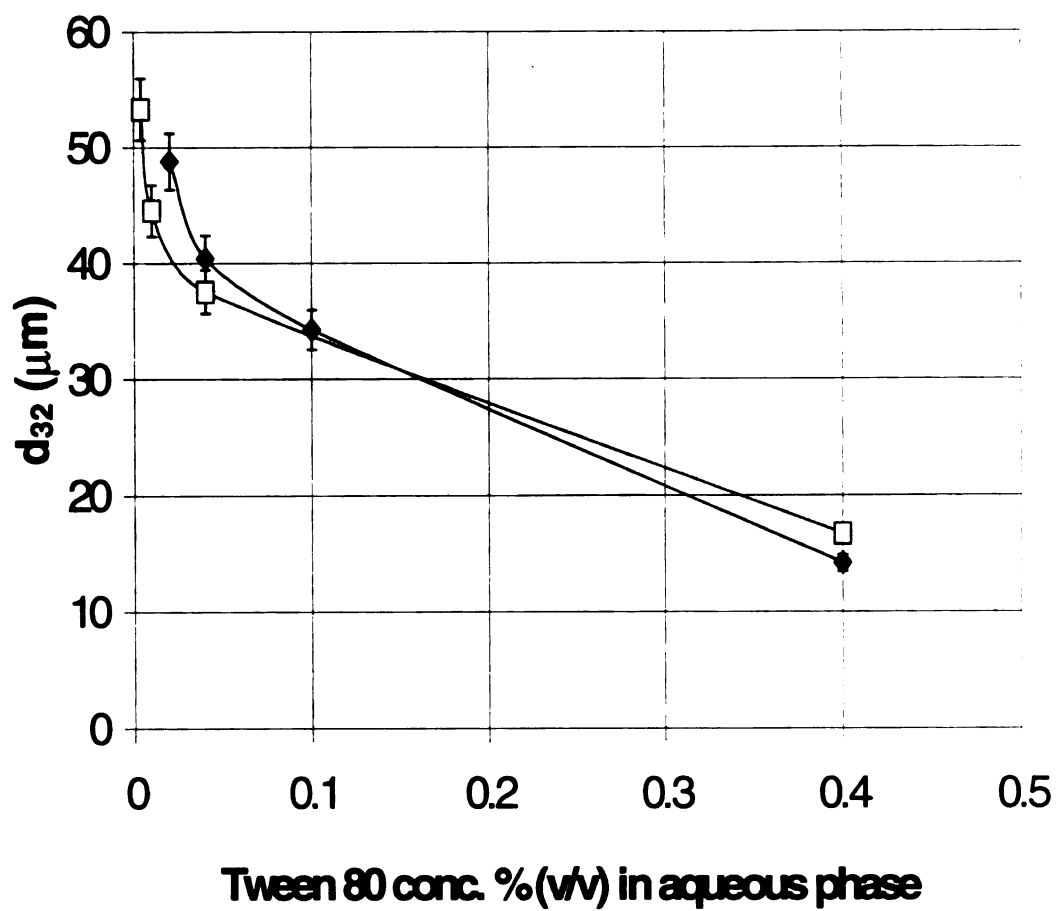


Figure 2.6 Variation of CLA droplet diameter with Tween 80 concentration in the aqueous phase at Tergitol 15-S-3 concentrations of 0.1% v/v ( $\square$ ) and 0.01% v/v ( $\blacklozenge$ ).

Table 2.3. Effect of surfactant concentrations on  $K_L$  and  $K_L a$

Run	Tween 80 (%)	Tergitol (%)	$d_{32}$ ( $\mu\text{m}$ )	$a$ ( $\text{cm}^2/\text{cm}^3$ ) <sup>+</sup>	$K_{L,\text{overall}}$ ( $\text{cm/s}$ ) $\times 10^3$	$K_L a$ ( $\text{h}^{-1}$ )
10	-	-	241 <sup>#</sup>	0.44	14.5	23
11	0.02	0.01	49	2.19	14.9	117
12	0.04	0.01	40	2.65	17.9	170
13	0.4	0.01	14	7.07	13.1	334
14	0.04	0.1	22	4.84	13.8	240
6	0.4	0.1	17	6.41	12.1	280

<sup>#</sup> Value calculated using Eqn. 6.

<sup>+</sup> Interfacial areas calculated from measurements of diameter using the equation

$$a = 6 \phi / d_{32}$$

the  $K_L$  values were essentially independent of impeller rate (see Figure 2.5). In this regime, the shell resistance is believed to be significant. Thus, the fact that  $K_L$  was largely unaffected by surfactant concentration in these experiments suggests that the surfactant concentration does not significantly affect the properties of the shell (e.g., shell thickness) under these conditions. Moreover, since the measured  $K_L$  values are similar in magnitude to those predicted by Eqn. 4 for the control experiment, the mass-transfer resistance contributed by the shell does not appear to be excessive. Consequently, at an equivalent dispersed-phase void fraction, the 7- to 16-fold higher  $a$  values provided by the CLA translate into 5- to 14-fold higher  $K_L a$  values.

This mass-transfer advantage provided by CLA would be expected to be even more significant at lower  $N_{RE}$  values. The value of  $a$  is inversely proportional to  $\overline{d_{32}}$ . Thus, according to Eqn. 6,  $a$  should be proportional to  $N_{RE}^{0.558}$  for conventional emulsions. The size distribution of the CLA (and hence  $a$ ), on the other hand, is determined exclusively by the conditions under which they are formed. As a result, decreasing  $N_{RE}$  would decrease  $a$  for conventional emulsions but have little effect on  $a$  for CLA.

Because CLA emulsions can provide several-fold higher interfacial areas and volumetric mass-transfer rates than conventional emulsions, they offer significant advantages for mass-transfer-limited applications of multiphase biocatalysis. However, a major impediment to the commercial application of CLA (and other surfactant-stabilized emulsions) is the difficulty in coalescing the

dispersed phase and separating the two phases once the contacting step is complete. It is possible to overcome this difficulty by stabilizing the emulsions with novel polymeric emulsifiers whose emulsification properties are pH sensitive (Mathur, *et al.*, 1998). The emulsions produced with these emulsifiers can be coalesced on demand by making a small change in the pH. These emulsions shall be discussed further in Chapter 6.

## 2.5 Conclusions

The mass-transfer properties of CLA emulsions of limonene in water have been measured experimentally. The CLA size distribution was found to be strongly affected by the aqueous-phase surfactant (Tween 80) concentration, but virtually unaffected by the nonpolar-phase surfactant (Tergitol-15-S-3) concentration. The  $\overline{d}_{32}$  values decreased from 49 to 14  $\mu\text{m}$  as the Tween 80 concentration increased from 0.02 to 0.4% v/v. The  $K_L$  values measured for CLA emulsions averaged about  $15 \times 10^{-3}$  cm/s and were essentially unaffected by surfactant concentration. The  $K_{L,\text{shell}}$  value was estimated to be about  $30 \times 10^{-3}$  cm/s, which is comparable to  $K_L$  values for surfactant-free, liquid-liquid systems at an equivalent  $\phi$  value. The  $K_L a$  values for CLA were 5- to 15-times higher than those for conventional emulsions. These results suggest that CLA may offer significant advantages over conventional emulsions for mass-transfer-limited, multiphase biocatalytic processes.

## 2.6 Nomenclature

$C$  = Concentration of solute ( $\text{mol L}^{-1}$ )

$K_L$  = Overall mass-transfer coefficient, ( $\text{cm s}^{-1}$ )

$K_{L,continuous}$  = Mass-transfer coefficient of the continuous phase ( $\text{cm s}^{-1}$ )

$K_{L,shell}$  = Mass-transfer coefficient of the CLA shell ( $\text{cm s}^{-1}$ )

$D$  = Diffusivity, ( $\text{cm}^2/\text{s}$ )

$a$  = interfacial area per unit volume in two phase mixture ( $\text{m}^2/\text{m}^3$ ), calculated as

$$\frac{6\phi}{d_{32}}$$

$\overline{d}_{32}$  = Sauter mean diameter defined by  $\frac{\sum n_i d_i^3}{\sum n_i d_i^2}$ , (m)

$d_i$  = diameter of the impeller, (m)

$N$  = impeller speed, (rps)

$K$  = cell constant for conductivity probe ( $\text{cm}^{-1}$ )

$T$  = tank diameter, (m)

$N_{OH}$  = Ohnesorge number, defined by  $\frac{\mu_c}{\sqrt{\rho_c d_i \sigma}}$

$N_{RE}$  = Reynolds number, defined by  $\frac{\rho_c N d_i^2}{\mu_c}$

$N_{WE}$  = Weber Number, defined by  $\frac{N^2 d_i^3 \rho_c}{\sigma}$

$V_C$  = Volume of the continuous phase, (L)

$V$  = Filled volume of the tank, given by  $(1+\phi)V_C$ , (L)

Greek

$\phi$  = void fraction of dispersed phase, dimensionless

$\mu$  = viscosity, ( $\text{Ns/m}^2$ )

$\rho$  = density, ( $\text{kg/m}^3$ )

$\sigma$  = interfacial tension, (N/m)

## 2.7 References

Bhave R.R. and Sharma M.M. 1981. Liquid-liquid reactors: operation under refluxing conditions: measurement of effective interfacial area, *Trans ICHME*, 59 161-168.

Bredwell M.D., Worden R.M. 1998 Mass-transfer properties of microbubbles. 1. Experimental studies, *Biotech. Prog.* 14: (1) 31-38.

Bredwell, M.D., Telgenhoff M.D., Barnard S., and R. M. Worden 1997. Effect of surfactants on Carbon monoxide fermentations by *Butyribacterium methylotrophicum*, *Applied Biochemistry and Biotechnology*, 63-5: 637-647

Bredwell, M.D., Srivastava, P., and R. Mark Worden 1999. Reactor Design Issues in Synthesis Gas Fermentations, *Biotechnology Prog.*, 15(5) 834-844.

Bruce, L.J and Daugulis, A.J. 1991. Solvent Selection Strategies for Extractive Biocatalysis, *Biotechnol. Prog.* 7, 116-124.

Dean J.A. 1992. Lange's Handbook of Chemistry, Fourteenth edition, McGraw Hill, Inc. New York, NY.

Fernandes J.B., Sharma M.M. 1967. Effective interfacial area in agitated liquid liquid contactors, *Chem. Engg.Sci.* 22, 1267-1282.

Kollerup, F. and Daugulis, A.J. 1985. A mathematical model for ethanol production by extractive fermentation in a continuous stirred tank fermentor, *Biotechnol. Bioeng.* 27: 1335-1346.

Lye G.J., Pavlou O.P., Rosjidi M., Stuckey D.C. 1996. Immobilization of *Candida cylindracea* lipase on colloidal liquid aphrons (CLAs) and development of a continuous CLA-membrane reactor, *Biotechnol. Bioeng.* 51: (1) 69-78.

Lye G.J. and Stuckey D.C. 1996. Predispersed solvent extraction of microlide antibiotics using colloidal liquid aphrons, in *Proceedings International Solvent Extraction Conference, Melbourne, Australia*, ed. by Shallcross DC, Paimin R and Prvcic LM, 1399-1405.

Mathur, A.M., B. Drescher, A.B. Scranton, and J. Klier, Polymeric Emulsifiers Based on Reversible Formation of Hydrophobic Units. 1998. *Nature*, 392, 567-370.

Mattiasson B. and Olle Holst 1991. Objectives for extractive Bioconversion, in *Extractive Bio Conversions*, ed. Bo Mattiasson and Olle Holst, Marcel Dekker, New York NY.

Larsson, M., Arasaratnam, V. and Mattiasson, B. 1989. Integration of bioconversion and down-stream processing. Starch hydrolysis in an aqueous two-phase system, *Biotechnol. Bioeng.* 33:758-766.

Matsushita K, Mollah A.H., Stuckey D.C., del Cerro C and Bailey A.I. 1992. Predispersed solvent extraction of dilute products using colloidal gas aphrons and colloidal liquid aphrons – aphron preparation, stability and size. *Colloids Surfaces*, 69, 65-72.

McCabe W.L., Smith J.C. and Harriot P. 1993. *Unit Operations of Chemical Engineering*, Fifth Edition McGraw Hill Inc, New York NY.

- Nanda A.K. and Sharma M.M. 1966. Effective interfacial area in liquid liquid extraction, Chem. Engg. Sci. 21 707-714.
- Nanda A.K., Sharma M.M. 1967, Kinetics of fast alkaline hydrolysis of esters, Chem. Engg. Sci. 22, 769-775.
- Porter M. R. 1994, Handbook of surfactants, 2<sup>nd</sup> ed. Chapman and Hall, London UK.
- Puziss, M. and Heden 1965. C.G., Toxin production by *Clostridium tetani* in biphasic cultures, Biotechnol. Bioeng. 7: 355-366.
- R Reid, and T. Sherwood 1958. Properties of Gases and Liquids: their estimation and correlation, 2<sup>nd</sup> ed., McGraw-Hill, New York, NY
- Roffler, S. 1986. Extraction fermentation-lactic acid and acetone/butanol production, Ph. D. Dissertation, University of California, Berkeley.
- Roffler S.R., Theodore W Randolph, Douglas A Miller, Harvey W. Blanch and John M Prausnitz 1991. Extractive Bio-conversions with non-aqueous solvents in *Extractive Bioconversions* ed. by Bo Mattiason and Olle Holst, Marcel Dekker, Inc. New York, NY.
- Rosjidi M., Stuckey D.C. and Leak D.J. 1994. Downstream Separation of chiral epoxides using colloidal liquid aphrons( CLA), in *Separations for Biotechnology*, Ed by Pyle D.L. , SCI publishing. 280-286.
- Rushton J.H., Nagata S., Rooney T.R. 1964. Measurements of mass transfer coefficients in Liquid-Liquid mixing, AIChE J. 10 (3), 298-302.
- Save S.V., Pangarkar V.G. and Kumar S.V. 1994. Liquid-Liquid extraction using aphrons, Separation Technology, 4: 104-111.

Schwuber, M.J. and Bartnik, F. G. 1980, in *Anionic surfactants: Biochemistry, Toxicology, Dermatology*, Ed. by Christian Gloxhuber, Marcel Dekker, New York. 1-49

Scott, C.D., T.C. Scott, H.W. Blanch, A.M. Klivanov, and A.J. Russell 1995. *Bioprocessing in Nonaqueous Media: Critical Needs and Opportunities*. ORNL/TM-12849, U.S. National Technical Information Service, Springfield, VA.

Sebba F. 1984. Preparation and properties of polyaphrons (bilibiquid foams), *Chemistry and Industry*, 367-372.

Scarpello J.T. and Stuckey D.C. 1996. Extraction of phenylalanine using colloidal liquid aphrons (CLA): stability in dispersion and rates of mass transfer, in *Proceedings of International Congress on Membranes and Membrane Processes*, Yokohama, Japan. 988-989

Scarpello J.T. and Stuckey D.C. 1999. The influence of system parameters in the stability of Colloidal liquid aphrons, *J. Chem Technol. Biotechnol.* 74: 409-416.

Sharma M.M., and A. K. Nanda 1968. Extraction with second-order reaction, *Trans Inst. Chem. Engrs.*, 46, 44-52.

Skelland A.H.P., Jai Moon Lee 1981. Drop size and continuous phase mass transfer in agitated vessels, *AIChE Journal* 27 (1) 99-111.

Soucaille, P., Joliff, G., Izard, A, and Goma G. 1987. Butanol tolerance and autobacteriocin production by *Clostridium acetobutylicum*, *Curr. Microbiol.* 14: 295-299

Toxicology Update *Journal of Applied Toxicology* 1995.15(6) 495-499.

Wallis D.A., Michelson D.L., Sebba F., Carpenter J.K. and Houle D. 1985.  
Applications of aphron technology to biological separations. *Biotech. Bioeng.*  
*Symp.* 15 : 399-408

Wilke, C.R., and P. Chang 1955. Correlation of Diffusion coefficients in Dilute  
solution, *AICHE J.*, 1, 264.

## Chapter 3

### 3. Enhancement of Mass Transfer using Colloidal Liquid

#### Aphrons: Measurement of Mass-Transfer Coefficients

#### Using Chemical Reaction

##### 3.1 Introduction

Many industrially important chemical, biochemical, and environmental processes involve a phase-contacting operation intended to transfer a solute between two immiscible liquids. The rate of solute mass transfer is often a rate-limiting factor that limits the overall efficiency of the process. For example, the nitration of aromatic substances like benzene, toluene, phenol, and naphthalene is practiced on large scales for the manufacture of intermediates for dyestuffs, polymers, pharmaceuticals and explosives. Most of these nitrations involve two phases: an organic phase and an aqueous, mixed acid ( $\text{HNO}_3 + \text{H}_2\text{SO}_4$ ) phase. Albright and Hanson (1975) determined that under industrial conditions the rate of nitration is typically controlled by diffusional factors. Similarly, the rates of alkaline hydrolysis of several formate esters and the rates of reduction of substituted nitroaromatics in mechanically agitated, liquid-liquid contactors are dependent on interfacial area per unit volume ( $a$ ), indicating that interphase mass transfer is rate-limiting.

Under mass-transfer-limiting conditions, the volumetric solute-transfer rate can be increased by decreasing the size of the dispersed-phase droplets, and

thereby increasing  $a$  (Kafarov *et al.*, 1974; Bhave and Sharma, 1981). CLA offer an attractive means to enhancing mass transfer in such processes.

Rational design of contacting processes involving CLA requires the overall interphase mass-transfer coefficient ( $K_L$ ) and  $a$  values be predicted (Fernandes and Sharma, 1967). The value of  $K_L$  will depend on the continuous phase mass-transfer coefficient ( $K_{L,continuous}$ ) and the shell mass-transfer coefficient ( $K_{L,shell}$ ). In this chapter, the rate of mass transfer of an ester (p-tolyl acetate) from CLA into aqueous solution was measured in a stirred tank having standard dimensions. The data were used to determine both  $K_L$  and  $a$  for a variety of impeller rates and surfactant concentrations. These results were then used, along with a literature correlation for  $K_{L,continuous}$  and a resistances-in-series model, to estimate the  $K_{L,shell}$  value.

## 3.2 Theory

### 3.2.1 Mass-transfer resistances in series

The overall resistance to mass transfer between the dispersed and continuous phases ( $1/K_L$ ) is the sum of the individual resistances. In this study, the CLA droplets contained pure p-tolyl acetate, which is sparingly soluble in the continuous, aqueous phase. Under these conditions, the main resistances are (1) the resistance of the continuous phase, and (2) the resistance of the shell. Assuming the thickness of the shell is small compared to the diameter of the aphron, a resistances-in-series model may be written:

$$\frac{1}{K_L} = \frac{1}{K_{L,continuous}} + \frac{1}{K_{L,shell}} \quad (\text{Equation 1})$$

### **3.2.2 Coupling of mass transfer and reaction**

Acetate esters ( $\text{CH}_3\text{COOR}$ ) are readily hydrolyzed in aqueous solutions by sodium hydroxide ( $\text{NaOH}$ ) as shown below:



If the R group is aromatic, the acidic phenol group ( $\text{ROH}$ ) formed in Reaction 1 reacts instantaneously with a second molecule of  $\text{NaOH}$  to give the corresponding phenoxide:



Because the solubility of the ester in the alkali solution is very low, the ester and  $\text{NaOH}$  must exist in two different phases, and the ester must be transferred into the aqueous phase for the reaction to proceed. Depending on the experimental conditions, either the mass-transfer step or the reaction step may be rate-limiting. Under conditions in which mass transfer is rate-limiting, the mass-transfer rate may be measured indirectly by measuring the rate of  $\text{NaOH}$  consumption in the aqueous phase.

### **3.2.3 Relative rates of mass transfer and reaction**

Nanda and Sharma (1966) developed methods to indirectly measure mass-transfer coefficients for an ester (referred to below as A) by monitoring the change in concentration of  $\text{NaOH}$  (referred to below as B) based on the following assumptions:

- (1) A is soluble in the aqueous phase, but B is insoluble in the nonpolar phase. Thus A must transfer into the aqueous phase before it can react, and the reaction occurs only in the aqueous phase.

(2) The reaction is slow enough that A diffuses through the interface into the bulk aqueous phase, and the reaction occurs uniformly throughout the aqueous phase containing B.

(3) The reaction is irreversible and first order with respect to both A and B.

To ensure that the reaction occurs uniformly throughout the aqueous phase and that the rate is controlled by the transfer rate of A into the aqueous phase, two conditions must be satisfied (Doraiswamy and Sharma, 1983). First, the rate of mass transfer must be less than the rate of reaction. This condition may be expressed using the following inequality:

$$K_L a \ll K_R C_{B0} \quad (\text{Condition 1})$$

Second, the amount of A that reacts in the film adjacent to the phase boundary should be negligible compared to that which reacts in the bulk B phase. This condition is satisfied when the following inequality holds:

$$\frac{(D_A K_R C_{B0})^{1/2}}{K_L} \ll 1 \quad (\text{Condition 2})$$

The reaction system used in this study was the alkaline hydrolysis of p-tolyl acetate. Because the aqueous solubility of p-tolyl acetate is low, the driving force for mass transfer is comparatively small. At the same time, the reaction rate is among the highest obtained for alkaline hydrolysis for aromatic esters of acetic acid (Tommila and Hinshelwood, 1938). Consequently this reaction system satisfies conditions 1 and 2, and is thus well-suited for determination of mass-transfer coefficients through the measurement of reaction rates.

When Conditions 1 and 2 are both satisfied,  $C_A$  is approximately zero, and the mass balance on A in the continuous phase may be written

$$\frac{dC_A}{dt} = -K_L a C_{Ai} \quad (\text{Equation 2})$$

where  $C_{Ai}$  is the equilibrium solubility of A in the aqueous phase. Assuming the formation of the phenoxide goes to completion, two moles of B are consumed per mole of A transferred, giving

$$\frac{dC_A}{dt} = \frac{1}{2} \frac{dC_B}{dt} \quad (\text{Equation 3})$$

Combining Equations 2 and 3 gives an expression for the interphase transfer rate of A per unit surface area ( $R_A$ ):

$$R_A = -\frac{1}{a} \left( \frac{1}{2} \frac{dC_B}{dt} \right) = K_L C_{Ai} \quad (\text{Equation 4})$$

Equation 4 indicates that  $K_L$  can be calculated from  $a$ , the rate of disappearance of B, and  $C_{Ai}$ .

The equilibrium solubility of non-electrolytes can be strongly affected by the presence of salts. This phenomenon, known as the "salting" effect, results from the activity coefficient of the non-electrolyte changing with the electrolyte concentration. Using thermodynamic considerations, Long and McDevit (1952) proposed the following expression to describe this effect for low non-electrolyte concentrations:

$$\ln \left( \frac{C_{Aw}}{C_{Ai}} \right) = K_s I \quad (\text{Equation 5})$$

where

$I$  = concentration of the electrolyte in solution

$K_S$  = salt parameter for electrolyte-nonelectrolyte interaction

The above expression, which is of the same form as the Setshenow Equation (Setshenow, 1889), was used by Nanda and Sharma (1966) to correlate the solubility of liquids in electrolyte solutions.

Using Equation 5,  $C_{Ai}$  can be expressed as

$$C_{Ai} = C_{Aw} \exp(-K_S I) \quad (\text{Equation 6})$$

where  $C_{Aw}$  is the equilibrium solubility concentration of the ester in pure water.

Substituting Equation 6 into Equation 4 gives:

$$R_A = K_L C_{Aw} \exp(-K_S I) \quad (\text{Equation 7})$$

Equation 7 indicates that a semi-log plot of  $R_A$  vs.  $I$  should give a straight line having a slope of  $-K_S$ .

The value of  $a$  can be computed from the Sauter mean diameter  $\overline{d}_{32}$  as shown below:

$$a = 6 \frac{\phi}{\overline{d}_{32}} \quad (\text{Equation 8})$$

where  $\phi$ , the void fraction of the dispersed phase, is defined as the ratio of the volume of nonpolar phase to the total volume. For most of the experiments presented in this paper,  $\phi$  was 0.0035. At such a low void fraction, the CLA

rarely collide, so coalescence can be ignored (Fernandes and Sharma, 1967).

The following expression (Tsouris and Tavlarides, 1994) can be used to describe the effect of  $\phi$  on the maximum stable drop size ( $d_{cr}$ ).

$$d_{cr} = c_m N_{WE}^{-0.6} d_i \left[ 1 + 2.5\phi \left( \frac{\mu_d + 0.4\mu_c}{\mu_d + \mu_c} \right) \right]^{1/2} \quad (\text{Equation 9})$$

The  $d_{cr}$  values calculated using Equation 9 ranged between 180 and 440  $\mu\text{m}$  for the hydrodynamic conditions used in this study. Above this size, drop breakup due to agitation becomes significant and can no longer be neglected. However, the mean drop size of the CLA was in the range of 20-75  $\mu\text{m}$ , with 99% of all drops measured below the  $d_{cr}$ . Hence breakage of CLA was neglected.

The  $K_{L,\text{continuous}}$  values were estimated using the following correlation by Skelland *et al.* (1981).

$$\frac{K_{L,\text{continuous}}}{\sqrt{ND}} = 1.864 \times 10^{-7} \phi^{-0.287} \left( \frac{d_1}{T} \right)^{0.548} (N_{RE})^{1.371} (N_{WE})^{-0.095} \quad (\text{Equation 10})$$

The diffusivity value for p-tolyl acetate in water was calculated from the Wilke-Chang correlation (Wilke and Chang, 1955). The molal volume of the p-tolyl acetate at its normal boiling point was obtained using Le Bas group contributions method (Reid and Sherwood, 1970).

### 3.3 Materials

Deionized water (Resistivity > 18M $\Omega$ -cm) drawn from a Milli-Q Plus<sup>®</sup> water purification system (Millipore Corporation, Bedford, MA) served as the aqueous phase. The dispersed, nonpolar phase was p-tolyl acetate (Aldrich Chemical Company, Milwaukee, WI). Nonionic surfactants were used in both the aqueous

and nonpolar phases. The aqueous-phase surfactant was polyoxyethylene sorbitan monooleate (Tween 80, Aldrich Chemical Company, Milwaukee, WI ), and the nonpolar-phase surfactant was a linear alcohol ethoxylate (Tergitol 15-S-3, Sigma Chemical Company, St. Louis, MO). Because these surfactants do not ionize in aqueous solution (Schick *et al.*, 1967), they do not interfere with measurement of NaOH concentrations using conductivity. The interfacial structure created by this combination of surfactants has been characterized in Chapter 1.

### **3.4 Methods**

#### ***3.4.1 CLA preparation***

The preparation conditions were found to influence the size distribution and stability of the CLA phase; consequently, a consistent preparation procedure was used in all runs. The CLA were prepared in a 50 mL glass beaker with an internal diameter of 40 mm. Five mL of p-tolyl acetate/Tergitol (0.01% v/v to 0.1% v/v ) solution were dispensed at a rate of 0.5 mL/min into a 5-mL volume of aqueous/Tween 80 (0.001% v/v to 0.4% v/v ) solution. A 20 mm magnetic stirring bar spinning at 1600 rpm was used to provide agitation. The resulting CLA emulsions were creamy white, with a phase-volume ratio (PVR) of 1. The PVR is defined as the ratio of the dispersed-phase volume to the aqueous-phase volume. The emulsions were very stable, with no phase separation evident over a period of 6 months.

### **3.4.2 CLA size measurement**

Particle-size distributions of CLA emulsions were measured using a Malvern Mastersizer X particle analyzer (Malvern Instruments, Worcestershire, UK). The instrument was fitted with a 15-mL sample chamber that was mixed using a small Nalgene Star Head magnetic stir bar (Fisher Scientific, Pittsburgh, PA). A 30  $\mu$ L sample of the CLA dispersion was added to 15 mL of deionized water in the cell; the size measurement was then made within 10 s of the CLA addition. The particle size was reported as a  $\overline{d}_{32}$  value.

### **3.4.3 Mass-transfer rate measurement**

Mass-transfer properties of the CLA were measured in a baffled, stirred tank having standard dimensions (McCabe *et al.*, 1993). The Plexiglass tank had an ID of 15 cm and a height of 20 cm. The liquid height in the vessel was maintained at 15 cm. The vessel was fitted with four, equally spaced, vertical, wall baffles with standard dimensions. The six bladed, Rushton impeller had a diameter of 5 cm and was axially centered in the tank 5 cm from the bottom. The impeller was driven using a Lightnin<sup>®</sup> Labmaster II unit (Mixing Equipment Company, Rochester, NY). A wooden shaft was used to minimize the electrical noise in the conductivity measurements. All experiments were conducted at 25°C. To initiate an experiment, the dispersed phase was injected into the vessel close to the rotating impeller using a pipette. The rate of change in alkali concentration was then measured by monitoring electrical conductivity, as recommended by Rushton *et al.* (1964). A YSI 3417 (K=1.0/cm) conductivity

probe (YSI Inc, Yellow Springs, OH),  $\frac{1}{2}$  in OD,  $5\frac{3}{4}$  in overall length used with a YSI Model 32 conductance meter at a range switch setting of  $200 \text{ ms}^{-1}$ . The probe support ring was grounded to the (-) recorder jack to minimize electrical noise in the signal. The output of the conductance meter was recorded by a CAMILE 2000<sup>®</sup> data acquisition system (Dow Chemical Company, Midland MI) at 1-s intervals. The time constant of this probe was much smaller than that of the interphase mass-transfer process, so the mass-transfer dynamics could be measured accurately during the batch runs. The experimental values of  $K_L$  were determined using Equation 4 along with experimental measurements of  $a$ ,  $C_{Ai}$ , and the slope of the  $C_B$  vs. time plot. The slope was determined over the region of the curve during which half of the ester was hydrolyzed.

#### ***3.4.4 Physical-property determination***

The aqueous solubility of p-tolyl acetate was measured using a Perkin-Elmer Autosystems gas chromatograph (Perkin Elmer, Norwalk, CT) equipped with a flame ionization detector and a packed AT-1000 column (Alltech Associates, Deerfield, IL) 0.085" ID x 6' length. Saturated aqueous solutions of p-tolyl acetate were prepared by adding 200  $\mu\text{L}$  of the ester to 1.3 mL of water and vortexing for 15 min. The mixture was then centrifuged at 14,000 rpm for 2 min to separate the phases. Eight hundred microliters of the top (aqueous) phase was drawn, and 4  $\mu\text{L}$  of HPLC grade ethyl acetate was added as an internal standard. One microliter of the resulting sample was injected to the gas chromatograph. The flow rate of the carrier gas was 17 mL/min. The inlet and detector temperatures were  $150^\circ\text{C}$  and  $250^\circ\text{C}$ , respectively. The following

temperature program was used: 60°C for 2 min, followed by a ramp of 20°C/min to 225°C, where the temperature was held for 3 min. The residence times for ethyl acetate and p-tolyl acetate were 2.8 min and 10.1 min, respectively. A response factor ( $R_{ic}$ ) of 0.48 was determined using the following set of standards: 1  $\mu\text{L}$  p-tolyl acetate and 25  $\mu\text{L}$  ethyl acetate in 5 mL of water; 3  $\mu\text{L}$  p-tolyl acetate and 25  $\mu\text{L}$  ethyl acetate in 5 mL of water; and 5  $\mu\text{L}$  p-tolyl acetate and 25  $\mu\text{L}$  ethyl acetate in 5 mL of water. The response factor was then used to calculate the concentration of the p-tolyl acetate in the saturated aqueous solution.

Viscosity was measured using a Brookfield DV-I+ viscometer (Brookfield Engineering Laboratories Inc., Middleboro, MA) using the small-sample adapter. A SC4-18/13R spindle size was used for these measurements at a shear rate of  $132\text{ s}^{-1}$ . The sample volume was 8 mL. Surface tension measurements were made with a Krüss Processor Tensiometer K 12 (Krüss GmbH, Hamburg) using the *Wilhelmy Plate* method. The sample volume was 20 mL.

## **3.5 Results and Discussion**

### ***3.5.1 Physicochemical properties***

The measured physicochemical properties of the fluids are listed in Table 3.1.

**Table 3.1 Physicochemical data for p-tolyl acetate-water system.**

<b>Solubility of p-tolyl acetate in pure water</b>	0.0135 mol/L
<b>Viscosity of p-tolyl acetate</b>	3.75 cP
<b>Surface tension of p-tolyl acetate</b>	31.66 mN/m
<b>Interfacial tension of p-tolylacetate/0.4% Tween 80</b>	4.6 mN/m
<b>Interfacial tension of p-tolylacetate,0.1% Tergitol 15-S-3/0.4% Tween 80</b>	1.75 mN/m
<b>Density of p-tolyl acetate</b>	1.048 g/L
<b>Reaction rate constant for hydrolysis of p-tolyl acetate<sup>a</sup></b>	0.3191 L/(mol s)
<b>Viscosity of water containing 0.4% Tween 80</b>	1.44 cP

<sup>a</sup>obtained from Tommila and Hinshelwood, 1938

### **3.5.2 Effect of Ionic Strength**

The rate of reaction was measured for initial alkali concentrations from 0.5 to 0.75 M (ionic strength of 1.0 to 1.5 M). As shown in Figure 3.1, the semi-log plot of R vs. I is linear, confirming the validity of Equation 7. This experiment was repeated at 300 and 550 rpm. The slopes of the lines obtained at both speeds were almost identical and gave an average  $K_S$  value of 0.60.

### **3.5.3 Mass-transfer coefficients**

Experimentally measured  $K_L$  values are plotted as a function of  $N_{RE}$  in Figure 3.2 for B values of 0.5 and 0.75 M. The  $K_{L,continuous}$  values predicted by the Skelland *et al.* (1981) correlation (Equation 10) are shown for comparison. The  $K_L$  values agree well with the  $K_{L,continuous}$  values up to a  $N_{RE}$  of about 12,500. Above this value the  $K_L$  values become independent of  $N_{RE}$ , while the  $K_{L,continuous}$  values continue to increase.

These trends suggest that the controlling resistance shifts from the continuous phase to the shell as  $N_{Re}$  increases. The structure of the multilamellar surfactant shell, and hence its mass-transfer resistance, should be largely unaffected by the turbulence in the continuous phase. On the other hand, Equation 10 shows that the resistance of the continuous phase ( $1/K_{L,continuous}$ ) should decrease with increasing  $N_{RE}$ . Equation 1 was used to calculate  $K_{L,shell}$  from the experimentally measured  $K_L$  values and the  $K_{L,continuous}$  values obtained using Equation 1. The resulting  $K_{L,shell}$  values ranged from 0.033 to 0.040 cm/s.

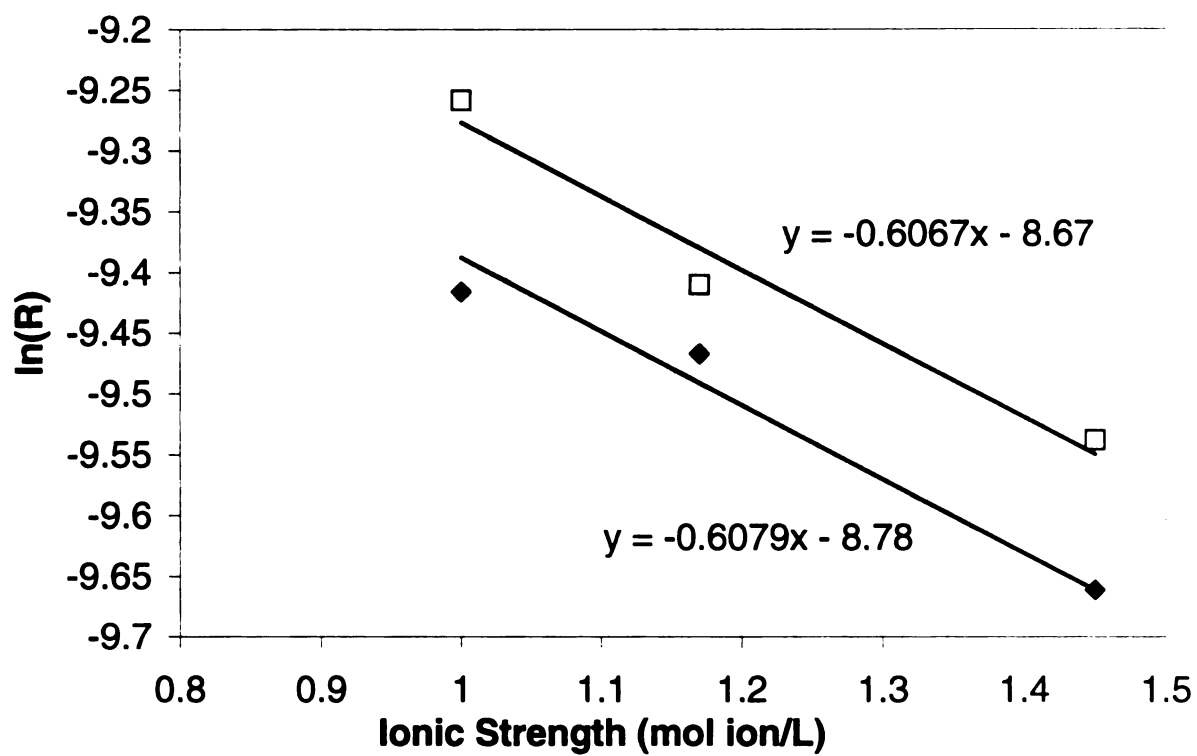


Figure 3.1: Semi log plot of specific reaction rate (R) vs. ionic strength (I) at 550 (□) and 300 (◆) rpm.

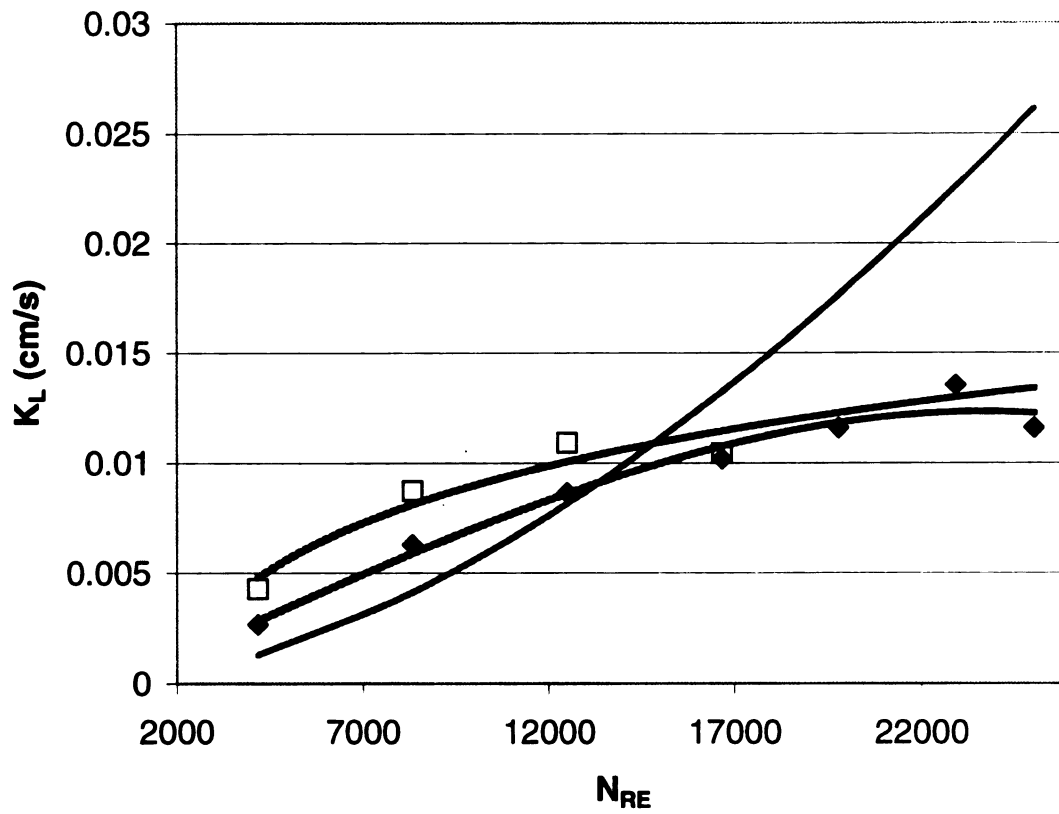


Figure 3.2. Effect of  $N_{RE}$  on  $K_L$  values measured in baffled stirred tank at initial alkali concentrations of 0.75M (□) and 0.5M (◆). The solid line represents the prediction of Equation 9 (Skelland *et al.*, 1981).

The experimentally measured  $K_L a$  values varied from 115 to 450  $\text{h}^{-1}$  over the  $N_{RE}$  range of 4,000 to 25,000, respectively. At a  $N_{RE}$  of 20,000, the  $K_L a$  was 400  $\text{h}^{-1}$ . Rushton *et al.* (1964) measured a volumetric mass-transfer coefficient of 300  $\text{h}^{-1}$  in a batch vessel in a system with similar dispersed phase viscosity (2.5 cP) at the same  $N_{RE}$  but a  $\phi$  value 25 times higher. To compare the mass-transfer efficiency of these two systems on an equivalent basis, the  $K_L a$  values were normalized by dividing by the  $\phi$  values. The resulting  $K_L a/\phi$  values were 114,000  $\text{h}^{-1}$  for CLA system and 5,400 for the system described by Rushton *et al.* This 20-fold difference illustrates the potential of CLA to enhance interphase mass transfer in liquid-liquid contacting operations. The enhancement would be expected to be even greater for contacting operations conducted at lower Reynolds numbers. Thus, the use of CLA offers the simultaneous advantages of extremely high mass-transfer rates and the potential for low agitation power requirements.

#### **3.5.4 Effect of surfactant concentration on $\overline{d_{32}}$ and $K_L$**

The effect of Tween 80 concentration on  $\overline{d_{32}}$  and  $K_L a$  is shown in Figure 3.3, and the corresponding  $K_L$  values are listed in Table 3.2. The  $\overline{d_{32}}$  values for the CLA decreased by about 50% as the concentration of the aqueous-phase surfactant increased from 0.02% to 0.4%. Because  $a$  varies inversely with  $\overline{d_{32}}$ , and the  $K_L$  values were essentially independent of surfactant concentration, the  $K_L a$  values increased by a comparable amount (about 50%) with increasing surfactant concentration.

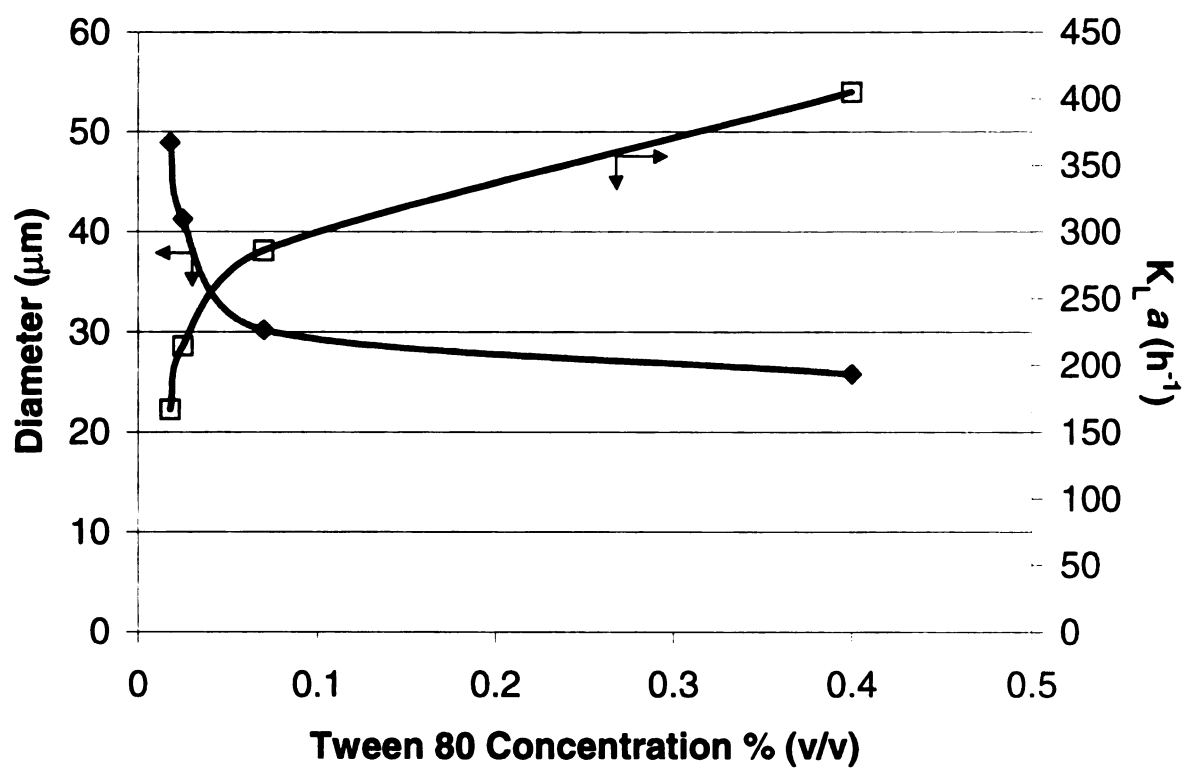


Figure 3.3. Variation of CLA Sauter mean diameter (◆) and volumetric mass transfer coefficient ( $K_{La}$ , □) with Tween 80 concentration (% v/v) in the aqueous phase.

**Table 3.2. Variation of interfacial area ( $a$ ), overall mass-transfer coefficient ( $K_L$ ), and volumetric mass-transfer coefficient ( $K_L a$ ) with Tween 80 concentration in aqueous phase.**

<b>Tween 80 conc (%v/v)</b>	<b><math>d_{32}</math> (<math>\mu\text{m}</math>)</b>	<b><math>K_L a</math> (<math>\text{h}^{-1}</math>)</b>	<b><math>a</math> (<math>\text{cm}^2/\text{cm}^3</math>)</b>	<b><math>K_L</math> (<math>\text{cm/s}</math>) x <math>10^3</math></b>
<b>0.4</b>	<b>25.8</b>	<b>405</b>	<b>8.3</b>	<b>13.5</b>
<b>0.07</b>	<b>30.2</b>	<b>286</b>	<b>7.1</b>	<b>11.1</b>
<b>0.025</b>	<b>41.2</b>	<b>214</b>	<b>5.2</b>	<b>11.5</b>
<b>0.018</b>	<b>48.9</b>	<b>167</b>	<b>4.4</b>	<b>10.6</b>

The result that the  $K_L$  values were relatively unaffected by the surfactant concentration suggests that the thickness of the shell is not significantly affected by the surfactant concentration. Alternatively, any differences in shell thickness may dissipate quickly after the CLA are transferred into the continuous aqueous phase. This transfer step suddenly decreases in the surfactant concentration surrounding the aphrons from greater than the critical micelle concentration (CMC) to far below the CMC. This change creates a large driving force for surfactant migration from the shell into the bulk solution and could lead to a rapid thinning of the shell. This explanation was offered by Bredwell and Worden (1998) to explain the observation that  $K_L$  values measured for surfactant stabilized microbubbles were considerably higher when measured in pure water than when measured in an aqueous surfactant solution above the CMC.

### **3.6 Conclusions**

The interphase mass-transfer properties of CLA emulsions in water have been measured by coupling the mass-transfer of the solute (p-tolyl acetate) to a chemical reaction. The overall  $K_L$  values, which ranged from 0.002 to 0.015 cm/s, increased with  $N_{RE}$  below a  $N_{RE}$  value of about 12,500. Above this value,  $K_L$  was essentially independent of  $N_{RE}$ . These trends suggest that as the degree of agitation is increased, the controlling resistance shifts from the continuous phase to the shell phase. The  $K_L$  values were essentially independent of the surfactant concentration used to prepare the CLA. A resistances-in-series model was used, along with a literature correlation for  $K_{L,continuous}$ , to estimate the  $K_{L,shell}$  value to be about 0.04 cm/s. At a nominal  $N_{RE}$  value of 20,000, the  $K_L a/\phi$  value

measured for CLA was about 20 times higher than that for conventional emulsions.

### 3.7 Nomenclature

$a$  = Interfacial area per unit volume in two phase mixture ( $\text{m}^2/\text{m}^3$ ), defined by  $\frac{6\phi}{d_{32}}$

$C$  = Concentration of solute ( $\text{mol L}^{-1}$ )

$C_{Aw}$  = Equilibrium solubility concentration of the ester in pure water ( $\text{mol L}^{-1}$ )

$D$  = Diffusivity, ( $\text{cm}^2 \text{s}^{-1}$ )

$\overline{d_{32}}$  = Sauter mean diameter defined by  $\frac{\sum n_i d_i^3}{\sum n_i d_i^2}$ , (m)

$d_i$  = Diameter of the impeller, (m)

$d_{cr}$  = Maximum stable drop size, (m)

$I$  = Concentration of the electrolyte or salt in solution ( $\text{mol ion L}^{-1}$ )

$K_L$  = Overall mass-transfer coefficient, ( $\text{cm s}^{-1}$ )

$K_{L,\text{continuous}}$  = Mass-transfer coefficient of the continuous phase ( $\text{cm s}^{-1}$ )

$K_{L,\text{shell}}$  = Mass-transfer coefficient of the CLA shell ( $\text{cm s}^{-1}$ )

$K_R$  = Reaction rate constant ( $\text{L mol}^{-1} \text{s}^{-1}$ )

$K_S$  = Salt parameter for ion - nonelectrolyte interaction ( $\text{L mol}^{-1}$ )

$N$  = Impeller speed, ( $\text{s}^{-1}$ ).

$N_{OH}$  = Ohnesorge number, defined by  $\frac{\mu_c}{\sqrt{\rho_c d_i \sigma}}$

$N_{RE}$  = Reynolds number, defined by  $\frac{\rho_c N d_i^2}{\mu_c}$

$N_{WE}$  = Weber Number, defined by  $\frac{N^2 d_I^3 \rho_c}{\sigma}$

$R_{ic}$  = Response factor defined by  $(C_{\text{analyte}}/C_{\text{std}}) \times (A_{\text{std}}/A_{\text{analyte}})$

T = Tank diameter, (m)

$V_C$  = Volume of the continuous phase, (L)

V = Filled volume of the tank, (L)

### Greek

$\phi$  = Void fraction of dispersed phase, dimensionless

$\mu$  = Viscosity, (Ns m<sup>-2</sup>)

$\rho$  = Density, (kg m<sup>-3</sup>)

$\sigma$  = Interfacial tension, (N m<sup>-1</sup>)

### Subscripts

d = dispersed phase

c = continuous phase

### 3.8 References

- Albright, L. F., and Hanson C. (1975). *Industrial and Laboratory Nitration* (Am. Chem. Soc. Symp. Ser. No. 22), American Chemical Society, Washington D.C.
- Bhave, R.R. and Sharma M.M. (1981). *Trans. Inst. Chem. Eng.*, 59, 161-170.
- Bredwell M.D., Worden R.M. (1998). Mass-transfer properties of microbubbles. 1. experimental studies, *Biotechnology Progress*, 14: (1) 31-38.
- Doraiswamy L.K., Sharma M.M., (1983), *Heterogeneous Reactions: Analysis, Examples, and Reactor Design, Vol 2: Fluid- Fluid-Solid reactions*, John Wiley & Sons, New York, NY p 17.

Fernandes J.B., and Sharma M.M. (1967) *Chem. Engg. Sci.*, 22,1267-1282.

Kafarov, V.V.; Reutli, V. A.; Zhuravleva, T. Yu. (1974), *J. Appl. Chem USSR*, 49(12), 2724.

Long F.A., and McDevit W.F. (1952). Activity coefficients of nonelectrolyte solutes in aqueous salt solutions, *Chem. Rev.* 51, 119-170.

McCabe W.L., Smith J.C., Harriot P (1993). *Unit Operations of Chemical Engineering*, Fifth Edition, McGraw Hill Inc, New York NY.

Nanda A.K. and Sharma M.M. (1966), Effective interfacial area in liquid-liquid extraction, *Chemical Engineering Sci.*, 21, 707-714.

Reid R.C., Sherwood T.K. (1970). *The Properties of Gases and Liquids: their estimation and Correlation*, 2<sup>nd</sup> ed., McGraw Hill book company, New York, NY.

Rushton J. H., Nagata S., Rooney T.R. (1964). Measurements of mass-transfer coefficients in liquid liquid mixing. *AICHE J.* 10 (3), 298-302.

Schick, M.J. (1967), in *Nonionic surfactants*, ed. by Schick M.J., Marcel Dekker Inc. New York. 1-5.

Setschenow,J., *Z. Physik. Chem.*, (1889) 4, 117.

Tommila E, and Hinshelwood C.N. (1938). The activation energy of organic reaction. Part IV. Transmission of substituent influences in ester hydrolysis, *J. Chem. Soc.(London)*, 2, 1801-1810.

Tsouris, C., and L.L. Tavlarides (1994). Breakage and coalescence models for drops in turbulent dispersions, *AICHE J.*, 40, 395-406.

Wilke, C.R., and P. Chang (1955). Correlation of diffusion coefficients in dilute solution, *AICHE J.*, 1, 264.

## Chapter 4

# 4. LIPASE CATALYZED DYNAMIC RESOLUTION OF AMINO ACIDS

### 4.1 Introduction

Chiral drugs are enormously important to both public health and the pharmaceutical industry. Worldwide sales of single-enantiomer drugs surged from \$36 billion in 1993 to \$90 billion in 1997 (Stinson et. al, 1998). The market of single-isomer fine chemicals (drug precursors) to pharmaceutical companies was \$25 billion in 1998 (Rogers, 1999).

Combinatorial chemistry methods are now providing an essentially unlimited number of chemical entities for screening (Brennan, 2000). Once new chemical entities are identified that bind to the desired biological targets and have desirable pharmacokinetics, they must be synthesized in sufficient quantities for clinical trials and, in some cases, commercial production. The ability to synthesize chiral compounds cost-effectively at the commercial scale is important to keeping health-care costs manageable. Enzyme-catalyzed biotransformations are commonly used for production of chiral drugs and drug precursors (Stinson et. al, 1999), often in tandem with conventional chemistry (Broxterman et. al, 1990).

The use of enzymes for biotransformations of drug precursors presents severe processing challenges. Ideal drug candidates would be hydrophobic to

allow passage through cell membranes (Brennan, 2000). Hence, many chiral resolution opportunities involve organic chemicals that are sparingly soluble in water. Low substrate solubility presents special problems when enzyme-based resolution methods are considered. One challenge is finding an enzyme that has activity and the desired stereoselectivity on what usually may be an unnatural substrate. Enzymes have been identified that are enantioselective, yet have broad substrate specificities to convert a non-natural substrate. These enzymes are particularly useful in the production or resolution of carboxylic acids, esters, and alcohols. Another challenge is to design bioreactors that make enzyme-based schemes economically feasible on a commercial scale.

The multiple mass transfer and reaction steps involved in dispersed-phase bioreactor systems make engineering of such systems complicated. Consider the generalized case in which it is desired to produce a resolved carboxylic acid. A preferred enzymatic approach is to use a hydrolytic enzyme, such as a lipase or esterase, to stereoselectively convert an ester to its respective acid and alcohol:



In many of the chiral compounds of commercial interest, the acyl moiety R' contains substituted benzyl, naphthyl, and/or aryl oxy functionalities, which reduce the aqueous solubility of the ester. The resulting acids, however, exhibit significant water solubility since the optimum pH for the reaction is usually above their pK<sub>a</sub> values.

Lipase enzymes have proven particularly valuable for such biotransformations (Patel et. al, 1996). Lipases (triacylglycerol acylhydrolase, E.C. 3.1.1.3) can be viewed as a special class of esterases. Esterases preferentially catalyze the hydrolysis of soluble esters, whereas lipases are distinguished by their ability to catalyze the hydrolysis of insoluble fatty acid esters. Interfaces provided by either aggregated or dispersed substrate in the aqueous medium constitute the primary sites for lipase catalysis. A stepwise increase in activity is observed for lipases when the solubility limit of the substrate is surpassed and substrate aggregates are formed (Entessangles and Desnuelle, 1968). Benzonana and Desnuelle (1965) have pointed out the importance of interfacial area rather than the bulk substrate concentration in determining the reaction rate, and have shown that lipolysis will apparently conform to Michaelis Menten kinetics when substrate concentration is expressed on the basis of interfacial area rather than bulk system volume. Adsorption of the enzyme to the interface may also change its intrinsic catalytic activity either as an immediate consequence of adsorption, or as a slow post adsorptive conformational change (Brockman, 1984).

The commercial potential of lipases and other multiphase enzymatic biotransformations has not been realized, due to processing limitations associated with conventional multiphase contacting systems. These limitations include poor reproducibility, low volumetric productivity, high energy requirement for dispersing the substrate during the reaction step, and difficulty in product separation (Patel et al. 1996). Clearly, more effective methods are needed to

provide intimate contact between the enzyme and its nonpolar substrate (Scott et. al, 1995).

The mass transfer properties of CLA in Chapters 2 and 3 have been characterized. CLA emulsions provide a 5-15 fold rise in interphase volumetric mass transfer rates over conventional emulsion systems. This result suggests that CLA emulsions can be used to enhance the rate of reaction in multiphase enzyme catalysed systems.

## **4.2 Model System**

One multiphase biocatalytic system that could benefit from accelerated mass transfer, is the dynamic resolution of amino acids to produce unnatural D-amino acids. As components of drugs, such amino acids would retain the chiral chemistry needed to bind with the biological target, but might be poor substrates for enzymes that would break the drug down (Stinson, 2000). Recently there has been enormous interest in D-phenylalanine for the development of HIV protease inhibitors (Bosswell, 1999). The Strecker reaction (the addition of cyanide to imines) is a direct strategy for asymmetric synthesis of alpha-amino derivatives. Although significant progress has been made in the stereoselective version of this reaction using imines bearing covalently attached chiral auxiliaries, gains have been limited for an enantioselective catalytic version (Jacobsen, 1999). One approach to purifying unnatural amino acids (D enantiomers) from racemic mixtures is dynamic resolution. This study investigated on the dynamic resolution of D-L Phenylalanine (D, L-PA) using lipase catalyzed hydrolysis of D-L phenylalanine methyl ester (D, L-PAM) (Figure 4.1). The use of CLA as enzyme-

immobilization supports has also been investigated. The amount of lipase immobilized on the CLA droplets formed using a variety of anionic and non-ionic surfactants was measured. Lye et al. (1997) found that when  $\alpha$ -chymotrypsin was immobilized on CLA, only about 1% of the activity was retained. Lamb et al (1999) investigated the immobilization of several other enzymes on CLA. An  $\alpha$ -amylase displayed superactivity when immobilized, while lipase, trypsin and lysozyme were inactivated. Both the above studies utilized sodium dodecyl sulphate, an anionic emulsifier) to form CLA emulsions. Sodium dodecyl sulphate (SDS) is used for estimating polypeptide sizes, either by gel-electrophoresis or by molecular-sieve chromatography, and is known to bind with water soluble proteins causing them to form rod like shapes that are then separated by the gel (Muga et al. 1993). Such a binding would disrupt the protein structure and function. The objective of this study was to identify a surfactant that interacts only weakly with the enzyme, so as to prevent protein refolding and denaturation. CLA emulsions formed using such a surfactant would provide high rates of mass transfer, while retaining the activity of the enzyme responsible for the resolution reaction.

Further, the influence of various environmental parameters such as pH, enzyme concentration and interfacial area on lipase catalyzed dynamic resolution of D-L phenylalanine in CLA emulsions has been studied.

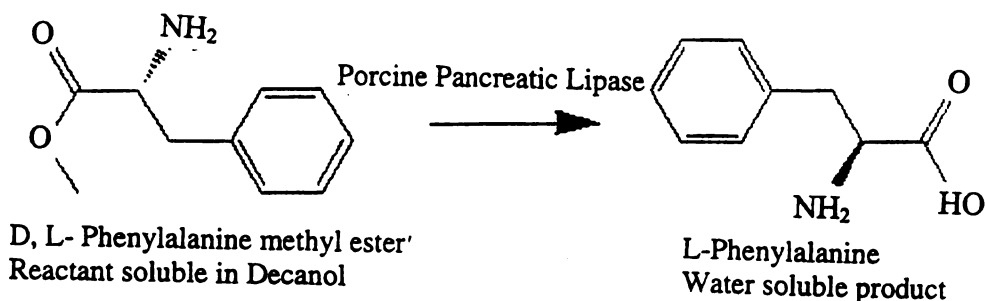


Figure 4.1 Lipase catalysed resolution of D,L-Phenylalanine using hydrolysis of D,L Phenylalanine methyl ester (PAM).

### 4.3 Materials and Methods

All the solvents used were HPLC grade. Water and methanol were obtained from JT Baker (Philipsburg, NJ, USA). Acetonitrile was obtained from EM Science (Gibbstown NJ). Buffer solutions ranging from pH 3 to pH 7 were prepared using the recipes described in Dean (1992). Table 1 outlines the recipes used to make the buffer solutions. Both the sodium phosphate dibasic and the citric acid were obtained from Sigma Chemical Company (Milwaukee, WI) and were ACS reagent grade.

Table 4.1. Buffer recipes for chiral resolution experiments

pH	x mL of 0.2 M Na <sub>2</sub> HPO <sub>4</sub> · 2H <sub>2</sub> O (35.599 g · L <sup>-1</sup> )	y mL of 0.1 M Citric Acid (19.213 g · L <sup>-1</sup> )
3	20.55	79.45
4	38.55	61.45
5	51.5	48.5
6	63.15	36.85
7	82.35	17.65

Crude porcine pancreatic lipase (SIGMA 3126, Sigma Chemical Company, Milwaukee, WI) was used as the biocatalyst in this study. This crude extract was analyzed for protein content using a Bradford DC protein assay. Bovine Serum Albumin was used as a standard for protein quantitation. Surfactants used in this study include Polyoxyethylene sorbitan monooleate (Tween 80), Polyoxyethylene sorbitan monolaurate (Tween 20), Sodium dodecyl sulphate (SDS), Hexadecyl trimethyl ammonium bromide (HTAB), and Tetradecyl trimethyl ammonium bromide (TTAB). Tween 80 and Tween 20 are non ionic emulsifiers, SDS is anionic and HTAB and TTAB are cationic emulsifiers. All the above emulsifiers were obtained from Sigma Chemical Company, Milwaukee, WI.

#### ***4.3.1 Experimental Methods***

##### ***4.3.1.1. Immobilization efficiency***

Immobilization experiments were carried out in 50ml total volume, containing 40mL of pH5 buffer solution, 80mg of surfactant (0.2%), 80mg of crude enzyme. A 0.5 mL sample was drawn from this solution. 10mL of decanol was added, followed by vigorous agitation to form CLA emulsions. The emulsion was allowed to cream and the aqueous phase was sampled using a micropipette. The protein content was determined using the Bradford DC protein assay. Calibration curves were constructed for each surfactant system and used to determine the amount of protein present in the samples. The percentage of enzyme immobilized was calculated based on the difference between the amount of enzyme present in the samples before the decanol was added and those taken after the CLA dispersion was formed.

#### *4.3.1.2. Chiral resolution experiments*

D,L- Phenylalanine methyl ester hydrochloride (Sigma Chemical Company) was dissolved in water in a separatory funnel and overlaid with a layer of diethyl ether. The water phase was neutralized with 25% stoichiometric excess of 10M NaOH solution accompanied by rigorous shaking. During this process the phenylalanine methyl ester (Phe-Me), formed by neutralization of the hydrochloride, was extracted into the ether phase. The phases were allowed to separate, and then pure Phe-Me was obtained by evaporation of the ether under vacuum. The ester was weighed, and stock solution of the ester in decanol was prepared. Over 90% yield was obtained in this process.

The experiments were conducted in 100 mL glass bottles. The appropriate amount of buffer was added to the bottle. Tween 80 (Aldrich Chemical Company, Milwaukee, WI) was added to the bottle and vortexed to ensure proper mixing. Decanol, which was used as the dispersed organic phase, forms molecular complexes with Tween 80 leading to the formation of lamellar micelles that stabilize CLA emulsions, as discussed in Chapter 1. The Phe-Me stock solution was dispersed into the aqueous phase and vigorously stirred to form CLA emulsions. The CLA emulsions formed were creamy white and extremely stable, with no phase separation evident over a period of several months. Appropriate amounts of crude lipase were weighed and added to the bottle, followed by vortexing for 30 seconds to ensure complete mixing. The bottle was then placed in a water bath (25°C) in an INNOVA 3000 platform shaker (New Brunswick Scientific Co. NJ) and shaken at 200 rpm. Samples were taken using 1 mL

syringes and placed in 10 mL vials after passing through a 25 mm Acrodisc<sup>®</sup> 0.2  $\mu\text{m}$  syringe filter (Pall Gelman, Ann Arbor, MI) to remove CLA droplets. This process was also effective in removing protein, as confirmed by adsorption of the filtered sample at 280nm.

#### *4.3.1.3. HPLC assay*

A common approach to separate enantiomers by chromatography is the use of a homo-chiral (single-enantiomer) derivatizing agent (HDA), which reacts with the two enantiomers to be distinguished (Gal, 1987). In this study, 2,3,4,6 tetra-O-acetyl-  $\beta$ -D- glucopyranosyl isothiocyanate (TAGIT) was utilized. This reagent reacts with primary or secondary amines to yield corresponding thiourea derivatives. The reaction products of TAGIT with L-D phenylalanine are shown in Figure 4.2. The two products of the reaction are no longer enantiomerically related, but are diastereomers. Unlike enantiomers, diastereomers have slightly different physical properties and can be separated under reversed-phase conditions using a C<sub>18</sub> HPLC column. The derivatization procedure used is a modification of the method of Kinoshita et al. (1981). Forty  $\mu\text{L}$  of sample was added to a 20 ml glass scintillation vial, along with 1 mL of 1% (v/v) triethyl amine (Spectrum Quality Prod., Gardena, CA) solution in water and 1 mL of TAGIT (Fluka Chemie AG, Buchs, Switzerland) stock in acetonitrile (0.1 g/10 g). The vial was vortexed for 10 seconds and placed on a shaker for 1hr at 200 rpm. The chromatographic system consisted of a WATERS 600 solvent delivery system, a reversed phase C<sub>18</sub> HPLC column (Novapak<sup>®</sup> C<sub>18</sub>, 3.9x150 mm, 4  $\mu\text{m}$  particles, WAT086344, Waters Corp, Milford, MA) and a Water 490 multiple

wavelength UV detector. The column was eluted at room temperature and at a flow rate of 1 mL/min with a mobile phase prepared by mixing 0.2 M pH 5 acetate buffer and methanol in a ratio of 55:45. The wavelength used for detection of the eluent was 250 nm. The retention times for L-phenylalanine and D-phenylalanine were 6.26 min and 9.41 min respectively. Response factors for the L and D diastereomers (429,726 and 474,434 respectively), were determined by running standards (in triplicate) between 0.125 g/L and 20 g/L. The reagent peaks were well separated from those of the amino acids and did not interfere with the detection. A sample chromatogram of the separation obtained is shown in Figure 4.3.

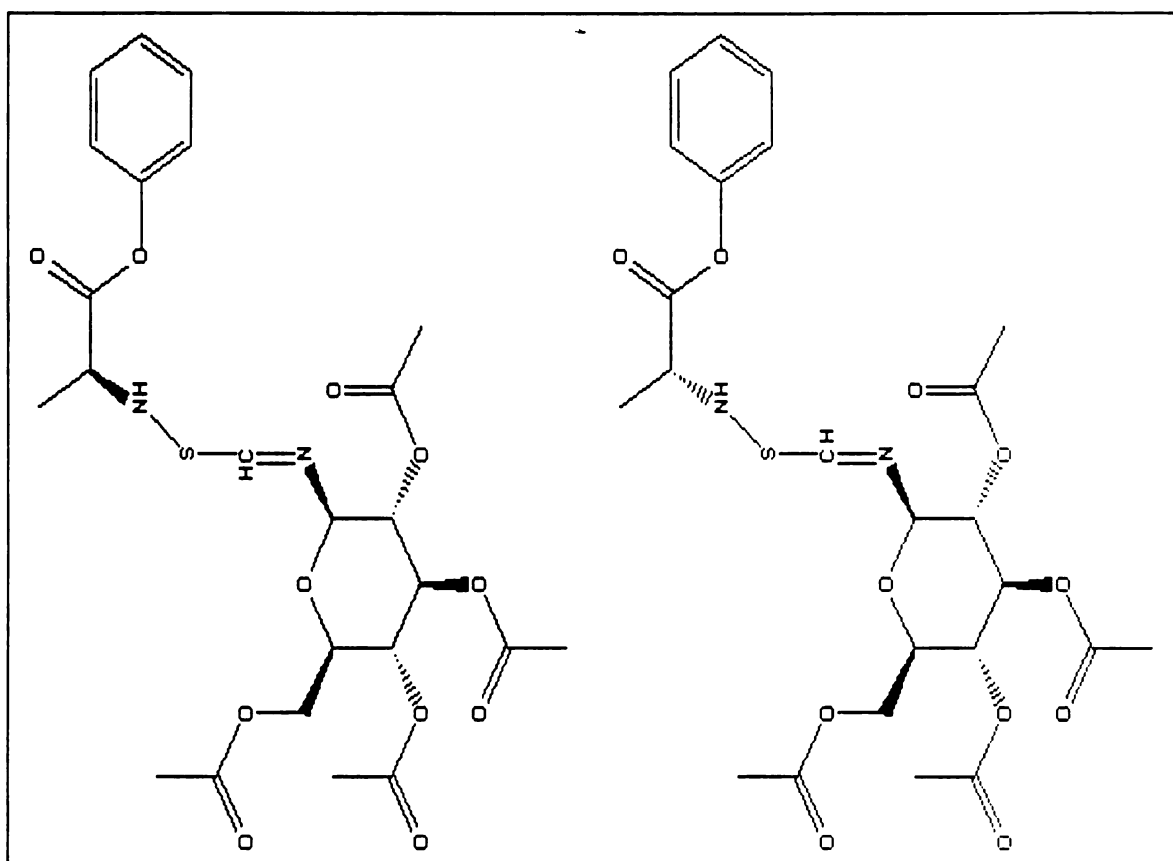


Figure 4.2. Reaction products of L,D PA with TAGIT

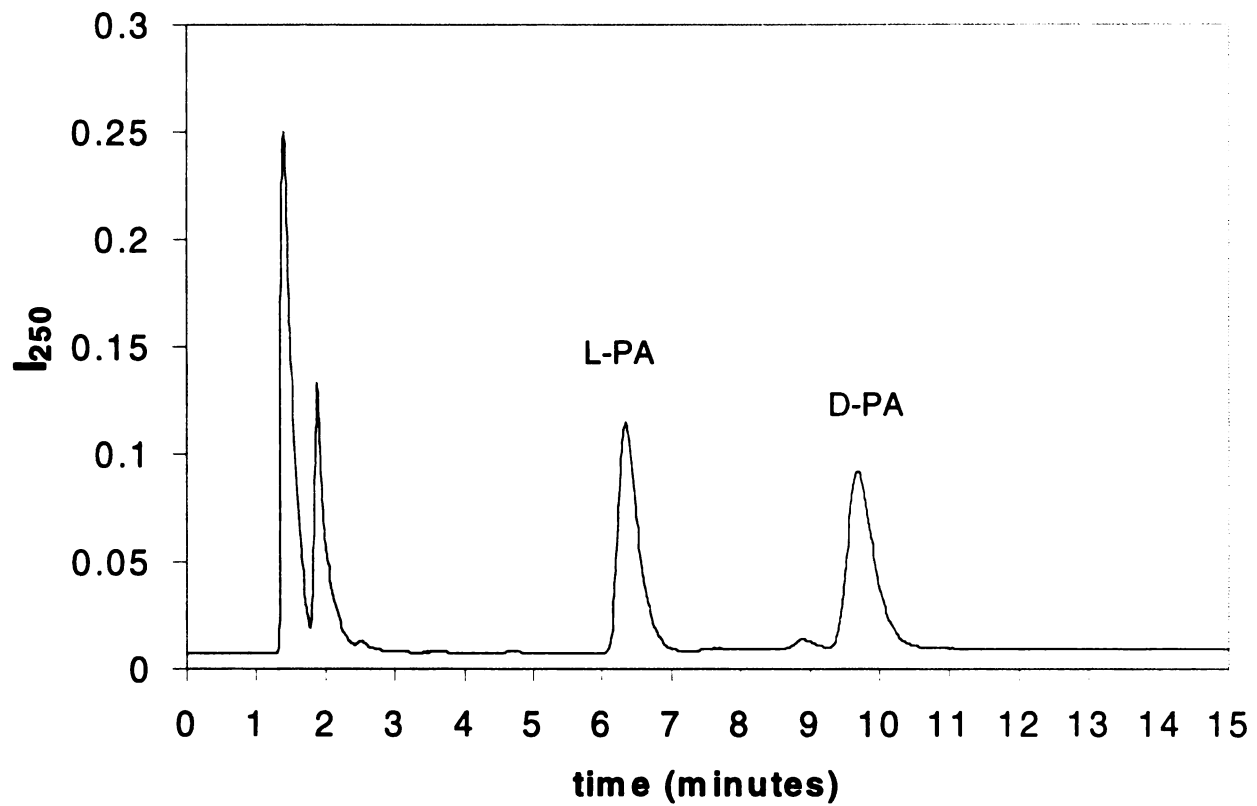


Figure 4.3. Sample HPLC Chromatogram of the enantiomeric separation of L and D Phenylalanine

### **4.3.2 Conversion and enantiomeric excess measurements**

A statistical experimental design, (central composite design) was implemented to determine the effect of process parameters and physical conditions on the equilibrium conversion and enantiomeric excess of the lipase catalyzed dynamic resolution reaction. Five factors were identified for the experiments, namely:

- 1) Surfactant concentration in aqueous phase
- 2) Void fraction
- 3) Amount of enzyme present
- 4) pH
- 5) Concentration of Phe-Me in the decanol phase

The experimental design involved running 32 experiments. Details on the factors studied and the levels chosen are discussed in the next section.

#### **4.3.2.1. Central Composite Design**

The central composite design (CCD) is an efficient design for fitting second order models that account for curvature effects in the response variable (Montgomery, 1997). A quadratic response to some of the variables was expected, most notably, to pH, because most enzymes exhibit an activity maximum at an intermediate pH. The design included a half fraction of  $2^5$  experiments with seven replicates on the center point of the design, augmented with nine points outside the five dimensional cubic space explored by the factorial

experiments. Regression was used to determine the linear main effects, curvature effects and interaction effects of the above mentioned variables. The solubility of L- phenylalanine is 29.6 g/L at 25°C (Kroschwitz et al., 1987). This places a constraint on the void fraction of the oil phase and concentrations of the Phe-Me in the oil phase that can be utilized in the chiral resolution process. The range of void fraction studied (20-40%), combined with the concentration range (0.1 M to 0.3 M) satisfies this constraint, maintaining maximum possible concentration of the product, L-phenylalanine, below 20g/L. Surfactant concentrations were chosen to be in the range of 0.2-0.4%. The center point of the CCD was chosen as void fraction 30%, pH 5 buffer containing 0.3% surfactant, 80 mg crude enzyme and 0.2M Phe-Me in decanol. The entire statistical design is shown in Table 4.2. Table 4.3 provides the coding for each individual variable. For example, Table 4.3 indicates that scaled variable P is given by the relation  $(\text{pH}-5)/1$ . Therefore, a value of P=1 in Table 4.2 would correspond to a pH of 6 in the experiment. The half fraction of the  $2^5$  set and the six center points were run first in the (random) order listed. An additional center point experiment and the axial experiments were run next.

Table 4.2. Central Composite Design  
(coded variables are defined as shown in Table 4.3)

Run	S	E	V	P	C
1	0	0	0	0	0
2	-1	1	1	1	-1
3	-1	-1	-1	-1	1
4	1	1	1	1	1
5	0	0	0	0	0
6	1	-1	1	-1	1
7	-1	1	1	-1	1
8	0	0	0	0	0
9	1	1	-1	-1	1
10	1	1	-1	1	-1
11	1	-1	-1	-1	-1
12	-1	-1	-1	1	-1
13	-1	1	-1	-1	-1
14	0	0	0	0	0
15	-1	1	-1	1	1
16	1	-1	1	1	-1
17	0	0	0	0	0
18	-1	-1	1	1	1
19	1	-1	-1	1	1
20	0	0	0	0	0
21	-1	-1	1	-1	-1
22	1	1	1	-1	-1
23	0	0	-2	0	0
24	0	0	2	0	0
25	0	0	0	-2	0
26	0	0	0	2	0
27	0	-2	0	0	0
28	0	2	0	0	0
29	0	0	0	0	2
30	-2	0	0	0	0
31	2	0	0	0	0
32	0	0	0	0	0

Table 4.3 Coding of variables for Central Composite Design

S	(Surf conc (%)-0.3)/0.05
E	(Enzyme amount(mg)-80)/25
V	(Void fraction(%) -30)/10
P	(pH-5)/1
C	(Concentration in decanol (Molar)-0.2)/0.1

## 4.4 Results and discussion

### 4.4.1 Enzyme interactions with CLA

The percentage enzyme immobilized for different surfactant systems is shown in Table 4.4. CLA emulsions made with nonionic surfactants (Tween 80 and Tween 20) appear to have low carrying capacity for the lipase enzyme. However, cationic or anionic surfactants appeared to immobilize 30-50% of the enzyme. Accounting for the purity of the crude enzyme (33%), it appears that about 2mg of pure lipase/ mL CLA is immobilized in the ionic surfactants. This value agrees well with the result obtained by Lye and Stuckey (1998). Lye and Stuckey (1998) have reported that pH had a strong effect on the binding of enzyme to CLA formed using ionic emulsifiers. However, in case of nonionic emulsifiers pH is not expected to affect enzyme binding to CLA, since their interactions are mainly hydrophobic. This expected trend was confirmed by the experimental results shown in Table 4.5.

Table 4.4 % Enzyme immobilized using different nonionic and emulsifiers to form CLA emulsions at pH 5.

Surfactant used	% immobilized
Tween80	8
Tween20	26
HMB	47.5
TTAB	45.3
SLS	31.2

Table 4.5 Effect of pH on % enzyme immobilized on CLA emulsions formed using Tween 80.

pH	% immobilized
4	12%
5	8%
6	11.20%
7	7.80%

#### **4.4.2 Reaction rate measurements**

Figure 4.4 shows the variation of conversion with time for experiments with and without CLA emulsions. It is evident that the equilibrium is attained within 1 h in the presence of CLA under these conditions, compared to over 4 h in the absence of CLA. This indicates that the CLA enable better contacting and faster rates of approach to equilibrium for this process.

#### **4.4.3 Chiral Resolution**

Data for equilibrium conversion ( $Y_c$ ) and enantiomeric excess ( $Y_{ee}$ ) are shown in Table 4.6. The data were analyzed using a linear regression procedure within the statistical computer package MINITAB. Polynomial models, which relate  $Y_c$  and  $Y_{ee}$  to the process variables through linear, quadratic and interaction coefficients, were fitted.

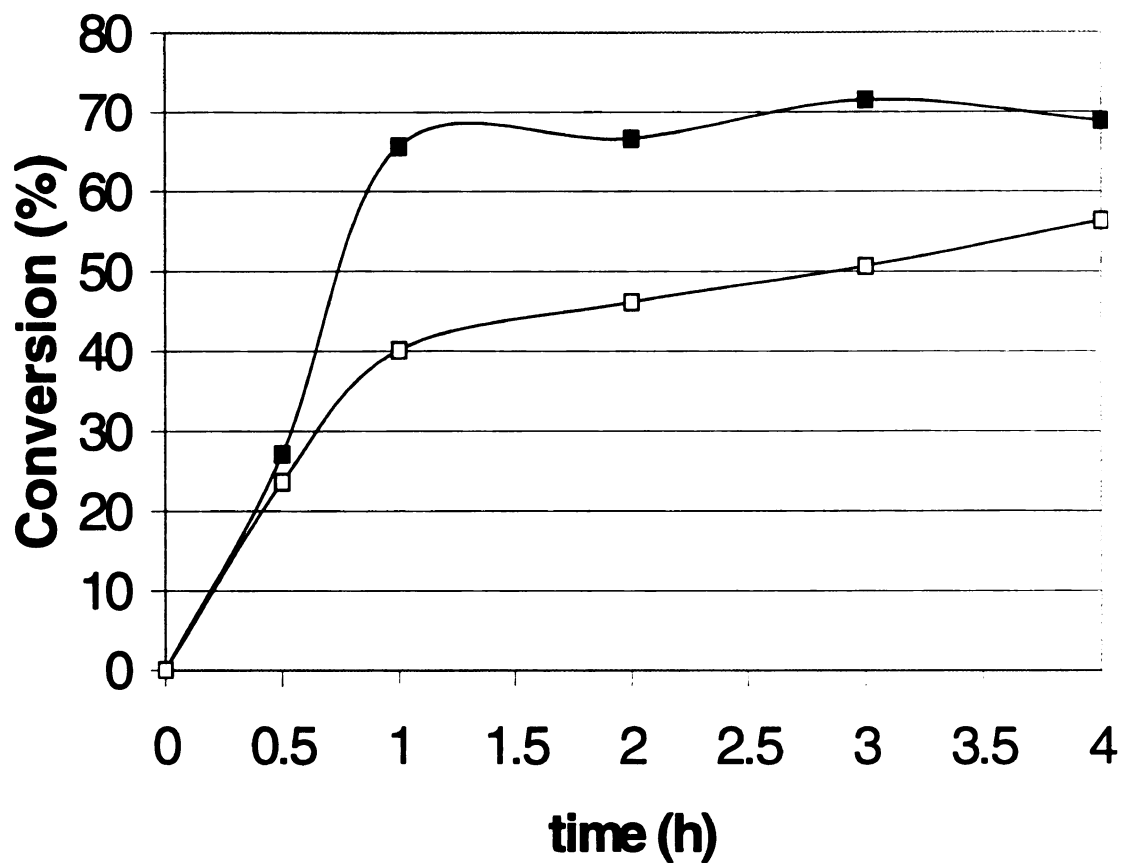


Figure 4.4 Conversion vs. time for chiral resolution experiments with (■) and without (□) CLA dispersions. Reaction conditions: pH 5, Void fraction 30%, 80 mg crude enzyme, 0.2M Phe-me in decanol.

Table 4.6. Experimental data for chiral resolution experiments.

Run #	Surf conc. %	Enzyme amount mg	Void Fraction %	pH	Conc. in Decanol (Molar)	Conversion $Y_c$	Enantiomeric Excess $Y_{ee}$
1	0.30	80	30	5	0.2	70.69	92.44
2	0.25	105	40	6	0.1	65.44	86.32
3	0.25	55	20	4	0.3	22.79	87.67
4	0.35	105	40	6	0.3	69.68	83.86
5	0.30	80	30	5	0.2	63.46	94.01
6	0.35	55	40	4	0.3	28.59	83.47
7	0.25	105	40	4	0.3	66.46	95.26
8	0.30	80	30	5	0.2	67.84	94.26
9	0.35	105	20	4	0.3	23.90	87.91
10	0.35	105	20	6	0.1	96.20	90.94
11	0.35	55	20	4	0.1	7.09	21.68
12	0.25	55	20	6	0.1	93.77	91.35
13	0.25	105	20	4	0.1	7.38	31.26
14	0.30	80	30	5	0.2	67.94	95.56
15	0.25	105	20	6	0.3	62.55	86.73
16	0.35	55	40	6	0.1	51.67	85.49
17	0.30	80	30	5	0.2	60.31	84.37
18	0.25	55	40	6	0.3	53.35	85.54
19	0.35	55	20	6	0.3	53.83	80.87
20	0.30	80	30	5	0.2	61.20	88.00
21	0.25	55	40	4	0.1	18.81	59.06
22	0.35	105	40	4	0.1	25.74	63.22
23	0.3	80	10	5	0.2	39.63	88.87
24	0.3	80	50	5	0.2	63.52	91.20
25	0.3	80	30	3	0.2	5.67	25.02
26	0.3	80	30	7	0.2	58.00	87.05
27	0.3	30	30	5	0.2	55.93	88.62
28	0.3	130	30	5	0.2	69.16	91.29
29	0.3	80	30	5	0.4	68.72	90.56
30	0.2	80	30	5	0.2	64.50	91.27
31	0.4	80	30	5	0.2	62.92	91.59
32	0.30	80	30	5	0.2	57.80	90.51

#### 4.4.3.1. Conversion ( $Y_c$ )

The results of a statistical analysis of the data are shown in Table 4.7. The plot of the residual vs. the fitted  $Y_c$  values (Figure 4.5) revealed the Run 25 has an unusually high residual compared to the rest of the data. The fitted value for this data point is negative, which is physically unrealizable. This experiment contributes heavily to the large standard deviation (8.14) observed for this model compared to the standard deviation (4.74) of the replicates for the center point of the design. Ignoring experiment 25 as an outlier, the rest of the data were refitted using the linear regression technique. This analysis was used to select the statistically most significant variables ( $p < 0.05$ ). The model was then refitted using only the selected variables. The results of the statistical analysis are given in Table 4.8. This fitted linear regression model is given as Equation 1.

$$Y_c = 63.83 + 4.40 E + 2.85 V + 21.4 P - 3.34 V^2 - 12.7 P^2 + 3.31 SE \\ + 3.38 EV - 9.56 VP + 6.63 VC - 9.92 PC \quad \text{(Equation 1)}$$

This equation shows that the most significant variables are the main effects E, V, P, quadratic terms for V, P, and some interaction effects namely VP, PC, PE, PC, SE. Plotting the residuals in time order of data collection is helpful in detecting the correlation between the residuals. A tendency to have runs of positive and negative residuals indicates positive correlation. This would imply that the independence assumption on the errors has been violated. A plot of residual vs. order of data is shown in Figure 4.6a. The variance from each run seems completely uncorrelated, so there is no reason to suspect any violation of

Table 4.7 Regression analysis for data presented in Table 4.6

The regression equation is

$$Y_c = 64.9 + 4.4 E + 18.4 P - 3.97 V^2 - 8.90 P^2 - 9.56 VP + 6.63 VC - 9.92 PC$$

Predictor	Coef	Stdev	T	P
Constant	64.905	3.029	21.43	0
S	-1.196	1.663	-0.72	0.487
E	4.4	1.663	2.65	0.023
V	2.846	1.663	1.71	0.115
P	18.42	1.663	11.08	0
C	2.098	1.978	1.06	0.312
S"	-0.937	1.509	-0.62	0.547
E"	-1.227	1.509	-0.81	0.433
V"	-3.968	1.509	-2.63	0.023
P"	-8.904	1.509	-5.9	0
C"	-1.371	1.986	-0.69	0.505
SE	3.307	2.037	1.62	0.133
SV	-0.913	2.037	-0.45	0.663
SP	1.13	2.037	0.55	0.59
SC	-1.01	2.037	-0.5	0.63
EV	3.377	2.037	1.66	0.125
EP	0.21	2.037	0.1	0.92
EC	2.019	2.037	0.99	0.343
VP	-9.56	2.037	-4.69	0.001
VC	6.631	2.037	3.26	0.008
PC	-9.919	2.037	-4.87	0

Analysis of variance

Source	DF	SS	MS	F	P
Regression	20	15936.73	796.84	12.01	0
Residual Error	11	730.12	66.37		
Total	31	16666.86			

S = 8.147    R-Sq = 95.6%    R-Sq(adj) = 87.7%

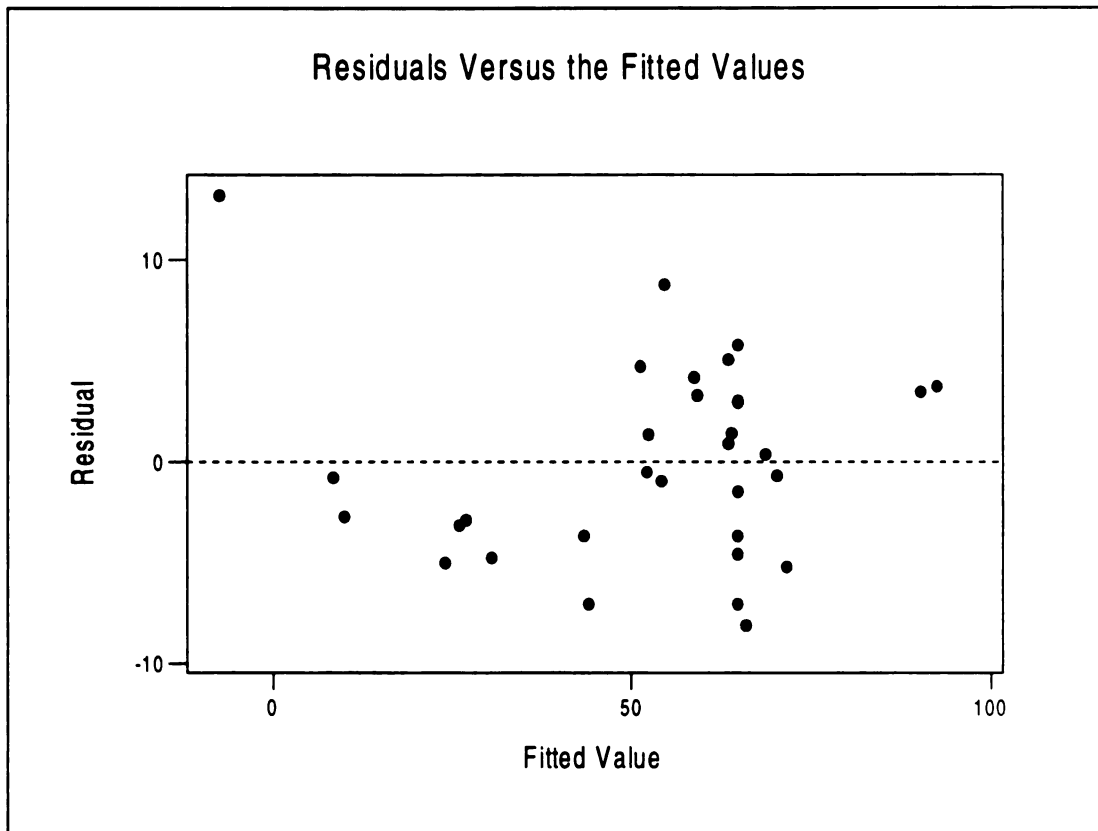


**Figure 4.5 Residuals vs. fitted values for full set of experimental data. (Note: The fitted value for one of the data points (experiment 25) is negative, and the residual is extreme)**

Table 4.8. Regression analysis results for model represented by Equation 1.

$$Y_c = 63.83 + 4.40 E + 2.85 V + 21.4 P - 3.34 V^2 - 12.7 P^2 + 3.31 SE + 3.38 EV - 9.56 VP + 6.63 VC - 9.92 PC$$

Predictor	Coef	StDev	T	P
Constant	63.83	1.364	46.79	0
E	4.4	1.021	4.31	0
V	2.846	1.021	2.79	0.011
P	21.369	1.199	17.82	0
V <sup>2</sup>	-3.3433	0.9254	-3.61	0.002
P <sup>2</sup>	-12.703	1.221	-10.4	0
SE	3.307	1.251	2.64	0.016
EV	3.377	1.251	2.7	0.014
VP	-9.56	1.251	-7.64	0
VC	6.631	1.251	5.3	0
PC	-9.919	1.251	-7.93	0

S = 5.004 R-Sq = 96.5% R-Sq(adj) = 94.8%

#### Analysis of variance

Source	DF	SS	MS	F	P
Regression	10	13863	1386.3	55.37	0
Residual Error	20	500.7	25		
Total	30	14363.8			

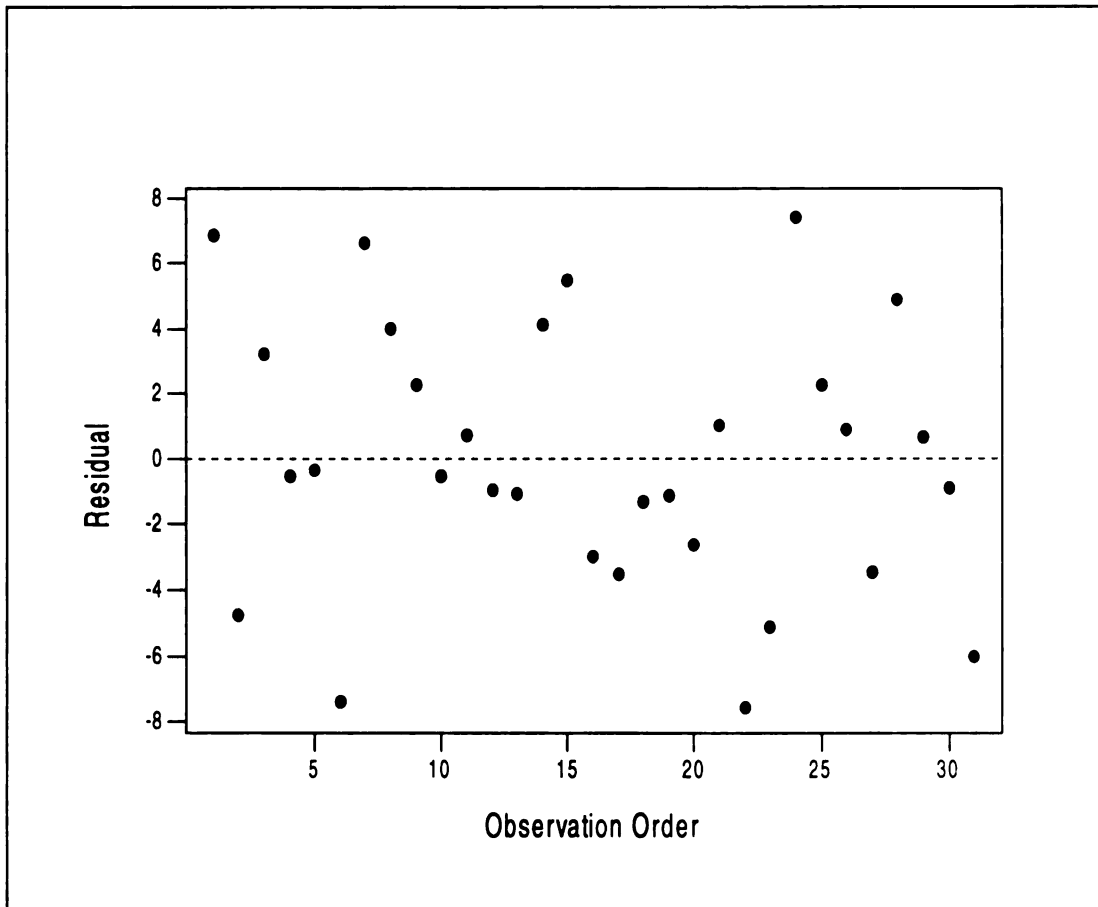


Figure 4.6a. Plot of residuals vs. order of data for regression model represented by equation 1.

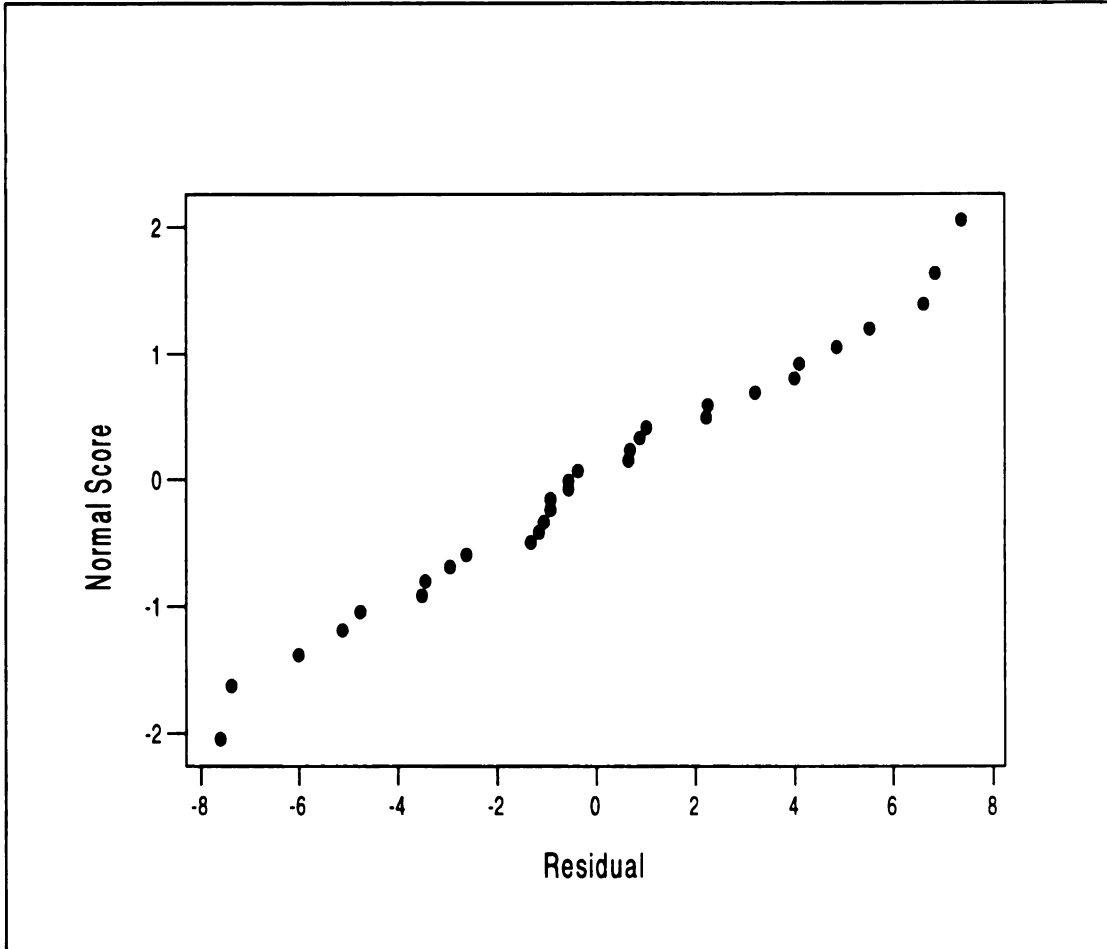


Figure 4.6b. Normal Probability plot for residuals based on Equation 1.

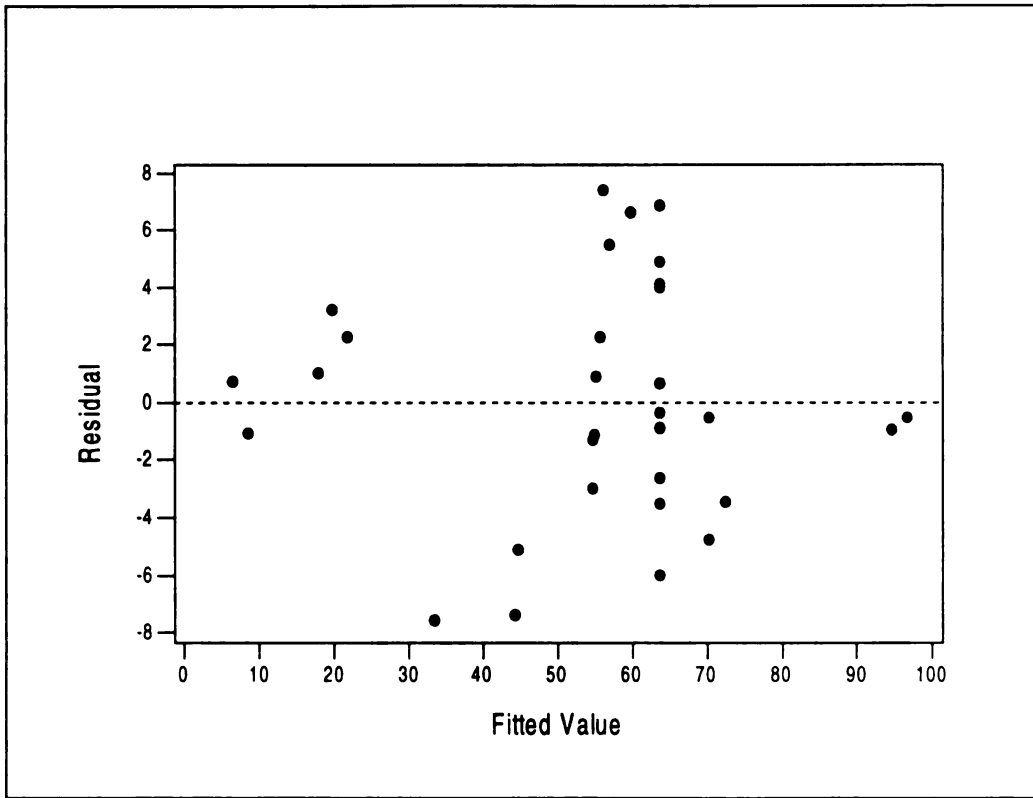


Figure 4.6c. Plot of residuals vs. Fitted values for regression model given by Equation 1.

the independence or constant-variance assumptions. The normal probability plot is shown in Figure 4.6b. The plot of the residuals vs. fitted values (Figure 4.6c) does not reveal an obvious pattern, indicating the adequacy of the model and its assumptions. The model presented as Equation 1 is obviously empirical, but it does highlight the effects in the response variables caused by the various factors.

Mechanistic aspects of the significant effects of each parameter is considered separately below:

1) Concentration of surfactant (S):

Within the range studied (0.2% -0.4%) Tween 80 concentration does not seem to affect the equilibrium conversion or the enantiomeric excess significantly. Weak interaction effects are present between amount of enzyme (E) and surfactant concentration (S). Although these effects are statistically significant, their influence on conversion is small from a process standpoint. In the presence of CLA, the volumetric rate of reaction may be limited by enzyme concentration and hence raising the concentration of the surfactant (i.e. reducing droplet size (Chapter 2) does not affect the reaction.

2) Amount of Enzyme (E):

The positive coefficient in the regression model for the main effect of enzyme concentration indicates that the higher the concentration of the enzyme the greater the conversion. This would imply that the system is reaction rate limited, rather than mass transfer limited. This interpretation is consistent with the

previous observations of the effect of surfactant concentration. However the increase in conversion obtained by raising enzyme concentration is not significant, due to the counteracting effects of the interaction terms (EV, since V is favored at low levels as discussed later in this section).

### 3) pH of the aqueous phase (P)

The pH of the continuous phase buffer seems to be the single most significant factor in the system. The presence of the quadratic term indicates curvature in the response variable. Since most enzymes have optimal pH, this trend is as expected. The interaction term between void fraction and pH, represented by VP, is also significant, suggesting a change in conformation of the active site for the enzyme. The conformation of the site would be affected by ionization (pH) as well as presence of water affecting protein folding collectively.

### 4) Void fraction (V):

The void fractions of substrate and water are critically important to the course of hydrolytic reaction. Both the main effect and the quadratic terms for void fraction are statistically significant, in addition to interactive effects with other variables. If a large amount of water is used, a high degree of hydrolysis may be achieved. However, higher amounts of water imply lower volumes of the oil phase containing substrate, and hence the total mass produced in the reactor would be lower. On the other hand, with smaller amounts of aqueous phase, the reverse reaction becomes significant due to increased concentration of methanol and decreased availability of water needed for hydrolysis. There is a significant interaction term between pH and void fraction. These terms combined, lead to

high equilibrium conversion at high pH and low void fractions as shown in the contour plot (Figure 4.7).

#### 5) Concentration of reactant in the decanol phase (C)

The signs of the various interaction terms (PC, VC) containing the reactant concentration C as a variable, coupled with the main effect of those variables (V and P) indicate that low reactant concentrations favor high equilibrium conversions. However, a lower mass yield also would result due to low concentrations in the organic phase. Figure 4.8 shows the effect of high concentrations at different void fractions, indicating that if a high mass yield is desired, high concentration would be favored at the expense of poorer equilibrium conversion.

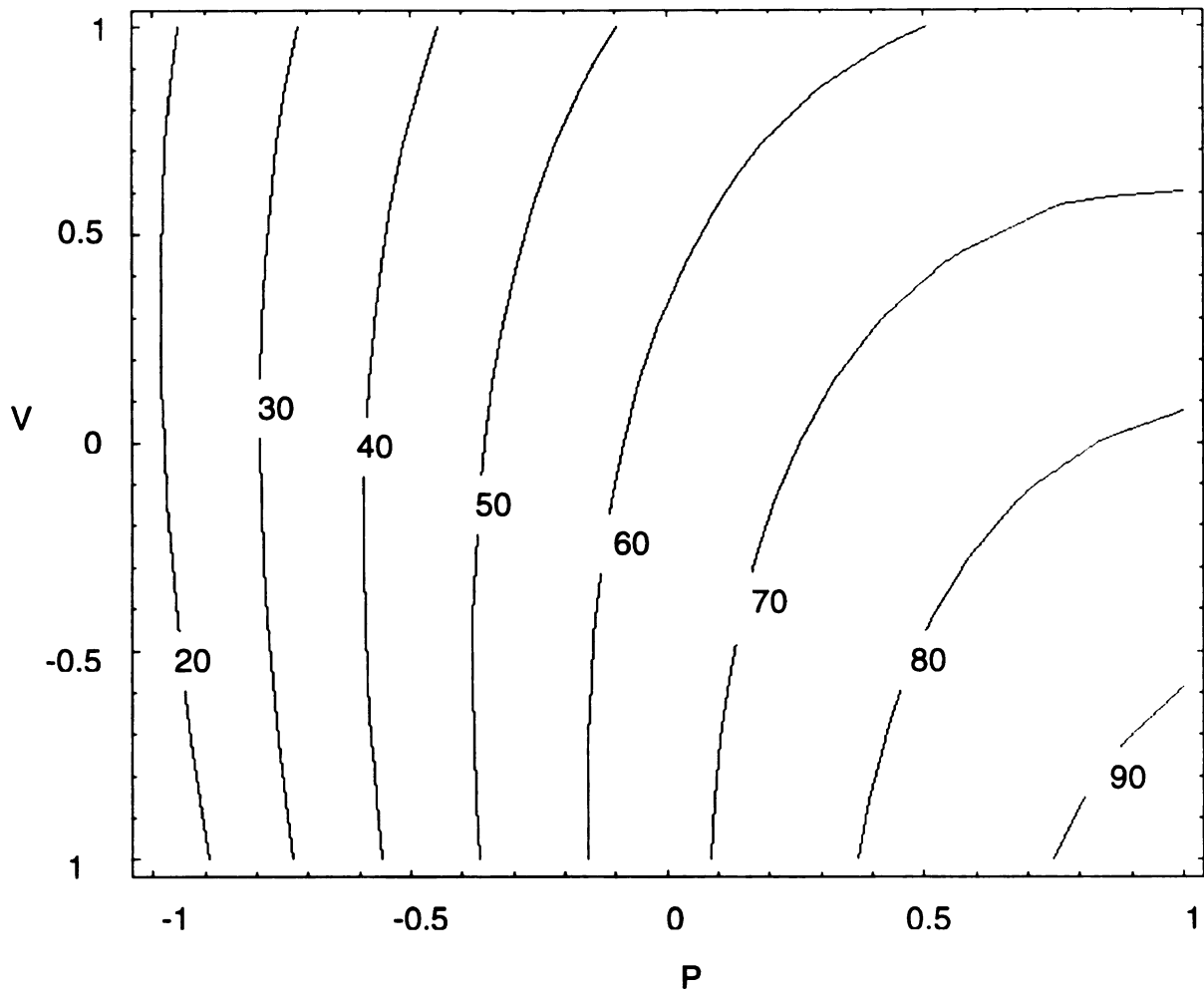


Figure 4.7. Contour Plot for  $Y_c$  for  $P$  and  $V$  ranging from -1 to 1, using Equation 1.

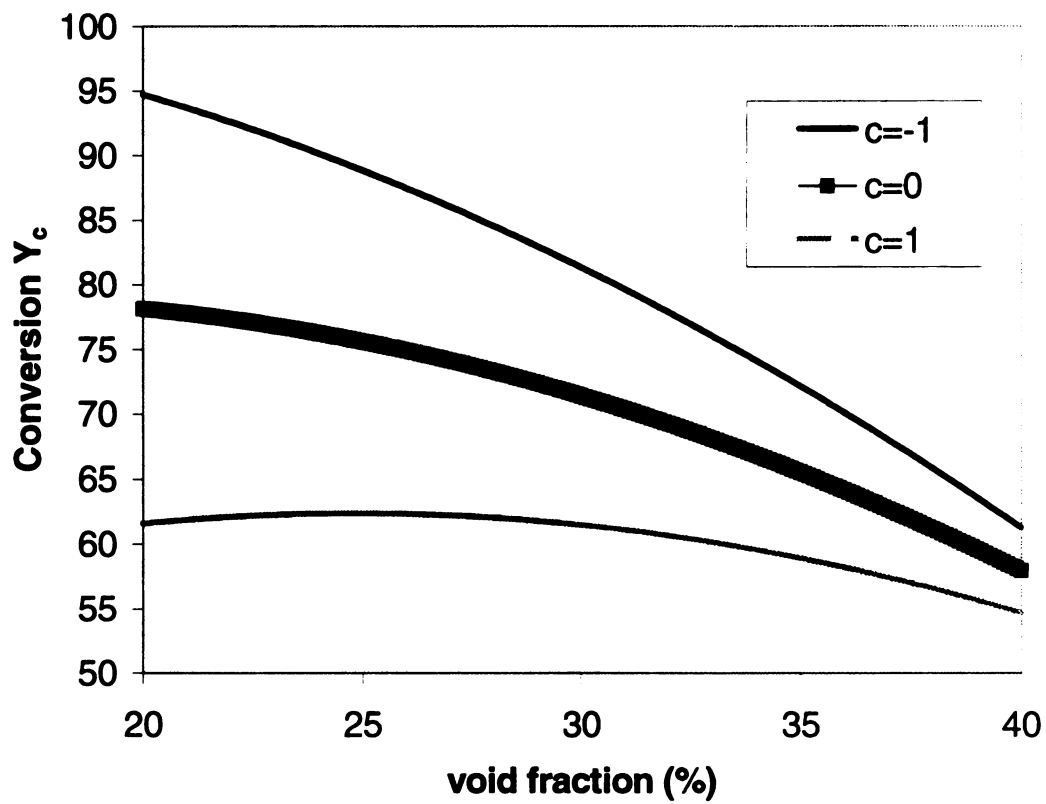


Figure 4.8. Plot of conversion vs. void fraction at varying initial concentrations of Phe-Me in the decanol phase

#### 4.4.3.2. Enantiomeric excess ( $Y_{ee}$ )

The statistical analysis of the data showed that pH, void fraction and concentration in the decanol phase are the most significant factors affecting enantiomeric excess. The results of the statistical analysis are given in Table 4.9. The enantiomeric excess showed no significant variation with surfactant concentration and amount of enzyme. The best-fit linear regression model is shown in Equation 2 with only the statistically significant terms

$$Y_{ee} = 90.5 + 3.22 V + 9.94 P + 11.1 C - 6.59 P^2 - 6.27 C^2 + 4.36 SE \\ - 5.62 VP - 2.83 VC - 12.8 PC \quad \text{(Equation 2)}$$

A plot of the residuals vs. the order of experiments is presented in Figure 4.9.

Under the optimal conditions identified for conversion, notably pH value of 6, high enantiomeric excess (90%) is predicted by equation 2 (Figure 4.10).

Table 4.9 Regression analysis for the model represented by Equation 2

$$Y_{ee} = 90.5 + 3.22 V + 9.94 P + 11.1 C - 6.59 P^2 - 6.27 C^2 + 4.36 SE - 5.62 VP - 2.83 VC - 12.8 PC$$

Predictor	Coef	StDev	T	P
Constant	90.45	1.007	89.84	0
V	3.2155	0.7729	4.16	0
P	9.9391	0.915	10.86	0
C	11.0504	0.915	12.08	0
P <sup>2</sup>	-6.5868	0.9519	-6.92	0
C <sup>2</sup>	-6.2651	0.9519	-6.58	0
SE	4.362	0.9466	4.61	0
VP	-5.6166	0.9466	-5.93	0
VC	-2.8262	0.9466	-2.99	0.007
PC	-12.8041	0.9466	-13.53	0

S = 3.786    R-Sq = 96.6%    R-Sq(adj) = 95.1%

Analysis of Variance

Source	DF	SS	MS	F	P
Regression	9	8543.99	949.33	66.22	0
Residual Error	21	301.05	14.34		
Total	30	8845.04			

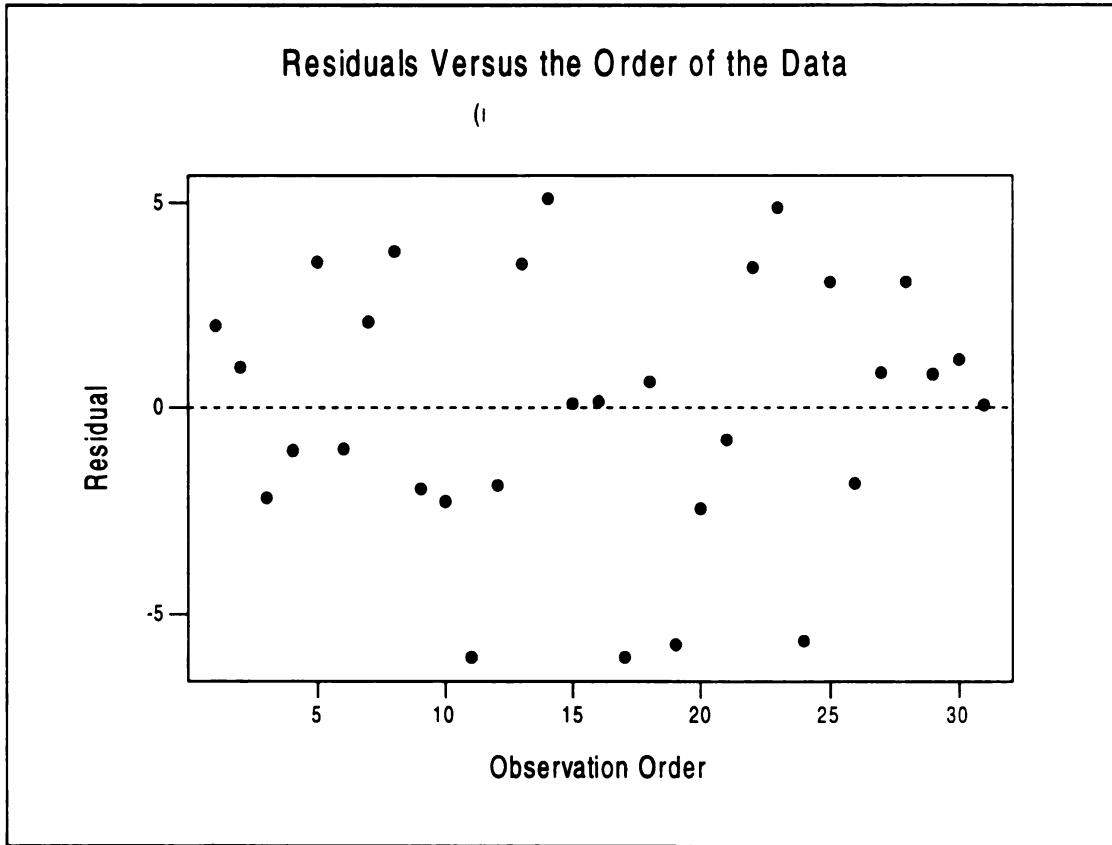


Figure 4.9 Plot of residuals vs. order of data for  $Y_{ee}$ .

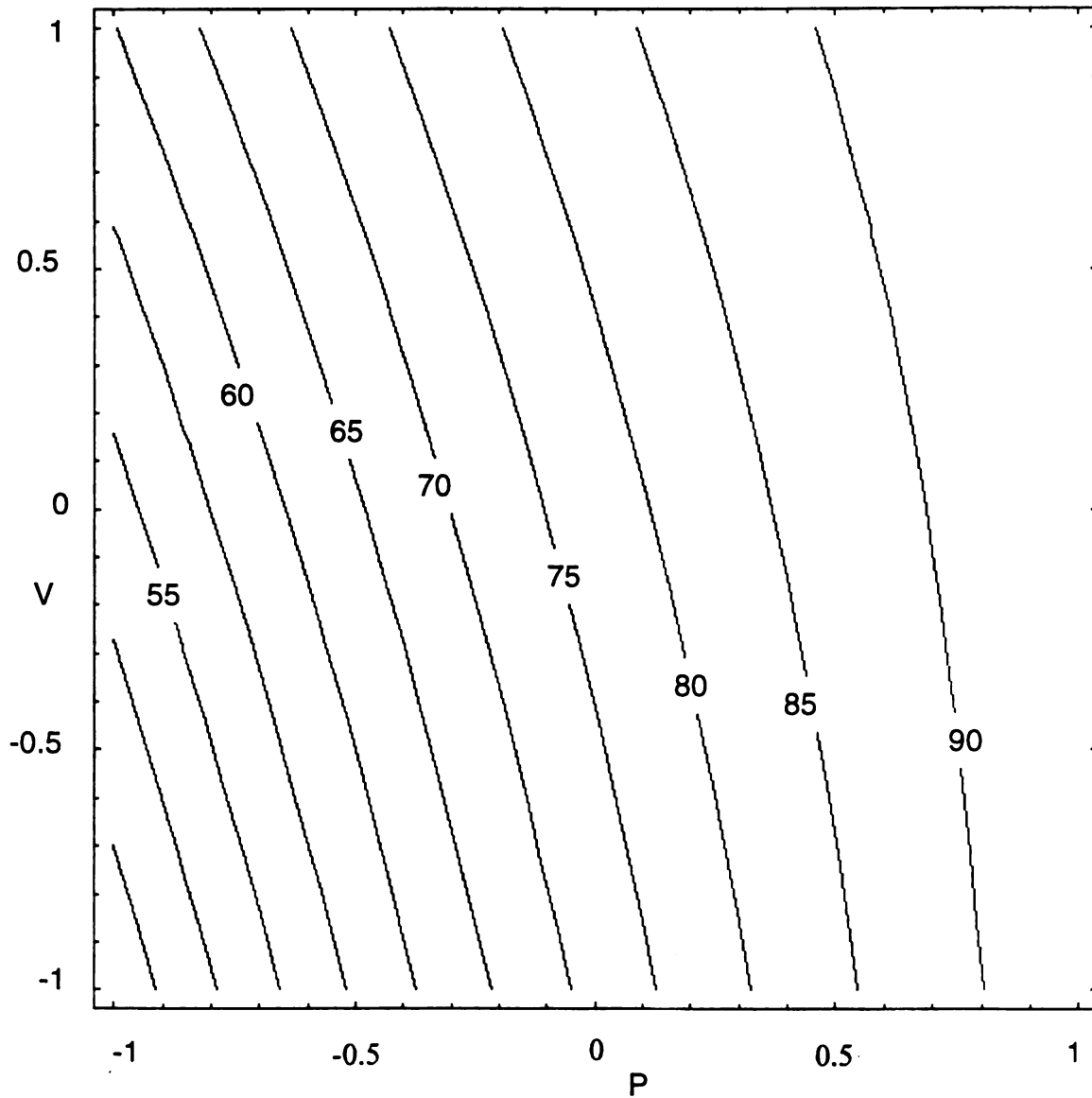


Figure 4.10 Contour plots for  $Y_{ee}$ , for  $P$  and  $V$  ranging from -1 to 1, based on equation 2.

## 4.5 Conclusion

The dynamic resolution of L,D phenylalanine was carried out in a multiphase system comprising CLA emulsions using crude pancreatic porcine lipase. A non-ionic emulsifier (Tween 80) used for the formation of CLA emulsions, exhibited minimal interactions with the biocatalyst. CLA emulsions provided a four-fold decrease in time required to attain equilibrium over conventional contacting methods. A statistical-design-of-experiment approach was used to identify the major variables affecting equilibrium conversion and enantiomeric excess in presence of CLA. The optimal conditions for high conversion (>90%) were identified as low void fraction (10%) and high pH (6). Under conditions that are optimal for high equilibrium conversion, the enantiomeric excess attained was also high (>90%), thus precluding a tradeoff between maximizing conversion and enantiomeric excess.

#### 4.6 References

Dean JA, 1992, Lange's Handbook of Chemistry, Fourteenth Edition, McGraw-Hill, Inc., p 8.111

Gal, J, 1987. Stereoisomer separations via derivatization with optically active reagents, Applications to Compounds of pharmacological Interest, LC-GC 5: 106-126.

Kroschwitz JI and Howe Grant M, Eds., Kirk Othermer Encyclopedia of Chemical Technology, 4th Edition, John Wiley and Sons, NY., 2, 514-515.

Kinoshita T, Kasahara Y, Nimura N, 1981. Reversed phase high performance liquid chromatographic resolution of non esterified enantiomeric amino acids by derivatization with 2,3,4,6 tetra-O-acetyl-  $\beta$ -D- glucopyranosyl isothiocyanate and 2,3,4 tri-O-acetyl-  $\alpha$ -D- arabino-pyranosyl isothiocyanate. Journal of Chromatography, 210 (1) 77-81.

Montgomery DC 1996. Design and analysis of experiments 4<sup>th</sup> edn John Wiley and Sons, New York NY

Bonzonana G and Desnuelle P. 1965. Kinetic study of pancreatic lipase on triglycerides in emulsion: enzyme action in heterogeneous medium. Biochim. Biophys. Acta., 105, 121.

Bosswell C, 1999. Building fine chemicals muscle with amino acids, Chemical Market Reporter, New York, NY June 14th.

Brennan MB, 2000. "Drug Discovery: Filtering Out Failures Early in the Game," C&EN, June 5, 2000, 63-73.

Brockman HL, 1984. General features of lipolysis: reaction scheme, interfacial structure and experimental approaches. in "lipases," B. Borgstrom and HL Brockman (ed.) Elsevier, New York, Chapter.1 p3.

Broxterman, QB, WHJ Boesten, J Kamphuis, M Kloosterman, EM Meijer, and HE Entessangles, B., and Desnuelle, P. 1968. Action of pancreatic lipase on aggregated glyceride molecules in an isotropic system, Biochim. Biophys. Acta, 159, 285

Jacobsen E, 1999, Assymetric synthesis of alpha-amino acids, Chemical Market Reporter 255 (24) p FR12-FR13.

Lamb SB, Stuckey DC. 1999. Enzyme Immobilization on colloidal liquid aphrons (CLAs): the influence of protein properties. Enzyme and Microbial Tech. 24 (8-9) 541-548.

Lye GJ 1997. Stereoselective hydrolysis of D-L phenyl alanine using aphron immobilized  $\alpha$ -chymotrypsin. Biotechnology Letters, 11, 611-616.

Patel, MT, R Nagarajan, and A Kilara, 1996. Lipase Catalyzed Biochemical Reactions in Novel Media: A Review, Chem. Eng. Comm., 152-153, 365-404.

Rogers, RS, 1999. Companies Turn to Biocatalysis: Drive to meet Customer Demand for Single-Isomer Intermediates Takes on Urgency," C&EN, July 19, 87-91.

Schoemaker, 1990. Chemo-enzymatic Production Methods for Optically Pure Intermediates of Potential Commercial Interest, In: Opportunities in Biotransformations, Elsevier Applied Science, New York, 148-169.

Scott, CD, TC Scott, HW Blanch, AM Klibanov, and AJ Russell, 1995.

"Bioprocessing in Aqueous Media: Critical Needs and Opportunities," ORNL/TM-12849, Department of Energy, 19-21.

Stinson, SC, 1998. Counting on Chiral Drugs, C&EN, Sept. 21, 83-104.

Stinson, SC, 1999. Prosperity for Fine Chemicals, C&EN, July 19, 1999, 65-87.

Stinson, SC, 2000. Fertile Ferment in Chiral Chemistry, C&EN, May 8, 59-70.

## **Chapter 5**

### **5. Whole Cell Biotransformations using Colloidal Liquid**

#### **Aphrons**

##### **5.1 Introduction**

The search for selective enzyme inhibitors and receptor agonists or antagonists is one of the keys for target-oriented research in the pharmaceutical industry. Increasing understanding of the mechanism of drug interaction on a molecular level has shown that chirality is the key to the efficacy of many drug products. It is now known that, in many cases, only one stereoisomer of a drug is effective, and the other stereoisomer may be inactive, exhibit reduced activity, or even cause detrimental side effects. Thus, pharmaceutical companies are aware that many new drugs should be homochiral. In many cases, where the switch from a racemic mixture to an enantiomerically pure compound is feasible, there is the opportunity to double the yield of an industrial process (Patel, 1997).

Chiral synthons can also be prepared by asymmetric synthesis using either conventional catalytic or biocatalytic processes. The advantages of biocatalytic reactions are that they are stereoselective and can be carried out at near ambient temperature and atmospheric pressure. This minimizes problems of isomerization, racemization, epimerization, and rearrangement that generally occur in conventional catalytic processes. Biocatalysis can be carried out using either individual enzymes or whole cells. The application of CLA emulsions for

enzyme based biocatalysis was described in Chapter 4. In this chapter the use of CLA emulsions for whole cell biocatalysis is demonstrated.

### **5.1.1 Whole Cell Biocatalysis**

The majority of reactions of organic-chemical interest require cofactors such as NAD(P)H or ATP. These cofactors are too expensive to be used in the stoichiometric amounts required (Jones, 1985). Viable cells can regenerate these cofactors efficiently in their metabolic cycles, and hence be used as efficient stereoselective catalysts for such reactions. Organic chemists prefer bakers yeast among microorganisms for biotransformations (Servi, 1990) because it is inexpensive, versatile, and is easy to grow to high cell densities. In particular, the asymmetric reduction of carbonyl compounds by Bakers yeast (*Sacchomyces cerevisiae*) has been widely used for preparing optically active alcohols largely because the reaction is easy to carry out and Baker's yeast is commercially available in large quantity (Brooks, et al. 1982; Deol, et al. 1976; Meyers, et al. 1980). Several review articles devoted to the use of baker's yeast in organic chemistry have been published (Jones, 1986; Simon et al. 1985; Van Middlesworth and Sih, 1987), and over 300 references to scientific works in this area have been reported (Servi 1990).

Development of yeast biotransformation processes suitable for implementation by the pharmaceutical industry presents significant engineering challenges. The two main issues involved with these transformations are:

- 1) Low aqueous solubility of substrates

Ideal drug candidates would be hydrophobic to allow passage through cell membranes (Brennan, 2000). Hence, many relevant biotransformations involve substrates that are sparingly soluble in water. Biocatalysts, such as microorganisms, are designed by nature to be effective in an aqueous medium. This results in low volumetric productivities in biocatalytic processes involving sparingly soluble substrates. In addition products streams are dilute and present challenges in downstream processing.

## 2) Competing reactions in yeast biotransformations

The presence of several intracellular enzymes that may compete for the same substrate may result in the formation of more than one product, leading to low selectivities. For instance, of the more than one thousand six hundred enzymes listed in the *Handbook of Enzymes* (Barman TE, 1985), several hundred have been purified from yeast and probably more are present in the organism. Yeast can catalyze the asymmetric reductive biotransformations of a variety of compounds containing a carbonyl group or carbon-carbon double bond. Oxidoreductases participating in these reactions have a relatively broad substrate specificity (Ward, et al. 1990). However, other side reactions such as acyloin condensation and Michael type of addition of a carbon nucleophile have also been reported (Lintner and Von Leibig, 1913, Oldrich H et al., 1986). Also, the presence of another group of enzymes (lyases), has been reported to cause water addition across the double bond of an  $\alpha,\beta$  unsaturated aldehydes such as crotonaldehyde (Fronza et al, 1988). Since most enzymes present in yeast will

display their properties under similar conditions, the problem of low selectivity, in biocatalytic processes involving yeast, is a major problem (Servi, 1990).

### **5.1.2 Organic solvents in whole cell biocatalysis**

There is much current interest in conducting biotransformations in the presence of organic solvents (Brink and Tramper, 1985; Adlercreutz and Mattiason, 1987; Laane et al., 1987a,b; Brink et al., 1988; Zaks and Klivanov, 1988). The organic solvent may serve as a reservoir for a hydrophobic substrate. It may also shift the equilibrium conditions in order to improve selectivity.

However, the presence of a nonpolar liquid phase can create processing difficulties. First, interphase mass transfer of sparingly soluble substrates is typically slow. Yeast biotransformations are often carried out using high cell densities (~250 g/L) and even cell slurries. At high cell densities the substrate consumption capacity can far surpass mass transfer capacity. Mechanical agitation can be used to disperse the solvent phase and thereby increase the interfacial area and mass transfer. However, this approach is energy-intensive and thus costly, particularly in large-scale systems (Bredwell, *et al.* 1998). Second, many organic solvents are toxic to cellular biocatalysts. This toxicity can either arise from the action of the trace amount of solvent that is dissolved in water, or from direct contact between the cells and the organic phase. The latter has been termed "phase" toxicity (Salter and Kell, 1995).

### **5.1.3 Colloidal Liquid Aphrons**

As shown in Chapters 2 and 3, CLA provide a 5-15 fold increase in interphase volumetric mass transfer rates over conventional emulsion systems even without the need for energy intensive agitation. They can be formed at low shear rates (Chapter 1) and pumped into the reactor as predispersed droplets of organic solvent. Scott et al. (1995) have suggested that cells inhibited in the presence of an organic phase may be at least partially protected by immobilization or the use of membranes. The presence of a lipid-like liquid crystalline "shell" stabilizing the CLA could prevent direct contact between cells and the solvent, thus reducing phase toxicity effects. Thus, CLA emulsions have potential to enhance whole cell multiphase bioconversions.

This research described in this chapter had two main objectives

1. To demonstrate the use of CLA produced using biocompatible organic solvents in whole cell biotransformations involving high cell densities.
2. To determine whether selectivity of whole cell biocatalysis can be influenced through the use of CLA emulsions and explore mechanisms for the variation in selectivity (if any).

### **5.1.4 Model system**

Carbonyl reductions are probably the most thoroughly studied and exploited biotransformations performed by Bakers yeast (Ward et al, 1990). In this chapter, the biotransformation of an  $\alpha,\beta$  unsaturated carbonyl compound **1** was studied (Figure 5.1). Baker's yeast fed D-glucose converts  $C_6$   $\alpha,\beta$  unsaturated aromatic

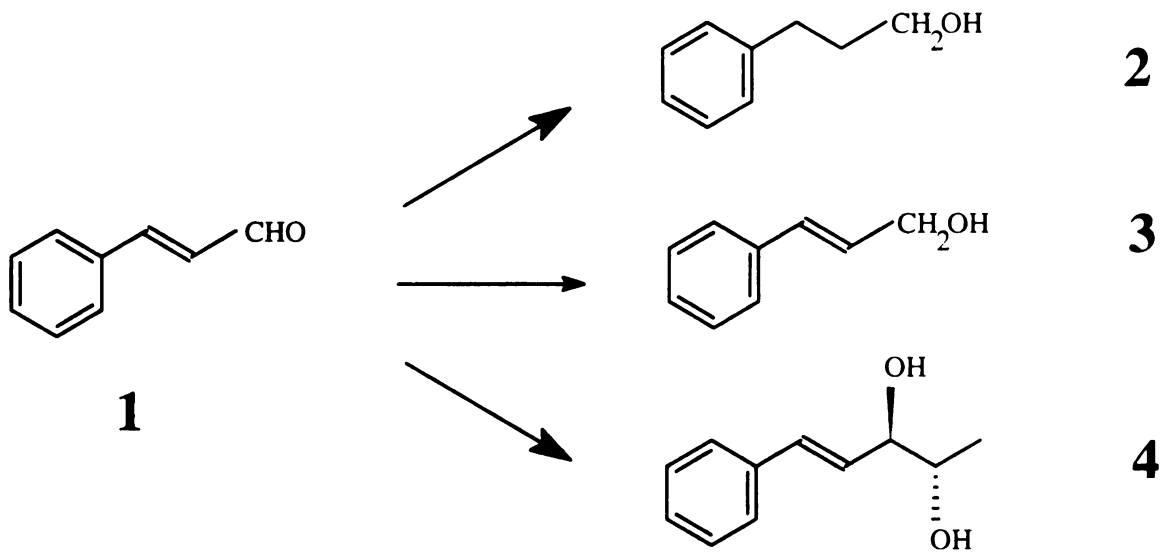


Figure 5.1. Biotransformation of cinnamaldehyde by baker's yeast.

aldehydes into corresponding 3-phenyl-propan-1-ols (**2**) and 3-phenylprop-2-en-1-ols (**3**) and into the 4 substituted (2S, 3R)-5-phenylpent-4-en,2,3-ols (**4**) (Fuganti and Grasselli, 1985)

The formation of (**2**) and (**3**) is interesting from a mechanistic point of view towards understanding and controlling selectivity whereas the production of (**4**), which contains two more carbon atoms than the precursor aldehyde and two chiral centers of the type R,R'CHOH, is interesting from both the mechanistic and synthetic points of view. The (2S, 3R)-diol possesses unique structural features that make it useful as starting material in the synthesis of enantiomerically pure forms of natural products (Fuganti, 1986). The (2S,3R) configuration matches the configuration at positions 5 and 4 of 6-deoxysugars of the L-series like L-amiacetose **5** (Figure 5.2). The double bond of the diol can be stereospecifically functionalized, the stereochemistry of the process being dictated by the stereochemistry of the adjacent allylic center. Once the double bond has been saturated it is possible to functionalize the derived products regioselectively at the benzylic position. In saturated products, degradation of the benzene ring with ozone gives 6-deoxyhexonic acids, which bear all the chiral centers present in the side chain of the parent compound. From suitably protected forms of the diol it is possible to extrude C<sub>4</sub>, C<sub>5</sub>, C<sub>6</sub> carbonyl compounds with ozone. The *erythro* forms of these compounds can be converted to  $\alpha$  epimers, with *threo* stereochemistry, on treatment with base. This diol can be considered as carbohydrate like chiral synthon, which can sometimes be used advantageously as an alternative to natural carbohydrates. For example, it may be used in the

synthesis of 2,3,6 tri-deoxy-3 amino hexoses of the L- series, which are present in the therapeutically important anthracycline glycosides adriamycin (doxorubicin) and 4'-adriamycin. The conventional route using D hexoses requires a critical inversion of the configuration at position 5 at some stage in the sequence which can be avoided using the 2S,3R diol as the starting compound.

Other products synthesized from the diol are shown in Figure 5.3.

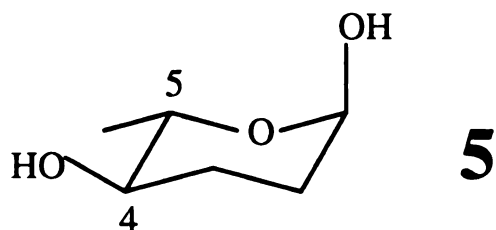


Figure 5.2. Structure of L- amiacetose

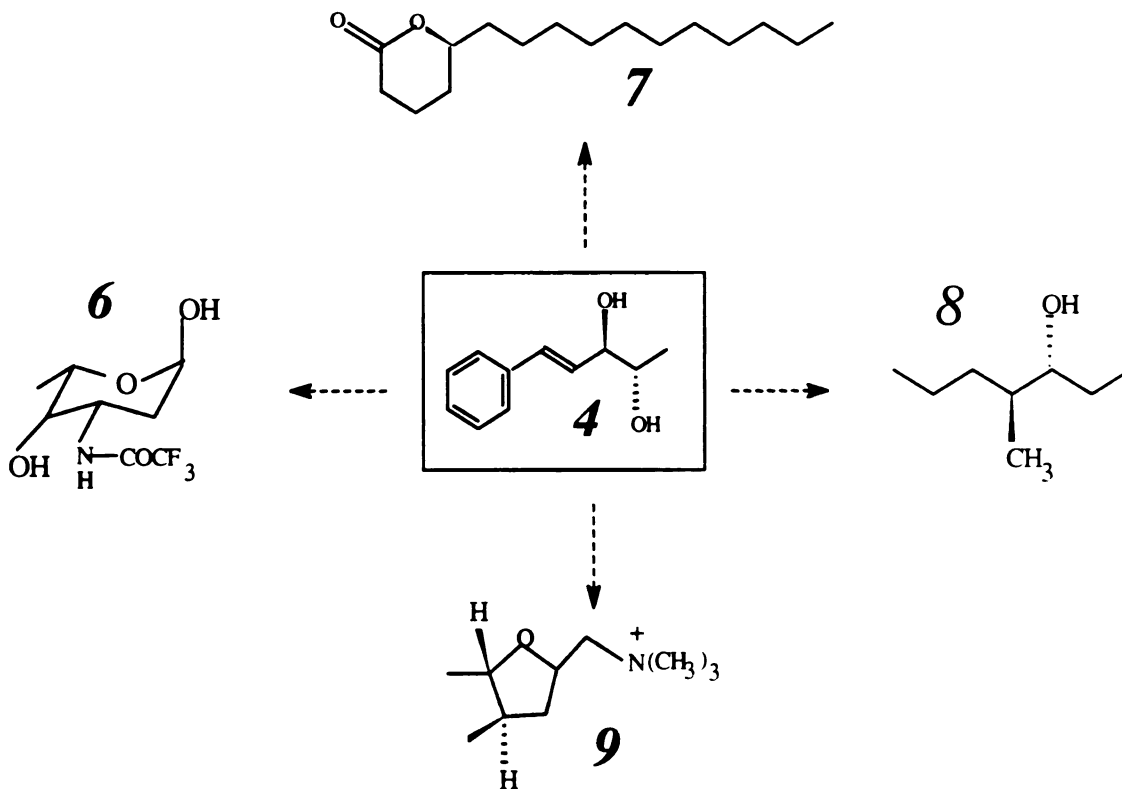


Figure 5.3. Compounds synthesised from (4)

## **5.2 Experimental Methods**

### ***5.2.1 Determination of solvent biocompatibility***

Five different experiments conducted under identical conditions (50 mL water, 12.5 mL yeast slurry, 28°C in 125 mL Erlenmeyer flasks, shaken in a horizontal shaker at 220 rpm), were started simultaneously, and 10 mL of organic solvent were added to each flask to screen for biocompatibility. The organic solvents tested were hexane, benzene, toluene, oleyl alcohol and 2,2,4-trimethylpentane. All solvents were HPLC grade and were obtained from Sigma Chemical Company (Milwaukee, WI). At time intervals of 30 min, 1 mL samples were centrifuged at 4000xg for 2 min. Ten microliters of the clear, cell free supernatant were added to 1 mL of glucose (Trinder) reagent (Sigma Chemical Company, Procedure 315). Each sample was incubated for exactly 18 min and its absorbance measured at 505 nm with a PE Lambda 3A UV/VIS spectrophotometer (Perkin Elmer Corp., Norwalk, CT). Conclusions about biocompatibility of each organic solvent were drawn by comparing the glucose concentration profile in each flask to that of a control experiment without organic solvent.

### ***5.2.2 Preparation of Colloidal Liquid Aphrons***

Two surfactants are typically used for the preparation of CLA emulsions. One of the two partitions primarily in the aqueous phase, and the other partitions primarily in the organic phase. The surfactant used in the aqueous phase was Tween 80 (Sigma Chemical Company, Milwaukee, WI). The surfactant in the

organic phase was a linear alcohol ethoxylate Tergitol 15-S-3 (Union Carbide Corp., Danbury, CT). The CLA preparation conditions influence the size distribution and stability of the CLA phase. Consequently, a consistent preparation procedure was used. The CLA emulsion was prepared in a 50 cm<sup>3</sup> glass beaker with an internal diameter of 40 mm. The solvent (2,2,4 trimethyl pentane)/Tergitol (0.5%) solution) was added to the aqueous phase (Tween 80 (2%)) at a rate of 0.5 mL per min, while stirring at 1600 rpm using a 25 mm magnetic stirrer bar. The resulting CLA phases were creamy white, with a phase volume ratio (volume of organic phase/volume of aqueous phase) of 1. They were very stable with no phase separation evident over a period of 4 months. One hundred milligrams of Cinnamaldehyde (1) was dissolved in the organic solvent prior to the formation of CLA dispersions.

### **5.2.3 Biotransformation Methods**

Trans-cinnamaldehyde (3-Phenyl-2-propenal) of the highest quality available was obtained from Aldrich Chemical Company (Milwaukee, WI). A 250 mL Erlenmeyer flask containing 50 mL tap water and 2.5 g Glucose was inoculated with 12.5 g of bottom fermented *Saccharomyces cerevisiae* (Harper's' Brewing Company, East Lansing, MI). The culture was grown in a controlled environment shaker (New Brunswick Inc, NJ) at 28<sup>0</sup>C, with 220 rpm shaking for 2 h; then the biotransformation was started by adding a known amount of substrate 1 (either dissolved in the organic phase of CLA or pure). The biotransformations were performed for 3, 8, 12 and 24 h. Whenever the glucose concentration dropped below 10 g/L, 2.5 g of glucose were added.

In some experiments, the substrate was immobilized onto a hydrophobic resin before being fed into the flasks. The resin, 250 mg of Amberlite XAD-4 (Supelco, Bellefonte, PA) was washed with de-ionized water (3 mL per 1 mL of resin) and acetone (3 mL for 1 mL of resin). The substrate was dissolved in acetone, and the resin, once dried, was added to this solution. The mixture was shaken for 2 min, and the acetone was evaporated. The resin so obtained was poured into the biotransformation flask.

The substrate (**1**) as well as all the biotransformation products, are nonpolar organic compounds that can be separated from the biotransformation medium by extraction with an organic solvent, e.g. chloroform ( $\text{CHCl}_3$ ). After fermentation the cells were centrifuged for 5 min at 4000  $xg$ , and the cell-free aqueous supernatant was extracted under vigorous shaking for 2 min with 40 mL of  $\text{CHCl}_3$ . Once again the mixture was centrifuged for 5 min at 4000  $xg$ . The solvent was removed by evaporating the clear organic bottom phase at 75°C under vacuum for 10 min. The oily product mix was dissolved in 1.5 mL of deuterated chloroform ( $\text{CDCl}_3$ ) for  $^1\text{H-NMR}$  analysis.

#### **5.2.4 Analytical procedures**

All spectra were recorded using a  $^1\text{H-NMR}$  INOVA 300 (Varian Inc., Palo Alto, CA) spectrometer operating at 300 MHz with a sample temperature of 20°C; the sample volume was 600  $\mu\text{l}$ . Samples were recorded in  $\text{CDCl}_3$  solutions containing succinic anhydride [ $^1\text{H-NMR}$   $\delta$  ( $\text{CDCl}_3$ ) 2.9 (4H,  $\text{CH}_2$ , d)] as an internal standard of known concentration.

All product peaks in the NMR spectra were identifiable from published data (Pouchert et al., 1993), except 5-phenyl-pent-4-ene-2, 3 diol. (4). One-dimensional total correlation spectroscopy (*TOCSY*) was performed on this compound to confirm its structure. Irradiation of the quartet of doublets (multiplet)( $J=6.5$ ,  $J=3.6$ ) peak at 3.97 ppm and observing the *TOCSY* spectrum at increasing mixing times indicated that the peak at 3.97 ppm was directly bonded to the methyl doublet ( $J=6.5\text{Hz}$ ) at 1.19 ppm. No further relays were observed in this direction. From the peak at 3.97, a relay was observed to quartet of doublets ( $J=7.15$ ,  $J=3.6$ ,  $J=1.01$ ) 4.25 ppm and further to the doublet of doublets ( $J=16.24$ ,  $J=7.0$ ) at 6.27 ppm and further to the doublet of doublets ( $J=16.0$ ,  $J=1.0$ ) at 6.67 ppm from which no other relays were observed.

A typical NMR spectrum is shown in Figure 5.4.



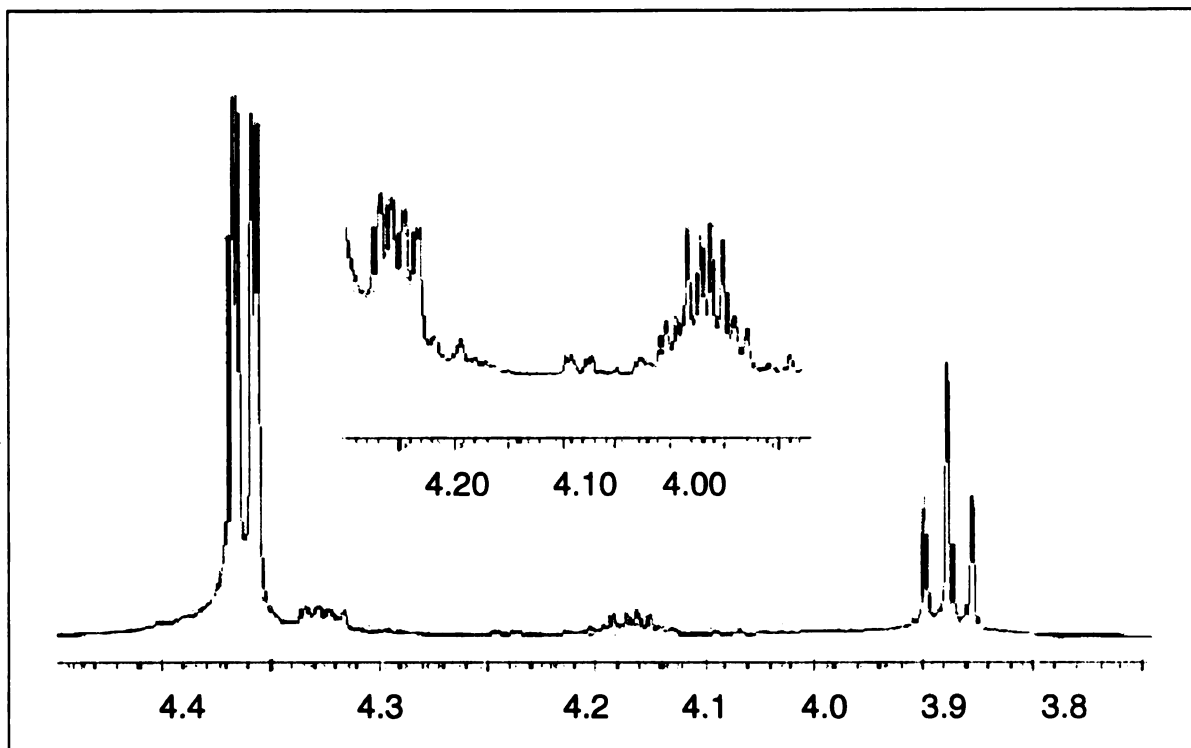


Figure 5.4. Typical NMR spectrum of biotransformation products

## **5.3 Results and discussion**

### ***5.3.1 Biocompatibility***

The solvents selected for the biocompatibility experiments were oleyl alcohol, hexane, benzene, toluene and 2,2,4-trimethylpentane. Oleyl alcohol has been widely accepted as a biocompatible solvent for extractive ethanol fermentations (Bruce and Daugulis, 1991). However, since the products of this biotransformation were non-volatile, product recovery considerations mandate the use of a volatile solvent. Among commonly used solvents, hexane, benzene, toluene, and isooctane were selected due to their high volatilities and low solubilities in water. Figure 5.5 shows the glucose utilization rate by yeast in the presence of organic solvents (20% v/v). Among the solvents studied oleyl alcohol and 2,2,4 trimethylpentane (also referred to as isooctane) exhibited minimal toxicity on yeast. Because of its favorable boiling point (99.2°C at 10<sup>5</sup> Pa) that allows easy solvent removal in the recovery process and its low water solubility (0.244 mg/100 g water), 2,2,4 trimethylpentane (isooctane) was chosen as the organic solvent for the biotransformation experiments. Using <sup>1</sup>H-NMR, the solubility of cinnamaldehyde was determined to be 30 g/L in 2,2,4 trimethylpentane. However keeping in view the inhibition of the cells in

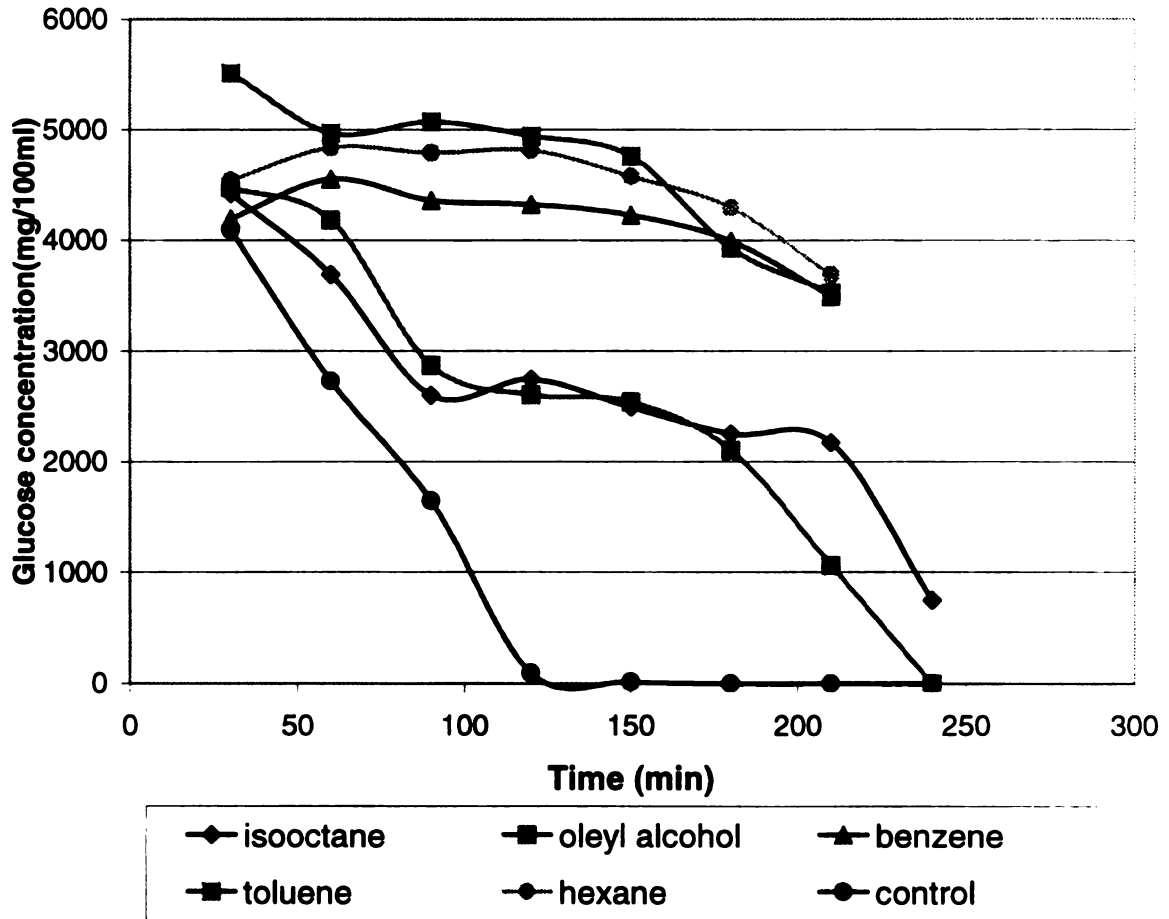


Figure 5.5. Biocompatibility of various solvents

presence of the solvent, the ability to use a large amount of organic solvent is limited.

### ***5.3.2 Biotransformations in presence of CLA***

The biotransformation experiments were performed with varying amounts (0-20 mL) of CLA emulsions present in the flasks. Over 95% of the cinnemaldehyde was converted after 3 h, in all experiments. The product compositions resulting from varying amounts of CLA are shown in Figure 5.6. The fraction of (2R, 3S) diol in the product increases as the volume of CLA emulsions increases, confirming that the selectivity of the biotransformation can be modified through the use of CLA. The yield of the diol obtained using CLA was three-fold higher than that in the absence of CLA.

Substrate concentration is known to be a major factor affecting the selectivity of microbial reductions (Wipf et al. 1983). The presence of the organic phase in the form of CLA dispersions could cause partitioning of the substrate between the phases, thus changing the apparent substrate concentration and the selectivity. Further experiments were conducted to identify whether the changes in selectivity could be attributed to the effect of substrate concentration.

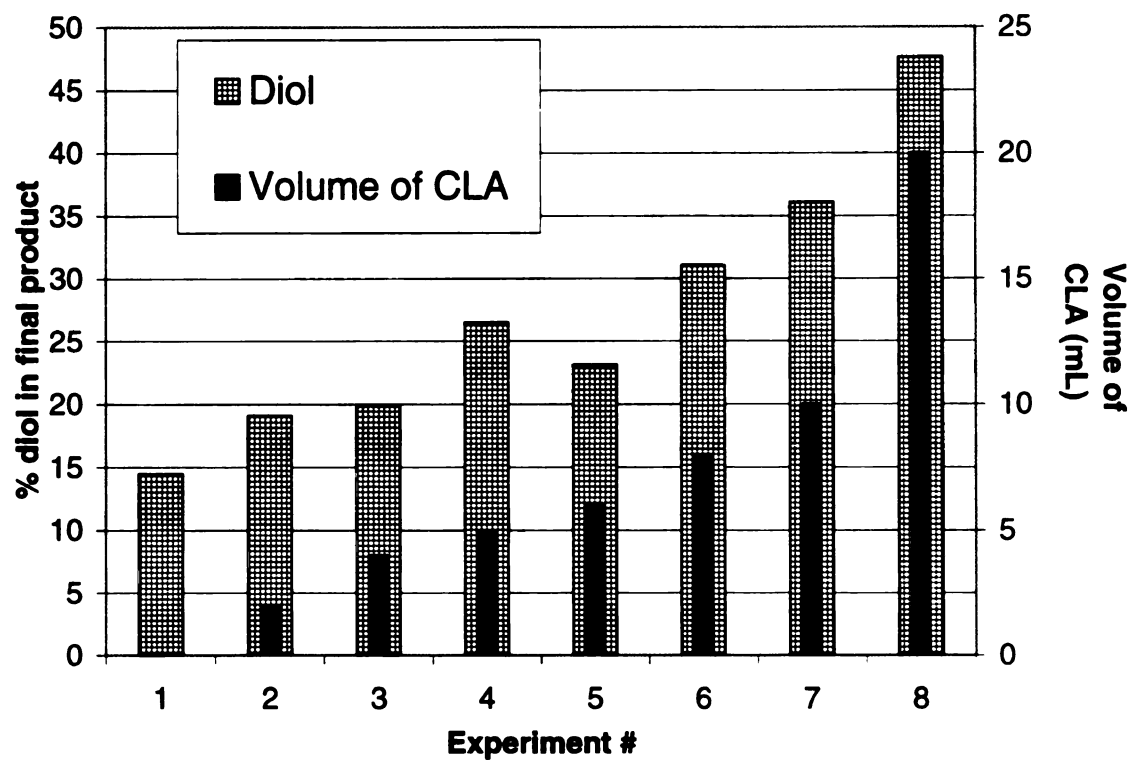


Figure 5.6. Effect of CLA volume on % diol in product

### ***5.3.3 Mechanisms for changing selectivity of whole cell biotransformations***

#### ***5.3.3.1. Effect of concentration on product composition***

The initial amount of cinnamaldehyde (1) added was varied from 6.6 mg to 132 mg per 50mL water in the biotransformation flask. Using <sup>1</sup>H-NMR cinnamaldehyde solubility was determined to be 1.0 g/L in water. At initial concentrations of (1) above 100 mg per 50 mL total-batch volume, product (2) was almost 50% of total product moles. This value rose to 100% when the initial amount of (1) was below 32 mg (Figure 5.7). This trend can be explained by competition for the same substrate between enzymes with different  $K_m$  and  $V_{max}$  values. However, in all the experiments, the yield of the diol (4) was low (<15%) compared to the experiments conducted in the presence of the CLA emulsions.

#### ***5.3.3.2. Effect of time on product composition***

Biotransformations were performed at different initial substrate concentrations (6.6, 33, 66, and 132 mg of (1) per 50mL water in flask) and the percentage of 3-phenyl-propanol (2) was determined after 8, 12 and 24 h, respectively. Results are shown in Figure 5.8. Initial cinnamaldehyde amounts less than 150 mg were completely converted after 3 h of fermentation. The product profile remained constant after 3 h, indicating that products 2,3, and 4 are not interconverted to a significant degree.

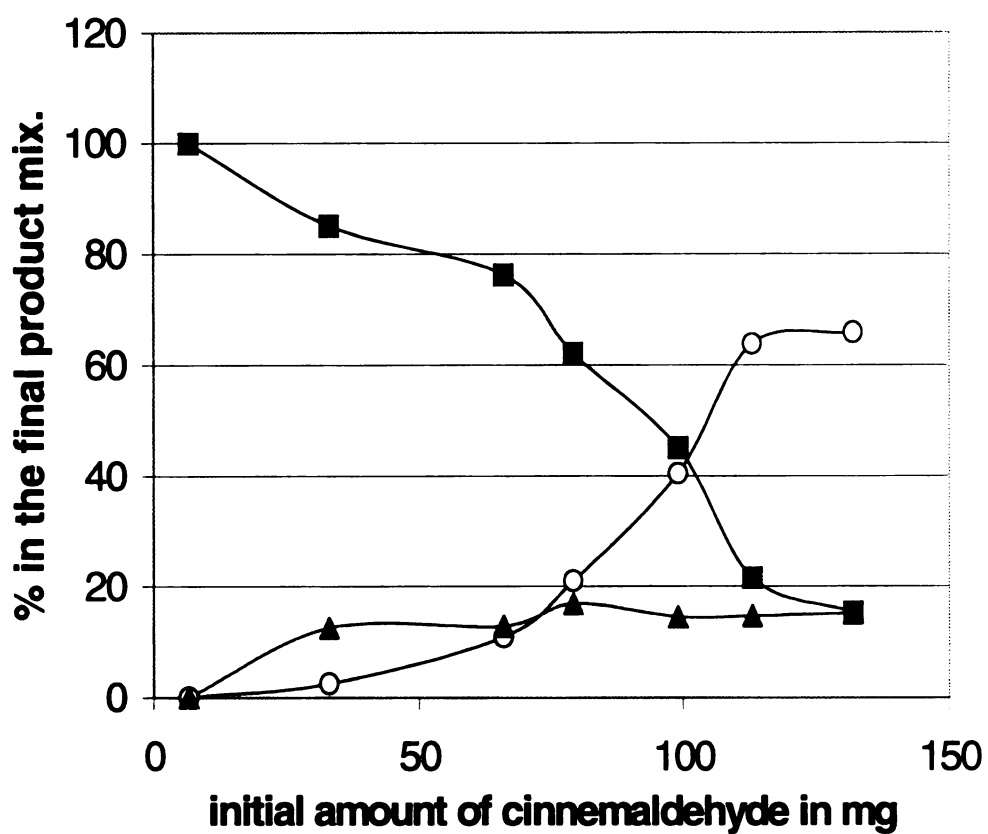


Figure 5.7. Change in product composition with initial concentration of cinnamaldehyde. Products represented are (■) 3 phenyl 1 propanol (2), (○) cinnamyl alcohol (3), and (▲) 2R, 3S Diol (4).

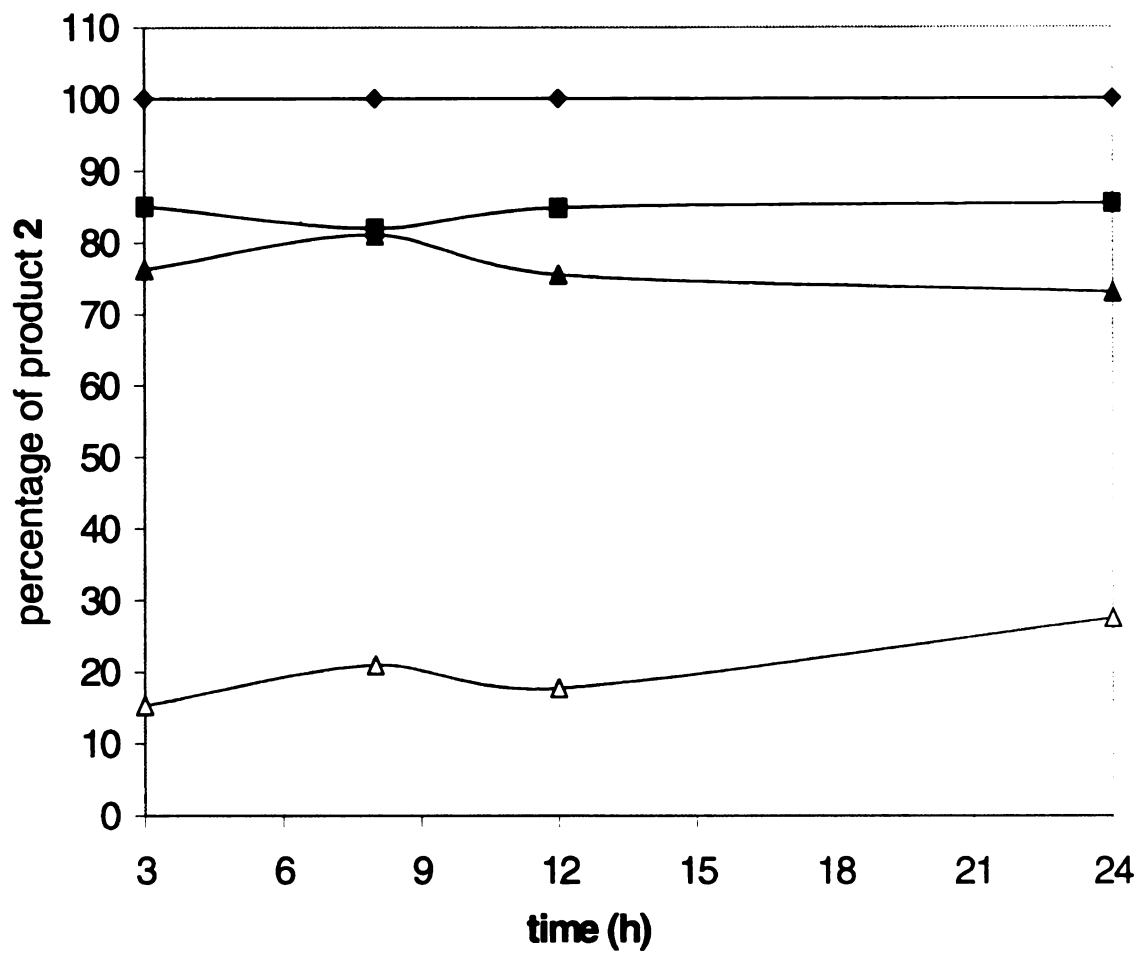


Figure 5.8. Effect of time on product composition. Plotted are data at different initial substrate (1) concentrations (◆)6.6 mg, (■) 33mg, (▲)66mg, (△)132 mg per 50ml.

#### **5.3.4 Selectivity control using hydrophobic resins**

Adding the starting material (1) adsorbed onto a resin would be expected to lower the concentration of the substrate in the broth (due to substrate partitioning between the resin phase and the aqueous phase) and change selectivity based on the experiments shown in Section 5.3.3.1.

Biotransformations were done with the same amount of substrate (100 mg); either in pure form or adsorbed onto 250 mg resin. The final product composition after 3 h is shown in Figure 5.9. This composition corresponds to what would be expected if the concentration in the broth was below 32 mg per 50 mL water. Thus it may be concluded that the presence of the resins lowered the apparent concentration in the broth, resulting in a change in selectivity towards (2), which is the favored product at low substrate concentration.

#### **5.4 Conclusion**

This study has demonstrated the use of CLA emulsions in the biotransformations of cinnemaldehyde by Baker's yeast at high cell densities (250g/L). The solvent 2,2,4 trimethyl pentane was identified as a suitable biocompatible solvent for yeast biotransformations. The presence of the organic phase in the form of CLA emulsion increased the fraction of 4 substituted (2S, 3R)-5-phenylpent-4-en,2,3-ols (4) by almost three-fold. The selectivity of the yeast biocatalyst appears to depend on substrate concentration. The change in selectivity due to the presence of hydrophobic resins is consistent with this hypothesis. However the variation in selectivity in presence of CLA, is not attributed to this phenomenon. More studies are required to clarify the

mechanism by which the presence of organic solvents affects selectivity.

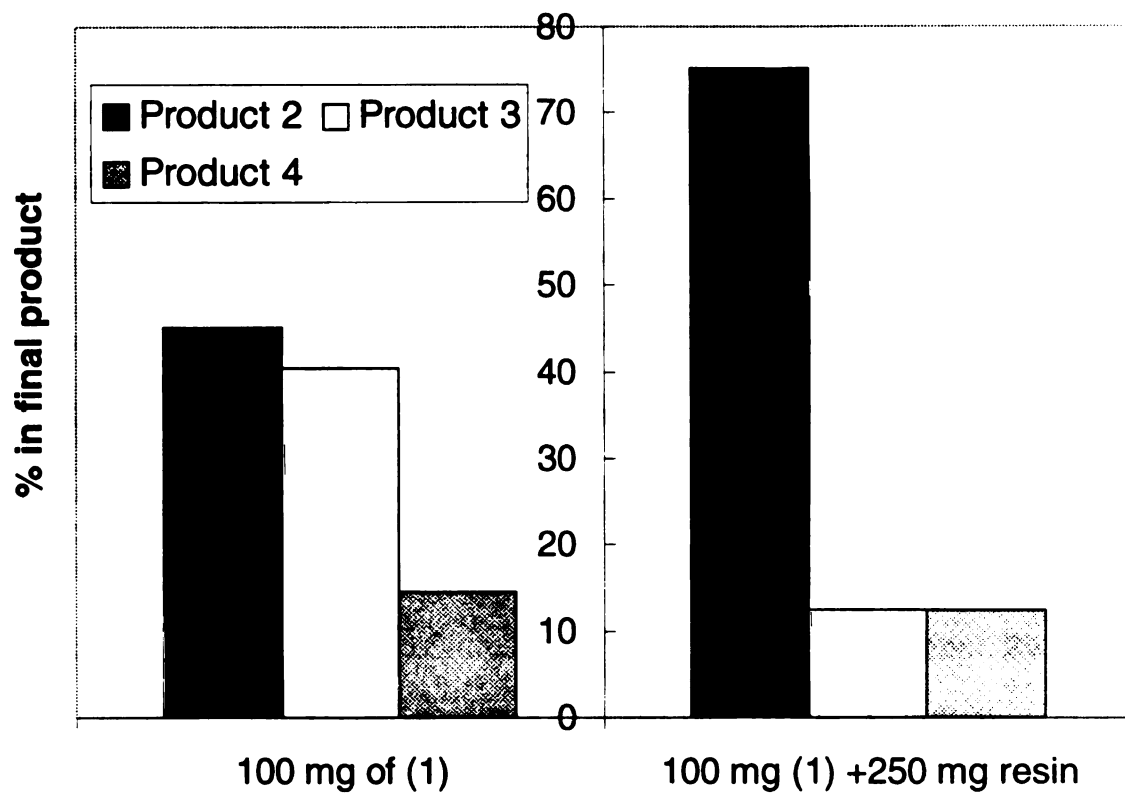


Figure 5.9. Effect of hydrophobic resins on product composition

## 5.5 References

Adlercreutz and Mattiason, 1987. Aspects of biocatalyst stability in organic solvents, *Biocatalysis* 1, 99-108

Barman TE, 1985. *Enzymes handbook*, Springer Verlag, Berlin.

Brink et al., 1988. LES, Tramper J, Luyben K Ch. A. M. and vant riet K:

biocatalysis in organic media. *Enzyme Microbial technology*, 10, 736-743

Brink LES and Tramper J, 1985. Optimization of organic solvent in multiphase biocatalysis. *Biotechnol. Bioeng.* 27, 1258-1269.

Brooks,D.W. ,Grothaus,P.G.,and Irwon,W.L.(1982).*J Org. Chem.* 47,2820.

Deol, B. S., Ridley, D.D., and Simpson, G. W. (1976) *Aust. J. Chem.* 29, 2459

Fronza G, Fuganti C, Grasselli P, Poli G, Servi S, Zorzella, A. (1988). *J. Org. Chem.* 53, 6153

Fuganti C, 1985, Bakers Yeast mediated preparation of carbohydrate-like synthons, in *Enzymes as catalysts in organic synthesis*, ed. M.P. Schneider, Kluwer Academic Publishers, Norwell, MA, USA. 3-17.

Fuganti, C.; and Grasselli, P.; in *Enzymes in Organic Synthesis*, Pitman London UK, 1985, pp. 112-127.

Jones JB, 1986, *Tetrahedron*, 42,3351

Laane C, Boeren S, Vos K., and Veeger C. ,1987b . Optimization of biocatalysis in organic media, In *Biocatalysis in Organic media* Eds Laane C, Tramper J and Lilly MD., Elsevier, Amsterdam, 65-84

Laane C, Tramper J and Lilly MD, 1987a. Eds. Biocatalysis in organic media, Elsevier, Amsterdam,

Lintner CJ and Von Leibig HJ, 1913, Z. Physiol. Chem. 88,109

Meyers, A. I., and Amos, R. A. (1980) J. Amer. Chem. Soc. **102**, 870

Oldrich H, Kakac B, Zvacek J, Tuma J, 1986. Czech Patent 231,401 (C1.C12Pz/24); C.A. 1987,106,3871.

Patel,R.N., Stereoselective Biotransformations in Synthesis of some pharmaceutical intermediates, Advances in Applied Microbiology,(1997),43,91-140

Pouchert, C.; Behnke, J.; *The Aldrich library of <sup>13</sup>C and <sup>1</sup>H FT-NMR spectra*, 1993, Aldrich Chemical Company, Milwaukee, WI.

Scott CD, Scott TC, Blanch HW, Klibanov AM, and Russel AJ 1995. Bioprocessing in nonaqueous media: Critical needs and opportunities. ORNL/TM-12849, U.S. National Technical Information Service, Springfield, VA.

Simon H, Bader J, Gunther H, Neumann S, Thanos J 1985, Angew. chem. int. Edn. Engl., 24, 539

Van Middlesworth F, Sih CJ 1987. Biocatalysis 1, 117

Wang, K.C., and Sih, C.J. (1963) Biochemistry **2**, 1238.

Ward, O.P.; Young, C.S.; *Enzyme Microbial Technol.* 1990,12, 482-493.

Ward,O.P., and Young C.S., Reductive biotransformations of organic compounds by cells or enzymes of yeast,Enzyme Microb. Technol., 1990, 12,482-493.

Wipf, B.; Kupfer, E.; Bertazzi, R.; Leuenberger, H.G. W. Helv. Chim. Acta. (1983). 66, 485.

Zaks A and Klibanov AM, 1988. J. Biol .Chem. 263, 3194-3201.

Zhou, B, Gopalan, A.S.; VanMiddlesworth, F.; Shieh, W.R,; Sih, C.J., J. Am.  
Chem. Soc. (1983), 105, 5925.

## Chapter 6

### 6. Reversible emulsions

#### 6.1 Introduction

Experimental evidence for the structure of CLA, and measurements of volumetric mass transfer coefficients for CLA in agitated vessels, has been presented in Chapters 1-3. Results presented in Chapters 2 and 3 showed a 5 to 15 fold increase in mass transfer rate using pre-dispersed CLA compared to conventional liquid dispersions. However, the high stability of the CLA emulsions makes phase separation, upon completion of the mass transfer, difficult. Separation of CLA from dispersion and their reconcentration can be effected by micro-filtration or centrifugation (Rosjidi et al., 1994). However, these processes can be energy intensive and substantially impact the economics of the extraction process.

Recently Mathur et al. (1998) have developed a novel class of co-polymeric block/graft emulsifiers whose emulsification properties are lost in response to small, predetermined changes in pH. The reversible stabilizer is a random-substitution copolymer of methacrylic acid (MAA) and methoxy-poly(ethylene glycol) methacrylate (MPEGMA). When mixed in the appropriate ratio the MAA forms a continuous linear polymer "backbone" into which the MPEGMA methacrylate groups are inserted randomly. The resulting comb-type co-polymer has a MAA backbone with poly(ethylene glycol) (PEG) side chains. In common with other polyacids such as poly(acrylic acid), the MAA backbone is

highly soluble in water at high pH, since its acid group are dissociated, and is less soluble at low pH (undissociated state). The PEG side chains are only slightly less soluble at low pH. However, when in close proximity, the hydroxyl groups of the PEG side chain form a hydrogen-bonded complex with the carboxylic acid groups of the MMA backbone, causing the side chains to fold against the backbone as illustrated in Figure 6.1.

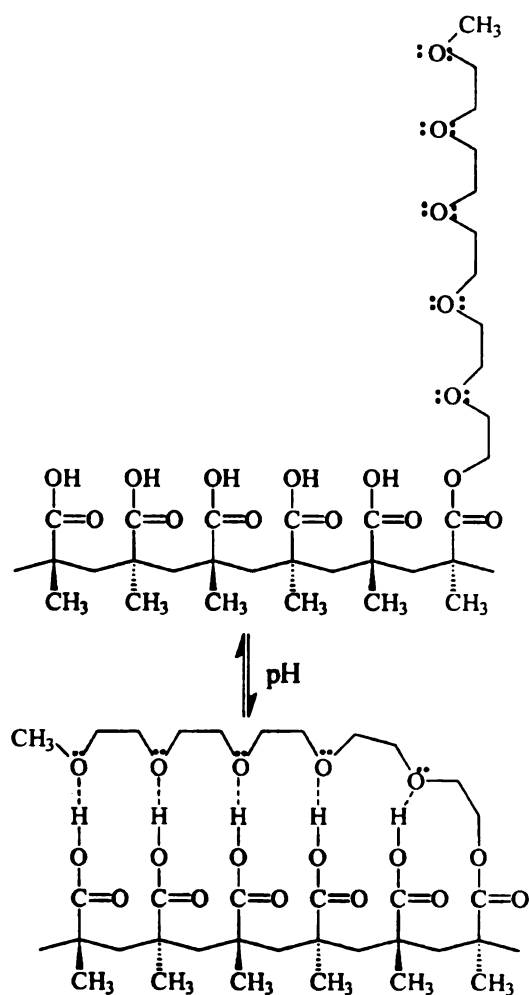


Figure 6.1 Complex formation in MAA-MPEGMA copolymers (redrawn from Mathur (1998)).

## **6.2 Materials and Methods**

The block/graft copolymers are synthesized via a free-radical solution polymerization of methacrylic acid (MAA) with methoxy poly(ethylene glycol) methacrylate (MPEGMA) using hydrogen peroxide (30% aqueous solution) as initiator and a 50/50 w/w mixture of ethanol/water as the solvent in a single step process. By choosing the ratio of methacrylic acid to ethylene glycol repeat units it is possible to form pseudo-multi-block copolymers consisting of a hydrophilic acid backbone interspersed with hydrophobic segments due to complexation. Such a polymer behaves like a multi-block polymeric emulsifier under acidic conditions and as a hydrophilic graft copolymer under basic conditions. Thus this reversible emulsification behavior can be repeatedly turned "on" or "off" by controlling the pH or other variables that affect complexation. As a result, the emulsions produced by using these novel polymeric emulsifiers can, in principle, be maintained stable as long as desired and then coalesced on demand by a small pH change. This study investigated the reversibility and mass transfer properties of emulsions formed using these novel emulsifiers.

The reversible emulsifier was prepared using the method of Mathur et al (1998). To produce an emulsifier with a 10:1 repeat ratio of MAA to EG: 0.55 g of MPEGMA 1000 was combined with 9.45 g of MAA, containing hydroquinone inhibitor, in 50g of a 50/50 mixture (v/v) of ethanol and water in a clear glass vessel. The mixture was briefly agitated by hand and then purged with a slow nitrogen feed for 5 min. The vessel was then capped with a silicone septum and

crimp cap under nitrogen gas. Fifty  $\mu\text{L}$  of 30% hydrogen peroxide was then added by injection through the septum, and the needle was left in place in the septum to act as a vent. The vessel was then placed in a temperature-controlled oven at  $70^\circ\text{C}$  for 3 days, with occasional agitation. The polymer was poured from the vessel and the solvent left to evaporate. For a repeat ratio of 20:1, the same procedure was followed with 0.275 g of MPEGMA and 9.725 g of MAA. This procedure resulted in a very viscous solution of polymer at the end of the three-day period (regardless of the ratio used). The emulsifiers synthesized contained 20:1, 15:1 and 10:1 ratio of the MA to EG repeat units.

The reversible emulsifiers were used as the stabilizer in the aqueous phase, and Tergitol 15-S-3 was added as the surfactant in the organic phase to lower the interfacial tension. Emulsions were prepared in a 50 mL glass beaker with an internal diameter of 40 mm. Five mL of Limonene/Tergitol (0.1% v/v) solution were dispensed at a rate of 0.5 mL/min into a 5-mL volume of aqueous/PMAA-PEG block graft emulsifier (0.4% v/v) solution. A 20 mm magnetic stirring bar spinning at 1600 rpm was used to provide agitation. The size distribution of the CLA dispersion was measured using a Malvern Mastersizer X. Mass transfer coefficient measurements were performed as previously reported using a conductivity probe (Chapter 2).

Coalescence properties of these emulsifiers were characterized by the percentage of organic phase recovered vs. pH. Emulsifier solutions (0.4% w/v) were titrated with 0.1N NaOH solution to find the amount of NaOH required to

change the pH of the emulsion (PVR 1). Twenty mL of emulsion (PVR 1) was stirred in a beaker for 30 min after addition of the appropriate amount of NaOH to change the pH to a desired value. The volume of organic phase recovered was recorded after 30 min. The experiment was repeated for emulsions stabilized by both 20:1 and 15:1 emulsifiers.

### **6.3 Results**

The 10:1 emulsifiers could not form stable emulsions with Tergitol 15-S-3 perhaps because of low hydrophilicity of these emulsifiers. However the 20:1 and 15:1 emulsifiers, being more hydrophilic, formed emulsions spontaneously. The size distribution measured for emulsions formed using the new emulsifiers and their comparison with sizes reported previously (Chapter 2) is shown in Table 6.1. The size data obtained indicate that the average size is about 2 fold larger than previously reported for CLA formed using Tween 80. The higher the MAA:EG repeat ratio, the more hydrophilic the emulsifier. Hydrophilicity aids in partitioning of the stabilizer in the aqueous phase, thus permitting better steric stabilization. Volumetric mass transfer coefficients measured for emulsions formed using reversible emulsifiers are similar to those measured in conventional emulsifier systems (Chapter 2). The comparison of measured  $K_L$  values to those measured for CLAs made using Tween 80 as the aqueous surfactant is shown in Table 6.2. The volumetric mass transfer coefficient  $K_{La}$  is about half that for CLA emulsions. However this still represents a 4-fold increase over conventional liquid liquid systems ( $29 \text{ h}^{-1}$ ) at the same Reynolds number ( $N_{RE}$ ).

**Table 6.1. Size distribution and mass transfer coefficients obtained for reversible emulsions and CLA.**

Aqueous phase surf. concentration	Tergitol conc.	Diameter ( $\mu\text{m}$ )	$K_{La}$ ( $\text{h}^{-1}$ )	$K_L$ ( $\text{cm/s}$ ) $\times 10^3$
0.4% (20:1)	0.1	43.9	126	14.4
0.4% (15:1)	0.1	81.7	53	11.2
0.4 % Tween 80	0.1	16.8	280	12.1

The titration curves for the two emulsifiers are presented in Figure 6.2. Figure 6.3 shows that after 30 minutes 95% of the oil phase was recovered from reversible emulsions formed using 20:1 emulsifiers at a pH of 8. At a pH of 9 about 80% of the oil phase was recovered from emulsions formed using the 15:1 emulsifier. Comparatively, less than 5% of the oil phase could be recovered from CLA formed using Tween 80 and Tergitol 15-S-3 at a pH of 10. Thus, the reversible emulsifiers hold considerable promise for applications where rapid dispersed phase recovery is desired. In order to undertake further studies on the reversible emulsions systems, the interfacial characterization of these reversible emulsions is essential. Phase behavior of several other polymeric emulsifiers is available in the literature. Hill et al. (1994) have characterized the  $L_2$ ,  $L_3$  and  $L_{\alpha}$  phases exhibited by four trisiloxane surfactants using small angle x-ray scattering (SAXS), small angle neutron scattering (SANS) and differential interference contrast microscopy. He et al. (1993) have studied the microstructure of polyoxyethylene trisiloxane surfactants in water and showed the presence of

hexagonally packed cylindrical micelles, using cryo-TEM, SAXS and SANS. However, before such studies can be undertaken current methods of polymer synthesis have to be improved. The polymers obtained by the current methods are highly polydisperse (polydispersities ranging from 2-5)(Drescher et al., in press). High polydispersities would significantly alter the aggregation behavior of the polymers making the interpretation of such results difficult. It is suggested that further work on the reversible stabilizer aggregation behavior be undertaken after further work on polymer synthesis and processing for this polymer class, so that a more practical and well-behaved system can be developed.

#### **6.4 Conclusions**

Preliminary studies indicate a high reversibility of emulsions formed using the 15:1 and 20:1 emulsifiers. Mass transfer studies indicate four fold higher volumetric mass transfer coefficients for such emulsions over surfactant free systems. However, these rates are three- fold lower than those reported for CLA (Chapter 2). The ease of coalescence due to the unique molecular architecture involves a tradeoff in mass transfer enhancement compared to CLA. The reversible emulsifiers hold considerable promise for applications where rapid dispersed phase recovery is desired.

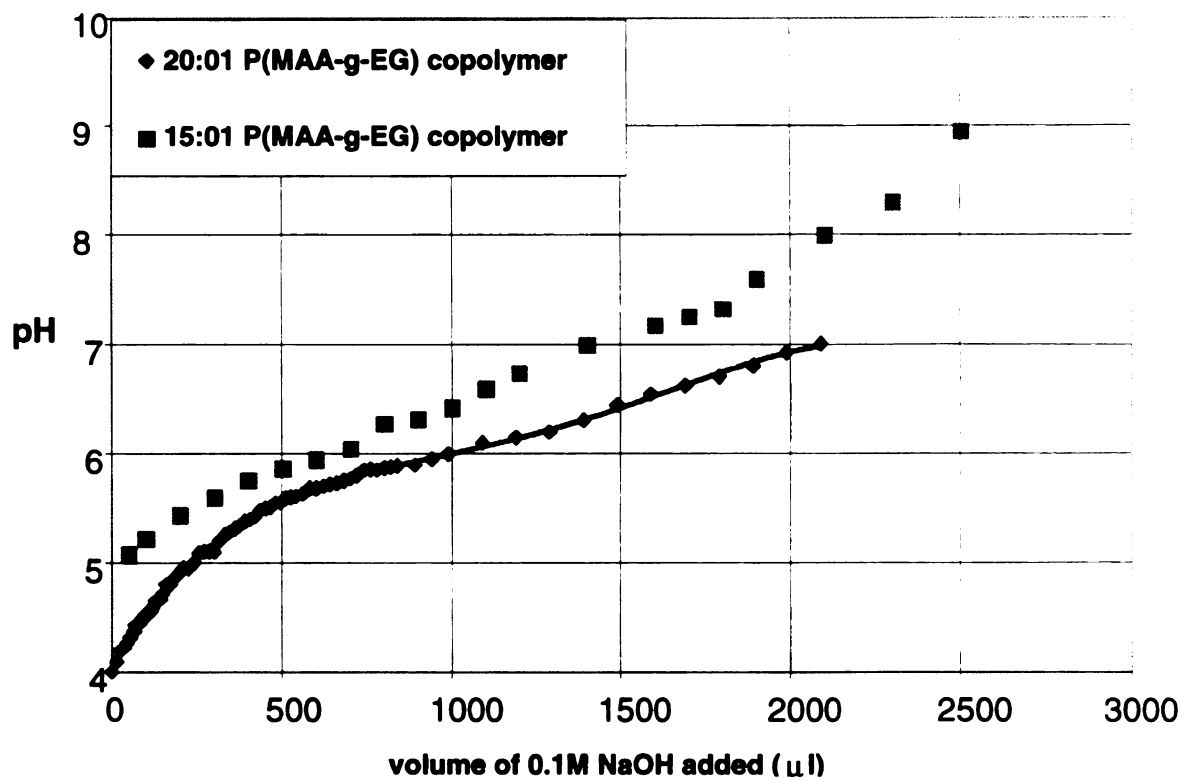


Figure 6.2. Titration curves for block copolymeric emulsifiers

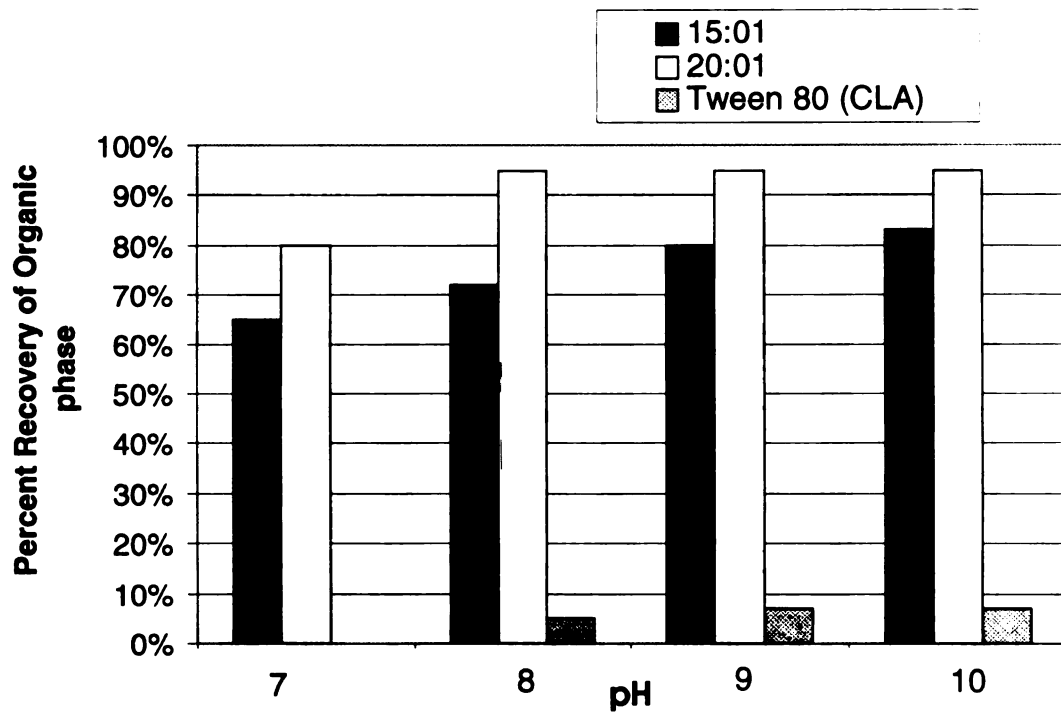


Figure 6.3 Percentage recovery of organic phase vs. pH for reversible emulsions, formed using different polymeric emulsifiers, and CLA emulsions.

## 6.5 References

- Rosjidi M., Stuckey D.C. and Leak D.J. 1994. Downstream Separation of chiral epoxides using colloidal liquid aphrons( CLA), in *Separations for Biotechnology*, Ed by Pyle D.L. , SCI publishing. 280-286.
- Drescher, Bernhard, A.B. Scranton, and J. Klier, 2000. Synthesis and Characterization of Polymeric Emulsifiers Containing Reversible Hydrophobes: Poly(methacrylic acid-g-ethylene glycol), Submitted to *Polymer* (in press).
- Arvind M. Mathur, Bernhard Drescher, Alec. B. Scranton and John Klier, *Nature*, 392(1998) 367.
- Hill RM, Mengtao He, Davis HT, and Scriven LE. 1994. Comparison of the liquid phase behavior of four trisiloxane superwetter surfactants. *Langmuir*, 10, 1724-1734.
- He M, Hill RM, Lin Z, Scriven LE, and Davis HT, 1993. Phase behavior and microstructure of polyoxyethylene trisiloxane surfactants in aqueous solution. *J Phys.Chem.* 1993, 97, 8820-8834.

## **Chapter 7**

### **7. Summary**

The interfacial structure and mass transfer properties of CLA emulsions were investigated in this research. Applications of these emulsions in multiphase biocatalysis were also developed.

Chapter 1 dealt with the characterization of the interfacial structure of CLA emulsions using FF-TEM, DSC, SAXS and ITC. Freeze fracture TEM demonstrated the lamellar interface formed in CLA emulsions. The formation of a rigid interfacial film, due to the interaction of the two unlike emulsifiers (Tween 80 and Tergitol 15-S-3) was found to be responsible for the stabilization of these emulsions. Differential scanning calorimetry results showed that this interfacial film forms a separate phase, apart from the aqueous and organic phases present in the emulsion. Isothermal titration calorimetry was used to characterize the energetics and stoichiometry of interaction between Tween 80 and Tergitol 15-S-3. Similarities and differences between properties and formulations of HIPE and CLA emulsions were elaborated. A model of lamellar micelles stabilizing the CLA interfaces was proposed based on the geometric theory of surfactant packing. Properties observed in the CLA literature were explained based on this model.

The mass-transfer properties of CLA emulsions of limonene in water were measured experimentally and presented in Chapter 2. The CLA size distribution was found to be strongly affected by the aqueous-phase surfactant (Tween 80) concentration, but virtually unaffected by the nonpolar-phase surfactant (Tergitol-

15-S-3) concentration. The  $d_{32}$  values decreased from 49 to 14  $\mu\text{m}$  as the Tween 80 concentration increased from 0.02 to 0.4% v/v. The  $K_L$  values measured for CLA emulsions averaged about  $15 \times 10^{-3}$  cm/s and were essentially unaffected by surfactant concentration. The  $K_{L,\text{shell}}$  value was estimated to be about  $30 \times 10^{-3}$  cm/s, which is comparable to  $K_L$  values for surfactant-free, liquid-liquid systems at an equivalent  $\phi$  value. The  $K_L a$  values for CLA were 5- to 15-times higher than those for conventional emulsions. These results suggest that CLA may offer significant advantages over conventional emulsions for mass-transfer-limited, multiphase biocatalytic processes.

Chapter 3 presented measurements of the interphase mass-transfer properties of CLA emulsions in water by coupling the mass-transfer of the solute (p-tolyl acetate) to a chemical reaction. The overall  $K_L$  values, which ranged from 0.002 to 0.015 cm/s, increased with  $N_{RE}$  below a  $N_{RE}$  value of about 12,500. Above this value,  $K_L$  was essentially independent of  $N_{RE}$ . These trends suggest that as the degree of agitation is increased, the controlling resistance shifts from the continuous phase to the shell phase. The  $K_L$  values were essentially independent of the surfactant concentration used to prepare the CLA. A resistances-in-series model was used, along with a literature correlation for  $K_{L,\text{continuous}}$ , to estimate the  $K_{L,\text{shell}}$  value to be about 0.04 cm/s. At a nominal  $N_{RE}$  value of 20,000, the  $K_L a/\phi$  values measured for CLA were about 20 times higher than that for conventional emulsions. These values, measured using chemical reaction, compare well to those obtained in Chapter 2 that were measured under extractive conditions.

The application of CLA emulsions in multiphase enzymatic biocatalysis was presented in Chapter 4. Dynamic resolution of L,D phenylalanine was carried out in a multiphase system using porcine pancreatic lipase. A non-ionic emulsifier (Tween 80), used for the formation of CLA emulsions, exhibited minimal interactions with the biocatalyst. The CLA emulsions provided a four-fold increase in reaction rates over conventional contacting methods. A statistical design of experiment approach was used to identify the major variables affecting equilibrium conversion and enantiomeric excess in presence of CLA. The optimal conditions for high conversion (>90%) were identified as low void fraction (10%) and high pH (6). Under conditions that are optimal for high equilibrium conversion, the enantiomeric excess attained was also high (>90%), thus precluding a tradeoff between maximizing conversion and enantiomeric excess.

Chapter 5 demonstrated the use of CLA emulsions in the biotransformations of cinnemaldehyde by Baker's yeast at high cell densities (250g/L). The solvent, 2,2,4 trimethyl pentane, was identified as a suitable biocompatible solvent for yeast biotransformations. The presence of the organic phase in the form of CLA emulsion increased the fraction of 4 substituted (2S, 3R)-5-phenylpent-4-en,2,3-ols (4) by three-fold upto 45%. The selectivity of the yeast biocatalyst appears to depend on substrate concentration. The observed change in selectivity due to the presence of hydrophobic resins was consistent with this hypothesis. However the variation in selectivity in the presence of CLA could not be attributed to this phenomenon. More studies are required to clarify

the mechanism by which the presence of dispersed organic solvents affects selectivity.

Chapter 6 presented preliminary studies on reversible emulsions formed using the 15:1 and 20:1 pH reversible emulsifiers. Results indicated a high degree of reversibility for emulsions formed using 15:1 and 20:1 emulsifiers. Mass transfer studies indicated a four-fold increase in volumetric rates of mass transfer for such emulsions compared to surfactant-free systems. The volumetric mass transfer rate was three-fold less than that measured for CLA systems. Thus, the ease of coalescence due to the unique surfactant architecture involves a trade off in mass transfer enhancement compared to CLA. In order to undertake further studies on the reversible emulsions systems, the interfacial characterization of these reversible emulsions is essential.